Carbon nanotube for differentiation of mouse stem cells and a non-invasive characterization method for cardiomyocytes

(マウス幹細胞のカーボンナノチューブによる分化誘導と分化心筋細胞の非侵襲画像解析)

Mohammad Mosharraf Hossain

Department of Applied Physics

Graduate School of Engineering

Osaka University

2010

Doctoral Dissertation

Carbon nanotube for differentiation of mouse stem cells and a non-invasive characterization method for cardiomyocytes

(マウス幹細胞のカーボンナノチューブによる分化誘導と分化心筋細胞の非侵襲画像解析)

Mohammad Mosharraf Hossain

A dissertation for the partial fulfillment for the degree of Doctor of Philosophy in Engineering

Department of Applied Physics

Graduate School of Engineering

Osaka University

September, 2010

Table of content

Chapter: One

Introduction

Chapter: Two

Non-invasive characterization of Mouse Embryonic Stem cell derived Cardiomyocytes based on the intensity variation in digital beating video

Chapter: Three

Effects of the exposure to functionalized multiwalled carbon nanotubes on embryoid body formation from mouse embryonic stem cells, their subsequent growth and cardiomyogenic differentiation

Chapter: Four

Carboxylate functionalized Multiwalled Carbon nanotube modified gelatin substrate enhances cardiac differentiation and promote neuronal differentiation of mouse embryonic stem cells

Chapter: Five

Microfluidic hanging drop chip for the formation of embryoid body with from mouse ES and iPS cells medium replenishment for long term culture

Chapter: Six

List of Schemes and Figures

Chapter: One

Chapter: Two

Chapter: Three

Chapter: Four

Chapter: Five

Chapter: 1

Introduction

Chapter: One

Introduction

1.0 Background

The era of regenerative medicine is emerging[1-4] as stem cells from embryonic and non-embryonic sources are showing unprecedented promises. The advent of the age of regenerative medicine has further been augmented by the creation of embryonic stem (ES) cell like induced pluripotent stem (iPS) cells through cellular reprogramming – a major breakthrough in developmental, cellular and molecular biology.[5,6] But the translational shift from research to clinical practices do have some real hurdles and formidable challenges. Before regenerative therapeutic applications of pluripotent stem cells, we have to achieve a comprehensive understanding of the factors involved with epigenetic fate determination through multi-lineage differentiations of these cells and finding out the exact clues to control the differentiation machineries to direct these cells towards a desired lineage to produce clinical grade terminally differentiated cells with all their *in-vivo* properties.[7-9]

The control of differentiation towards a particular lineage have so far been achieved with limited success for limited number of lineages with approaches ranging from culture medium optimization,[10,11] modification of cell growth and attachment substrates,[12,13] provision of physical and chemical induction factors,[14,15] creation of three dimensional *in-vivo* like growth environment[16] etc. As we know, in their natural niches, stem cells grows in special environments

that provides them, firstly with a unique surface to stick to and then a practically inimitable surroundings to get the chemical and physical clues from, for initiating and directing differentiation as needed while maintaining the pool of pluripotent cells at desired population

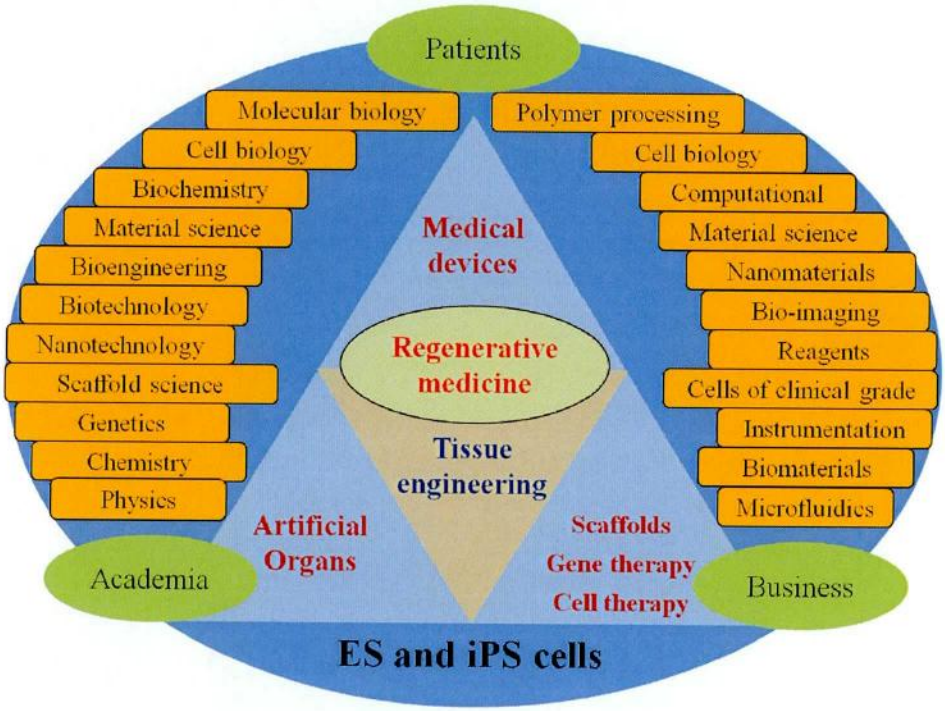

Figure 1 *The field of regenerative medicine in the context of Academia, Business and the Therapy seeking patients. Different faculties of human intellects play a concerted role in the development and evolution of the fields with breakthroughs coming from all of these fields.*

size. Hence, we need to address the problem from multiple directions at the same time rather than only chemical or only physical or only biological approach. But to combine these three approaches together, we need precise understanding what any of these has to offer in that pursuit. At this juncture, the field of regenerative medicine can be sought of an assortment of efforts from

academia and business endeavors to make ES/iPS cells' potentials available for patient care through segmented but concerted efforts (Fig 1).

ES and iPS cells are known to differentiate into spontaneously beating cardiac muscle cells and neuronal cells upon exposure to different chemicals[17-19] or if grown on special substrates[20,21]. The current state of understanding suggests that any particular environment and factor favors only a particular lineage commitment unlike the ultimate environment for ES cell growth – the mother's womb where these cells get all the necessary environment and clues to create all the different types of cells of a functional organism with unprecedented precision in spatial and temporal harmony of the differentiation. But the need to create only one desired population of cells from pluripotent cells is also of paramount importance for regenerative medicine.

Based on our understandings so far from the translational research of pluripotent stem cell, we observed that the differentiation research poses three major challenges (Fig 2) for being addressed.

The first challenge is to control the initiation of epigenetic events for directed differentiation at the ES or iPS cell aggregation step where the formation of three germ layers *viz.* ectoderm, mesoderm and endoderm containing different progenitors and precursor cells for different organ system is achieved.

The second challenge is to direct the ES/iPS cell lineage commitment or epigenetic events to favor a particular group of progenitors off the pool of progenitors from three germ layers for getting a particular type of terminally differentiated cells in subsequent culture after stem cell aggregation.

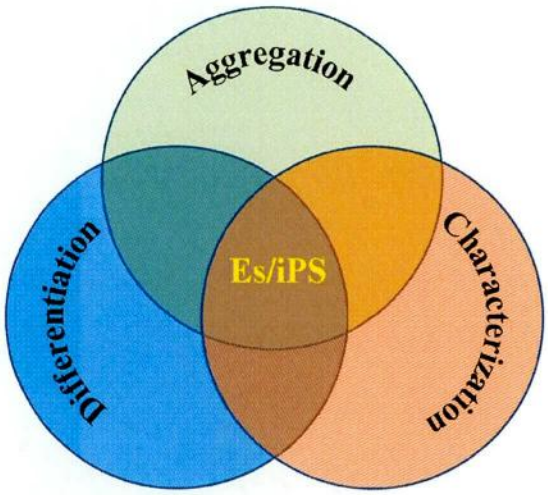

Figure 2 *The Major challenges in ES/iPS cell research - initiation of cell differentiation through controlled aggregation, controlling the actual differentiation and characterization of differentiated cells.*

The third but not-least-important challenge lies in the precise and quick characterization of differentiated cells of different lineages in a non-invasive and easy manner. After the onset of differentiation, characterization is necessary for the purpose of assessing their maturity, functionality and most importantly for purifying them from the collection of different kinds of cells including undifferentiated ES/iPS cells.

1.1 Scope of the Study

In this doctoral study, I intended to address these three basic issues related to ES cell differentiation in three related but separate approaches. Firstly, the development of a novel image analysis method for non-invasive characterization of ES derived cardiomyocyte by constructing the beating profile from the intensity variations in beating video images due to contraction and relaxation *i.e.* systolic and diastolic movements of synchronously beating cardiomyocytes over

time. Changes in the beating patterns give clues to the properties of differentiated cardiomyocytes and their response to external stimulations – such as chronotropic agents or drugs.

Secondly, application of a nano-material approach to direct the ES cell lineage commitment by using the direct and mediated interaction of functionalized carbon nanotubes with mouse ES cells. In the direct approach, the cells were exposed to functionalized and humanized multiwalled carbon nanotubes (f-MWCNT) to follow the effects of carbon nanotubes on the stem cell behaviors from primary aggregation step till the differentiation. In the indirect approach, however, mES cell aggregates or embryoid bodies were placed on functionalized MWCNT modified gelatin substrates to see the role of such novel composites in directing the cell fates.

Thirdly, adopting a microfluidic approach to improve the hanging drop embryoid body formation method in order to get better control over the formation of ES cells aggregates and enabling long time culture of them with medium replenishment.

1.2 Non-invasive intensity variation analysis to characterize differentiated cardiomyocyte

One of the major causes of worldwide mortality is cardiac diseases which cause millions of deaths every year. Cardiac diseases remained a major challenge to the medical practitioner though numerous breakthroughs in cardiac treatments have been made over the years.[22,23] Application of regenerative medicine to repair the damaged heart by the use of stem cell derived cardiomyocytes is yet a possibility[24,25] with some really promising successes to that end are surfacing from recent efforts of the researchers.[26] From ES/iPS cells, generation of functional beating cardiomyocytes is relatively easy and there are quite a number of protocols developed to

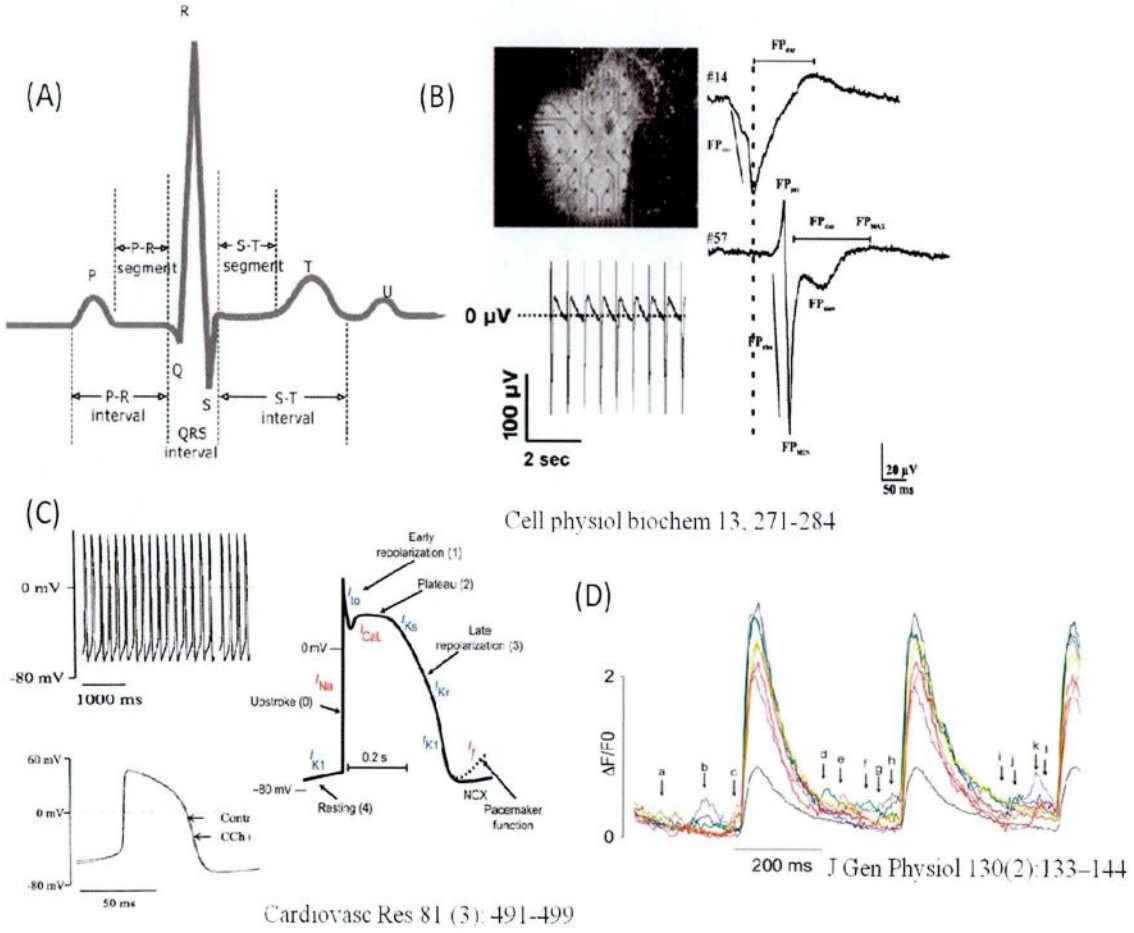

Figure 3 *The usual means of cardiac and cardiomyocyte characterization. (A) The whole heart function characterization is done by* ***E****lectro****C****ardio****G****raphy (ECG) which is not very useful in differentiated cardiomyocyte characterization. (B) Micro Electrode Array (MEA) based cardiomyocyte characterization - many details can be obtained in this method but it is invasive, expert oriented and requires expensive setups. (C) Patch clamp based cardiomyocyte characterization – the ion channel functionality can be measured but this method also is invasive, expert oriented and requires expensive setups. (D) Flourescence based* Ca^{++} *oscillation imaging – also an invasive process and cells can't be used further.*

that end but the real hurdles remained in purifying the differentiated cardiomyocytes from heterogeneous cell mixture including pluripotent cells[27,28] and characterizing them properly for clinical applications safely.

There are a number of widely used methods – conventional and modern - available for the characterization of ES and iPS derived cardiac muscle cells (Fig 3), for example, immunocytochemistry, micro electrode array (MEA) based electrophysiology, patch-clamp based electrophysiology, fluorescent imaging and other cell assays. But these approaches have one or more of the following limitations - invasiveness, expensiveness, requiring time and expertise, and needing the sacrifice of valuable differentiated tissue. Most of these approaches are not also amenable to automation for high throughput operations.

There are some analytical methods based on image analysis which focuses on single beating cardiomyocyte or a tiny patch of beating tissue consisting of few contractile cells.[29,30] In some approaches, changes in the selected cardiac myocytes' membranes[31] or the changes in Ca^{2+} intensities during beating are taken into consideration for characterizing differentiated contractile cells.[32] But measuring the contractile activity of one single cell or in patches of few cells is quite challenging and unreliable while Ca^{2+} intensity measurement requires expensive set-up and expertise.

Consequently, the development of a simple method to characterize ES and iPS derived cardiomyocytes based on easy to avail set-ups is very crucial to the development of high throughput screening of differentiated cardiac muscle cells in the emergence of cardiac regenerative medicine. In this thesis, a novel and non-invasive method for differentiated cardiomyocyte characterization based on optical microscopy is proposed. The approach is simple, easy, quick, inexpensive and above all amenable to automation. The applicability of the

approach has been illustrated by using it in measuring the response of differentiated cardiac myocytes to inotropic drugs.

In this approach, unlike the current approaches, we have considered the entire beating segment on the tissue for our analysis to ensure the simplicity and to reveal more information from the large patch of beating cells. The changes in the total pixel intensities in derivative images captured from in-vitro beating tissues were analyzed and converted it into the time and frequency domain intensity patterns. The method was successfully applied in monitoring the initiation, propagation and maturation of beating of mESC derived cardiac muscle cells. Moreover, using our method - the beating frequency, the strength of beating, number of distinctly beating patches at a certain location on the culture dish could be obtained. Moreover, we used our proposed method in evaluating the response of differentiated cells to positive and negative inotropic agents. All of these are important in evaluating stem cell derived cardiomyocytes for subsequent applications after differentiation.

1.3 Carbon nanotubes for directing ES cell differentiation

Mesoscale materials are getting more attention as owing to their size scale in the range of cell organelles, proteins and other biomolecules, they have greater and more meaningful functional and structural interactions with cells. Mesoscale interactions (Fig 4) between nanomaterials and cells are getting wider research focus with time and more mysteries related to such interactions are unraveling slowly. Nanomaterials of interest includes - carbon nanotubes and other carbon allotropes like fullerene, metallic nanoparticles from gold, silver, silicon or platinum, diverse range of organic and inorganic nano-particles. Wide range of cells is also under investigation in this field involving primary cells, immortalized cells, carcinoma cells and above all ES and iPS

cells. The interests involve the potential toxicity of such nanomaterials, their cellular uptake and processing, their interactions with culture medium, cell membrane and upon cellular uptake, with the cytosolic organelles. The potential uses so far reported include the use of nanomaterials in gene delivery, drug delivery, boosting cell performances, differentiation, targeted killing of cancer cells and imaging.

There are differences in the mode of action potential generation between neurons and cardiomyocytes, yet they have things in common – both are electro-active in nature and both prefer elastic surfaces with electrical activity for growth. Soft matrix is preferred by neurons and rigid matrix is suited for cardiomyocytes[13]. For this reason, we speculated that it might be possible to direct ES and iPS cells to commit towards cardimyogenic and neurogenic paths by providing them a substrate which will support their normal growth and proliferation and will favor their commitment towards electro-active lineages over other types of cells (Fig 5). It had been reported that carbon nano-tube (CNT) favors neurogenic differentiation[33-35] but there are reservations against the toxic role of CNT towards cells,[36,37] for which, in any scheme of using CNT for cellular differentiation, the direct exposure to cells should be kept to a minimum so that the toxicity of CNT, if any, will not affect the cells. Gelatin, in one hand, is very good substrate for adherent culture of ES cells in vitro, while on the other hand, it is known to be a very good dispersant of CNT[38].

CNTs are materials of very high aspect ratio and posses metal-like electrical properties. These made CNT a material of choice when we wanted composite materials with modified electrical properties and elastic behavior both of which can define lineage commitment of stem cells. CNT dispersion in gelatin, mixed with cell culture media, proved the non-toxic nature of such dispersion to different types of cells including cardiomyocytes,[39] neurons,[40] mesenchymal

stem cells[41] etc. In line with these facts, we decided to study the role of CNT on mES cell differentiation from two perspectives – firstly, by growing the ES cell derived embryoid bodies on CNT modified gelatin matrix and secondly by exposing the EB forming cells to CNT dispersion in gelatin.

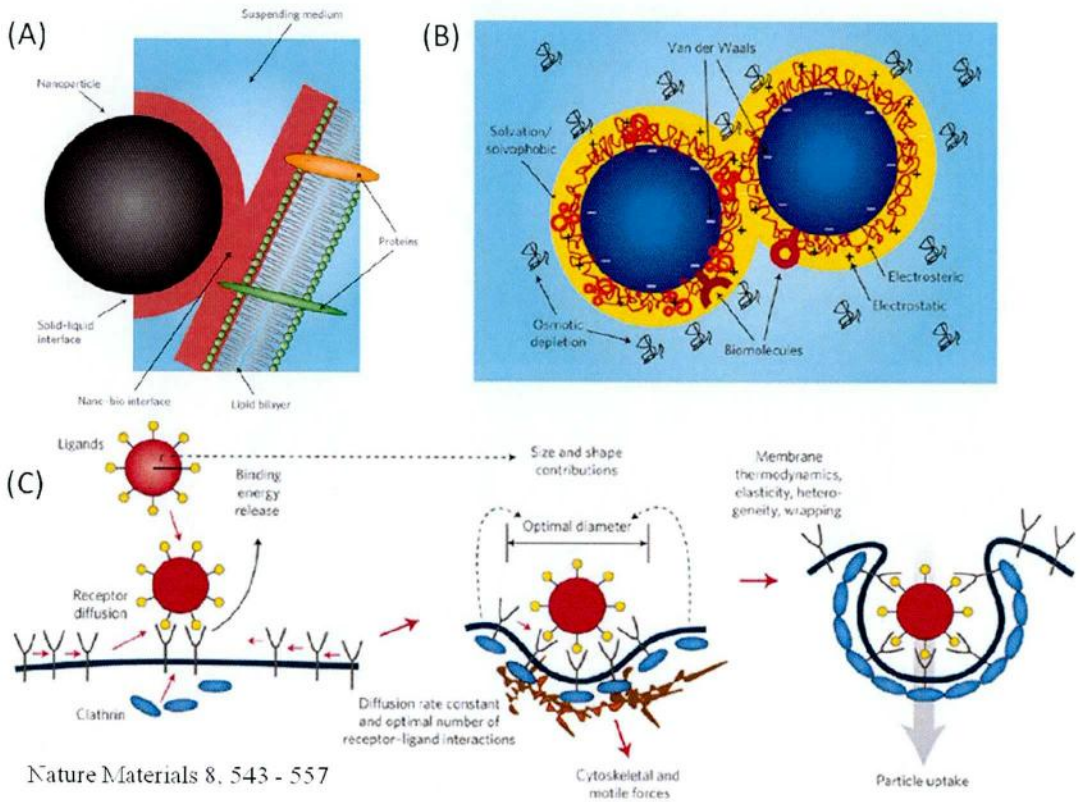

Figure 4 *Nano-bio interactions at different interfaces. (A) Nano material interaction with the cell culture medium at solid liquid interface and nano-bio interface. (B) The active forces and interactions at nanoscale solid liquid interfaces. (C) Nanobio interactions – one plausible mechanism.*

Consequently, in this work, we used CNT dispersed in 0.01% gelatin to coat the polystyrene culture dishes and we grew the ES cell derived embryoid bodies to see the lineage defining role of this composite substrate towards electro-active cardiac and neuronal lineages. Differentiation

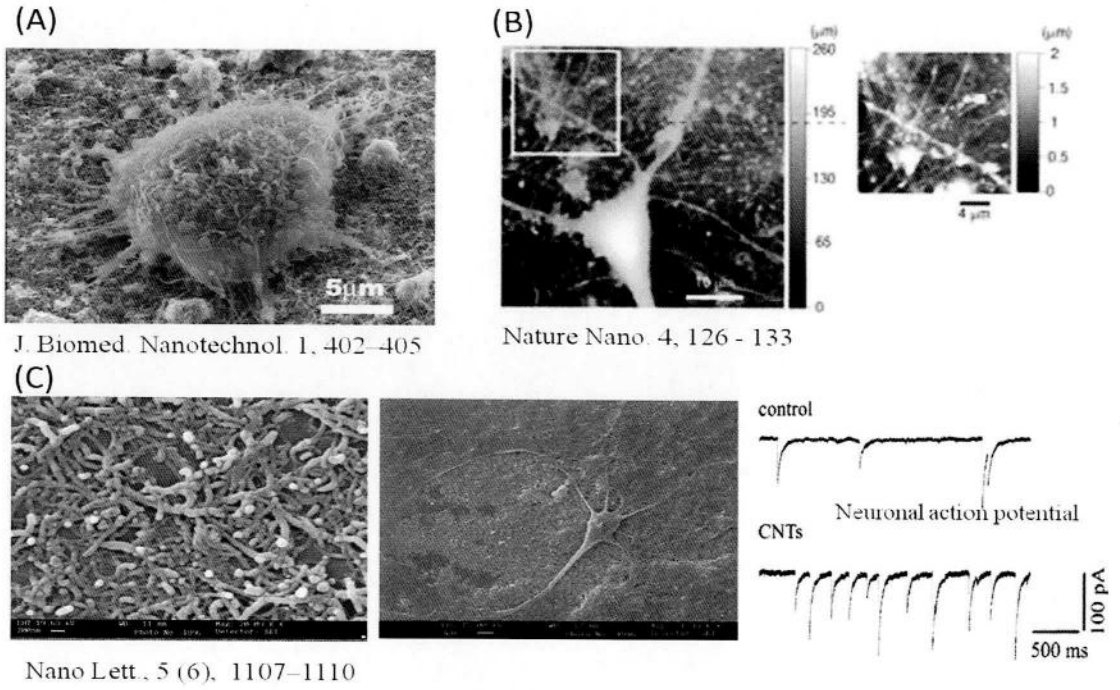

Figure 5 *Cell growths on the functionalized multiwalled carbon nanotube containing substrate. (A) Cells remained alive and (B, C) neurite outgrowth from neurons were favored by the presence of CNTs and CNTs boosted the neural action potential.*

is initiated by making ES cell aggregate *i.e.* embryoid body by keeping 20 μl to 30uL hanging drops containing defined number of cells in LIF free medium. These EBs were plated onto the gelatin-CNT modified culture substrate. The toxicity of CNT-gelatin matrix was evaluated by MTS assay, propidium iodide (PI) staining and green fluorescence protein (GFP) tracking since the ES cell line we used express GFPs ubiquitously.

The cultures were routinely investigated to study subsequent growth and differentiation through optical imaging and immunostaining. Transmission electron microscopic (TEM) study was done to see the uptake and localization of CNT in the cells as well as to see the ultra-

structural effects of CNT on cell. The differentiated cardiomyocyte properties have also been analyzed over time in relation to the control cultures. The role of exposure of ES cells to different concentrations of CNT at the EB formation stage was investigated.

We characterize the CNT-gelatin substrate by using Fourier Transform Infrared (FTIR) spectroscopy, Atomic Force Microscopy (AFM), Scanning Electron Microscopy (SEM), Raman spectra analysis and conductivity measurements. We observed the presence of CNT fibers embedded into the gelatin. This composite substrate material was non-toxic and did not affect the viability and proliferation of ES cells and ES cell derived EBs. The biocompatible substrate supported the growth and differentiation of murine embryonic stem cells and directed the ES cells towards concurrent differentiation towards cardiomyocytes and neuronal cells where neuronal differentiation came after cardiac differentiation. The immunostaining using cardiac markers α-actinin, ANP and Troponin we confirmed the presence of differentiated cardiomyocytes in significantly higher numbers and patches compared to control culture on bare gelatin. The immunostaining using neuronal markers Neu-N and neurofilament confirmed the presence of differentiated neurons whereas in control cultures no such differentiation was seen. The beating profiles of cardiomyocytes showed stronger beating compared to control. Though, on successful differentiation, the removal of residual CNTs may become a concern for the therapeutic applications of generated cells, but the high biocompatibility of the generated tissue to CNT and gradually decreasing concentration of CNTs in the cells due to successive cell divisions allowed us to ignore, for the time being, the CNT removal issue. We agree that this will be a major focus of research in CNT based stem cell differentiation for therapeutic purpose.

Based on aforementioned facts, we tried another approach to expose the mouse embryonic stem cells to functionalized carbon nanotubes in another way. Usually, for the initiation of

differentiation, we make ES cells to form spherical cell aggregate, known as Embryoid body (EB) through keeping 20 µl to 30uL hanging drops containing defined number of cells in LIF free medium. We supplemented the medium with carboxylate modified multiwalled CNT dispersion made in 0.1% gelatin solution. This approach made relatively direct exposure of the cells to CNT. After formation of embryoid bodies we investigated the role of CNT on EB formation and EB morphology. The toxicity of CNT in EBs was investigated by MTS assay, PI staining and GFP tracking. The formed EBs were plated onto 0.1% gelatin coated culture dishes for subsequent growth and differentiation. We studied the differentiation through optical imaging and immunostaining. The role of exposure of ES cells to different concentrations of CNT at the EB formation stage was investigated. We have seen the formation of EBs of comparable size and shape with better sphericity in case of CNT treatment. The EB did not show any toxicity affect in the toxicity assays. The attachment of EBs to gelatin substrate was remarkable and upon continuous culture we got beating cardiomyocyte from CNT exposed EBs as confirmed in immunostaining with cardiac specific markers.

1.4 Microfluidic chips for Embryoid Body formation

EBs are three dimensional cell aggregates, preferably spherical in shape, derived spontaneously from suspension culture or hanging drop culture of *embryonic stem cells* or *induced pluripotent stem* (iPS) cells in the absence of the feeder cells and anti-differentiation factors such as Leukemia Inhibitory Factor (LIF). Usually, for the initiation of differentiation, we make ES cells to form cell aggregates, known as Embryoid body (EB) by keeping 20 µl to 30uL hanging drops containing defined number of cells in LIF free medium at 37°C in 5% CO_2 for 3~5 days on the inverse side of the lid of a culture dish which contains autoclaved water to inhibit evaporation from the drops. Embryoid bodies are capable of emulating the phases of early

gastrulation, at least to some extent, for which there is rising interest in EBs as a model for studying early embryogenesis.[42-45] Moreover, EBs are important in the investigations involving drug screening, the cell fate determination,[47-49] the production of terminally differentiated cells like cardiomyocytes, neurons, pancreatic islets cells for regenerative medicine, are few examples. The means to generate EBs are several,[44] for example, suspension culture in bacterial grade dishes, methylcellulose culture (MC culture), hanging drop culture (HD culture) on inverted cell culture ware lids, suspension culture in low-adherence well plates, and spinner flask and bioreactor techniques for scalable production. Each of these methods has intrinsic limitations with some advantageous points. Suspension culture do not produce uniform size EBs and EBs formed are not spherical. Hanging drop culture produces EBs of uniform in size and spherical shape and the cells are aggregated at the bottom of the spherical hanging drops under the force of gravity which keeps them in an environment of favorable gaseous exchange. The main drawback of traditional hanging drop method is the nutrient deprivation suffered by EBs since media replenishment is impossible without disturbing the EBs under formation over a usual three day culture regime.

Methylecellulose culture is more preferable as a mean to preserve already formed EBs than for EB formation itself. Formation of EBs from single cell clones in methylecellulose culture is reported, but there is always a mechanical pressure against expanding EB sphere due to high viscosity of methyl cellulose media. Moreover, replenishing medium is also cumbersome in this method. We are still in a quest for a simple and more efficient mechanism for high throughput production uniform and spherical EBs. On the other hand, microfluidic is an emerging technology offering greater control over fluid manipulation at micron scale. In order to address the limitations of traditional hanging drop approach, we decided to construct a simple

microfluidic platform that ensures production of EBs of uniform sizes and shapes employing the gravitational force to aggregate the cells in a similar way to traditional hanging drop.

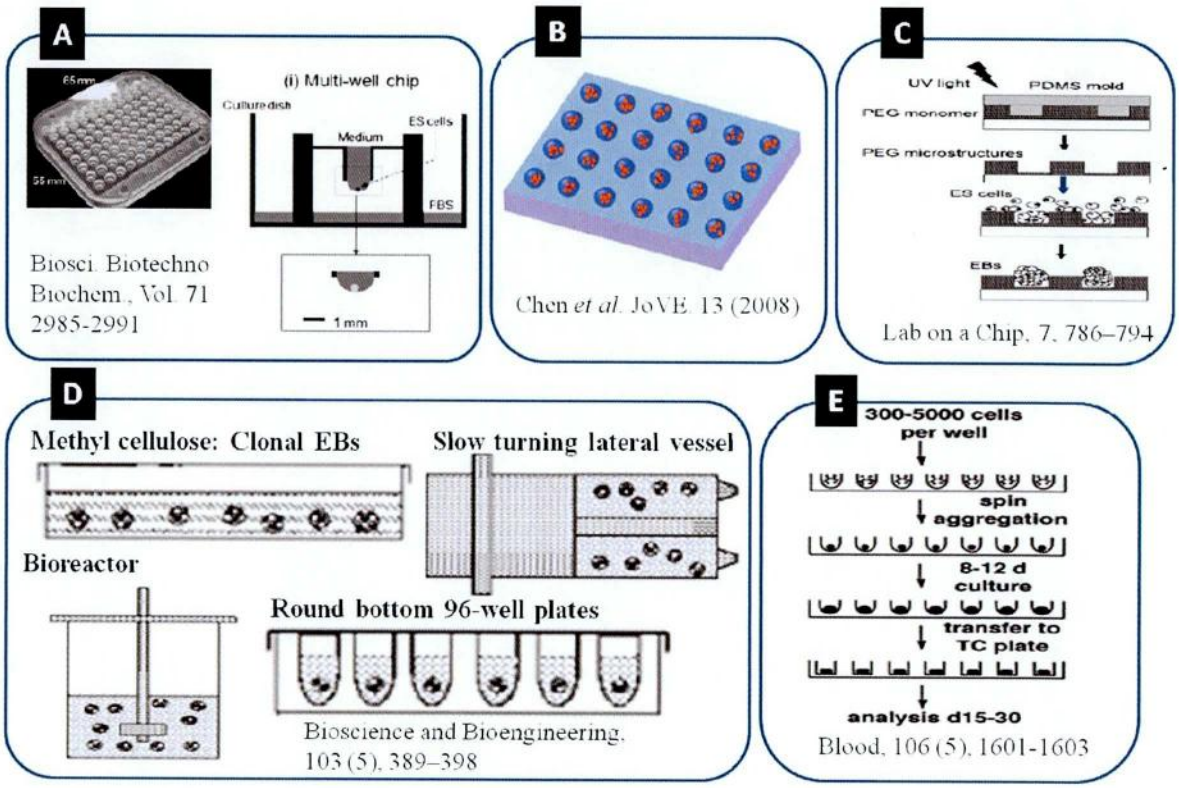

Figure 6 *Different available methods for EB formation. (A) Multi-well hanging drop platform, (B) Shrinky dink well structures, (C) PEG micro-wells based aggregation platform, (D) Bioreactors, round bottom wells, methylecellulose based aggregation systems, (E) Spinning based forced aggregation.*

We fabricated several chips with different designs and schemes for our work and most of them worked well. Briefly, the chips consisted of one inlet for cell suspension and several outlets receiving equal volume of cell suspension to form 20-30 µl droplets at the opening of each outlet. Considering the need for high throughput EB production, we expanded our design to make it into high throughput chip for EB formation. The polydimethylesiloxane (PDMS) chips

were constructed through replica molding from SU-8 master mold fabricated through photolithography at clean room facility available at our LAB. After tubing and setting chips were sterilized and fixed to the lid of tissue culture dish. We then pumped the cell suspension manually using syringe till we achieved droplets of desired and uniform sizes containing uniform number of ES cells. The chips were then kept inverted on the culture dish with water and incubated for 3~4 days before collecting the EBs. EBs formed were characterized and compared to the EBs from control traditional hanging drops. We observed uniformly sized EB formation with comparable sphericity and shapes to the control EBs. The quality of the EBs were also ascertained by doing he subsequent differentiation study where we confirmed the formation of beating cardiomyocyte from chip derived EBs. Our method also showed the promise for long term growth of EBs in hanging fashion in order to let them go into maturation during in-vitro gastrulation and research in that direction is underway.

1.5 Organization of the thesis

Chapter 1: Introduces the thesis with a general background and identifying the location of the works reported in the thesis within the broader field of regenerative medicine and ES/iPS research.

Chapter 2: In this chapter the novel and non-invasive video image analysis method for characterization of differentiated cardiomyocytes for ES cells have been described and the applicability of the method has been demonstrated.

Chapter 3: This chapter includes our investigation into the role of functionalized multiwalled carbon nanotubes (f-MWCNTs) dispersed into gelatin or water in ES cell aggregation during

hanging drop culture. The subsequent growth and differentiation of mouse ES cells have also been reported.

Chapter 4: In this chapter, the Mesoscale modification of gelatin substrate by using functionalized multiwalled carbon nanotubes (f-MWCNTs) is reported. The characterization of CNT modified gelatin substrate is included along with the study on the growth and differentiation of mouse ES cells on the modified substrate.

Chapter 5: The development of a microfluidic chip for hanging drop based mES and iPS cell aggregation is reported in this chapter. It includes the characterization of the chip, and EBs formed thereof.

Chapter 6: This chapter wraps up the thesis with a final discussion relating all other chapters.

4.0 References

[1] Christou, Y. A.; Moore, H. D.; Shaw, P. J.; Monk, P. N. *Neuropathology and Applied Neurobiology* **2007**, *33*, 485–498.

[2] Amabile, G.; Meissner, A. *Trends in Molecular Medicine* **2009**, *15*, 59–68.

[3] Gurtner, G. C.; Callaghan, M. J.; Longaker, M. T. *Annual Review of Medicine* **2007**, *58(1)*, 299-312.

[4] Mimeault, M.; Hauke, R.; Batra, S. K. *Clinical Pharmacology & Therapeutics* **2007**, *82*, 252–264.

[5] Okita, K.; Nakagawa, M.; Hyenjong, H.; Ichisaka, T.; Yamanaka, S. *Science* **2008**, *322*, 949.

[6] Takahashi, K.; Tanabe, K.; Ohnuki, M.; Narita, M.; Ichisaka, T.; Tomoda, K.; Yamanaka, S. *Cell* **2007**, *131*, 861–872.

[7] Hwang, N. S.; Varghese, S.; Elisseeff, J. *Advanced Drug Delivery Reviews* **2008**, *60*, 199–214.

[8] Graf, T.; Enver, T. *Nature* **2009**, *462*, 587–594.

[9] Mantalaris, A.; Randle, W. L.; Polak, J. M. *Stem Cell Repair and Regeneration* **2008**, 45.

[10] Gong, Z.; Calkins, G.; Cheng, E.; Krause, D.; Niklason, L. E. *Tissue Engineering Part A* **2008**, *15*, 319–330.

[11] Shi, X. L.; Mao, L.; Xu, B. Y.; Xie, T.; Zhu, Z. H.; Chen, J. H.; Li, L.; Ding, Y. T. *Cell Biology International* **2008**, *32*, 959–965.

[12] Dawson, E.; Mapili, G.; Erickson, K.; Taqvi, S.; Roy, K. *Advanced Drug Delivery Reviews* **2008**, *60*, 215–228.

[13] Engler, A. J.; Sen, S.; Sweeney, H. L.; Discher, D. E. *Cell* **2006**, *126*, 677–689.

[14] Borowiak, M.; Maehr, R.; Chen, S.; Chen, A. E.; Tang, W.; Fox, J. L.; Schreiber, S. L.; Melton, D. A. *Cell Stem Cell* **2009**, *4*, 348–358.

[15] Schugar, R. C.; Robbins, P. D.; Deasy, B. M. *Gene Therapy* **2007**, *15*, 126–135.

[16] Ferreira, L. S.; Gerecht, S.; Fuller, J.; Shieh, H. F.; Vunjak-Novakovic, G.; Langer, R. *Biomaterials* **2007**, *28*, 2706–2717.

[17] Willems, E.; Bushway, P. J.; Mercola, M. *Pediatric Cardiology* **2009**, *30*, 635–642.

[18] Xu, Y.; Shi, Y.; Ding, S. *Nature* **2008**, *453*, 338–344.

[19] Greco, S. J.; Rameshwar, P. *Molecular BioSystems* **2010**, *6*, 324–328.

[20] Horton, R. E.; Millman, J. R.; Colton, C. K.; Auguste, D. T. *Regenerative Medicine* **2009**, *4*, 721–732.

[21] Reilly, G. C.; Engler, A. J. *Journal of Biomechanics* **2009**.

[22] Gardner, T. J. *Circulation* **2009**, *119*, 1838-1841.

[23] Strong, K.; Mathers, C.; Bonita, R. *The Lancet Neurology* **2007**, *6*, 182-187.

[24] Boheler, K. R.; Czyz, J.; Tweedie, D.; Yang, H. T.; Anisimov, S. V.; Wobus, A. M. *Circulation Research* **2002**, *91*, 189.

[25] Narazaki, G.; Uosaki, H.; Teranishi, M.; Okita, K.; Kim, B.; Matsuoka, S.; Yamanaka, S.; Yamashita, J. K. *Circulation* **2008**, *118*, 498.

[26] Liao, L.; Chunhua Zhao, R. *Stem Cells and Development* **2008**, *17*, 613–618.

[27] Jungling, K.; Nagler, K.; Pfrieger, F. W.; Gottmann, K. *The FASEB Journal* **2003**, 301181.

[28] Heng, B. C.; Haider, H. K.; Sim, E. K.; Cao, T.; Ng, S. C. *Cardiovascular Research* **2004**, *62*, 34.

[29] Stummann, T. C.; Wronski, M.; Sobanski, T.; Kumpfmueller, B.; Hareng, L.; Bremer, S.; Whelan, M. P. *ASSAY and Drug Development Technologies* **2008**, *6*, 375–385.

[30] Weisensee, D.; Bereiter-Hahn, J.; Schoeppe, W.; L\öw-Friedrich, I. *International Journal of Immunopharmacology* **1993**, *15*, 581–587.

[31] Wassermann, D.; Mejail, M. *Progress in Pattern Recognition, Image Analysis and Applications* 420–430.

[32] Sasse, P.; Zhang, J.; Cleemann, L.; Morad, M.; Hescheler, J.; Fleischmann, B. K. *Journal of General Physiology* **2007**, *130*, 133.

[33] Lee, W.; Parpura, V. *Progress in Brain Research* **2009**, 110–125.

[34] Chao, T. I.; Xiang, S.; Chen, C. S.; Chin, W. C.; Nelson, A. J.; Wang, C.; Lu, J. *Biochemical and Biophysical Research Communications* **2009**.

[35] Jan, E.; Kotov, N. A. *Nano Letters* **2007**, *7*, 1123–1128.

[36] Firme III, C. P.; Bandaru, P. R. *Nanomedicine: Nanotechnology, Biology and Medicine* **2009**.

[37] Inoue, K.; Yanagisawa, R.; Koike, E.; Nishikawa, M.; Takano, H. *Free Radical Biology and Medicine* **2010**.

[38] Kim, Y.; Minami, N.; Kazaoui, S. *Applied Physics Letters* **2005**, *86*, 073103.

[39] Krajcik, R.; Jung, A.; Hirsch, A.; Neuhuber, W.; Zolk, O. *Biochemical and Biophysical Research Communications* **2008**, *369*, 595–602.

[40] Sucapane, A.; Cellot, G.; Prato, M.; Giugliano, M.; Parpura, V.; Ballerini, L. *Journal of Nanoneuroscience* **2009**, *1*, 10.

[41] Mooney, E.; Dockery, P.; Greiser, U.; Murphy, M.; Barron, V. *Nano Letters* **2008**, *8*, 2137–2143.

[42] Choi, D.; Lee, H. J.; Jee, S.; Jin, S.; Koo, S. K.; Paik, S. S.; Jung, S. C.; Hwang, S. Y.; Lee, K. S.; Oh, B. *Stem Cells* **2005**, *23*, 817–827.

[43] Hwang, Y. S.; Polak, J. M.; Mantalaris, A. *Stem Cells and Development* **2008**, *17*, 971–978.

[44] Kurosawa, H. *Journal of Bioscience and Bioengineering* **2007**, *103*, 389–398.

[45] Nishikawa, S. I.; Jakt, L. M.; Era, T. *Nature Reviews Molecular Cell Biology* **2007**, *8*, 502–507.

[46] Bauwens, C. L.; Peerani, R.; Niebruegge, S.; Woodhouse, K. A.; Kumacheva, E.; Husain, M.; Zandstra, P. W. *Stem Cells* **2008**, *26*, 2300–2310.

[47] Bratt-Leal, A. M.; Carpenedo, R. L.; McDevitt, T. C. *Biotechnology Progress* **2009**, *25*, 43.

[48] Mohr, J. C.; Zhang, J.; Azarin, S. M.; Soerens, A. G.; de Pablo, J. J. *Biomaterials* **2009**.

Chapter: 2

Non-invasive characterization of Mouse Embryonic Stem cell derived Cardiomyocytes based on the intensity variation in digital beating video

Chapter Summary

The interest on cardiomyocytes derived from differentiation of Embryonic Stem (ES) cells or induced pluripotent stem (iPS) cells is increasing due to their potential for regenerative therapeutics and as a pharmaceutical model of drug screening. Characterization of ES or iPS derived cardiomyocytes is challenging and inevitable for the intended usage of such cells. In this paper we have outlined a novel, non-invasive method for evaluating *in vitro* beating properties of cardiomyocytes. The method is based on the analysis of time dependent variation in the total pixel intensities in derivative images obtained from the consecutive systolic and diastolic frames from the light microscopic video recordings of beating tissue. Fast Fourier Transform (FFT) yielded the frequency domains for these images. The signal to noise ratio for the analysis met the Rose criterion. We have successfully applied our method for monitoring mouse ES cell (mESC) derived cardiac muscle cells to determine the initiation of beating, organization and maturation of beating tissue, calculating the beating rhythms in terms of beating interval or frequency and the strength of beating. We have shown the successful application of our image analysis method direct monitoring of the response of differentiated cardiomyocytes towards caffeine hydrate, *p*-hydroxyphenyleacetamide and calcium chloride dehydrate respectively as positive, neutral and negative inotropic agents. This non-invasive method of characterizations will be useful in studying the response of these cells to various external stimulations, such as differentiation promoting agents or treatments as well as in preliminary drug screening quickly, inexpensively and without much need of expertise.

2.0 Introduction

A paradigm shift in medicine from drug based symptomatic treatment towards regenerative treatment is becoming discernible.[1,2] With the wider investigations of embryonic stem (ES) cells[3] and induced pluripotent stem (iPS) cells[4,5] for regenerative purposes,[6-8] regenerative medicine is gaining wider appreciations.[9] The long term goal of all stem cell research is to regenerate desired tissue[10, 11] with reasonable efficiency. Its ultimate aim is to generate working organs from stem cells[12] while adequately addressing the issues like immune responses against grafted tissue, complete differentiation of stem cells to desired cells of acceptable quality.[13] Though we believe that ES and iPS cells are capable of meeting these ends, our understanding of differentiation and the factors that control it are sketchy. So far derivation of various cell types including cardiomyocytes,[14] adipocyte and osteoblast,[15] neural,[16] pancreatic,[17] renal cells[18] etc from ES and iPS has been reported. With the better understanding of differentiation, we need efficient and non-invasive methods for characterizing the differentiated cells.

Cardiac diseases cause millions of deaths and they remained a major challenge to the medical practitioners even after numerous breakthroughs in cardiac treatments.[19, 20] Repairing the damaged heart by stem cell derived cardiomyocytes is yet a possibility[8, 21] and some promising successes to that end are becoming evident from recent reports.[2] Though it is relatively easy to produce cardiomyocytes from ES/iPS cells, hurdles remained in purifying them from heterogeneous cell mixture and characterizing them properly before clinical application.[22, 23] On the other hand, characterization of cardiac cells with conventional methods like immunocytochemistry, electrophysiology, fluorescent imaging or other cell

assays are invasive, time consuming and require the sacrifice of valuable tissue and are less amenable to automation.

There are some analytical systems based on image analysis focusing on single beating cardiomyocyte or a tiny patch of beating tissue consisting of few contractile cells[24, 25] or the changes in the selected cardiac myocytes' membrane[26] or the changes in Ca^{2+} intensities during beating.[27] But measuring contractile activity in patches of few cells is quite challenging and unreliable[28] while Ca^{2+} intensity measurement requires expensive set-up and expertise.

In this chapter, the study on a non-invasive, quick and inexpensive method for characterizing ES cell derived cardiomyocytes is described. This novel method of cardiomyocyte characterization is amenable to automation. Unlike aforementioned approaches, as investigated by other researchers, we have considered the entire beating segment of the mESC derived tissue for our analysis to ensure the simplicity of the procedure and to reveal more information from the large patch of differentiated beating cells.

We analyzed the changes in the total pixel intensities in the derivative images captured from *in vitro* beating tissues and converted it into the time and frequency domain intensity patterns which revealed information about cardiomyocyte beating patterns, their maturation and other characteristics. We have also investigated the possible application of this proposed non-invasive image analysis method in following the response of differentiated cardiomyocytes to different types of inotropic agents. The results showed that, the novel method can be used to investigate the response of cardiomyocytes to such agents and it exhibited the strength of the method for being applied in cardiac drug screening studies of differentiated cardiomyocytes.

2.1 Materials and Methods

2.1.1 Cell culture

Mouse ES cells B6G2 (Riken cell bank) were cultured in 5% CO_2 and 37 °C incubator on mitomycin C-treated STO (ECACC) feeders in medium containing DMEM high glucose (Nacalai Tesque) supplemented with 15% FBS (Gibco), 1 mM nonessential amino acids (NEAA, Invitrogen), 2 mM L-Glutamine (Invitrogen), 50 U mL^{-1} penicillin and 50 µg mL^{-1} streptomycin (Invitrogen), 0.1 µM β-mercaptoethanol (Invitrogen), and 1000 U mL^{-1} recombinant Leukemia Inhibitory Factor (LIF, Chemicon) with daily replenishment of fresh medium. STO cells (ECACC) were grown in 5% CO_2 and 37 °C incubator in medium containing DMEM high glucose (Nacalai Tesque) supplemented with 10% FBS (Gibco), 1 mM L-Glutamine (Invitrogen), 50 U mL^{-1} penicillin and 50 µg mL^{-1} streptomycin (Invitrogen) with daily medium replenishment. As they reached confluent stage, STO cells were exposed to 50 µg mL^{-1} Mitomycin C (Wako) for 2.15 h. The mitomycin C-treated MEF cells were washed in PBS, trypsinized and plated at 75000 cells cm^{-2} on gelatin-coated tissue culture dishes as feeder layer and incubated overnight before plating ES cells.

2.1.2 Hanging drop culture for EB formation

After 2-days in culture on the MEF feeder cells with change of medium on every day, mESC monolayer on feeder cells were trypsinized (0.05% Trypsin-EDTA, Invitrogen) to prepare single cell suspension and the cell number was counted manually using hemacytometer. The single cell suspension was used for hanging-drop cultures to form mES cell aggregates popularly known as embryoid bodies (EB) in differentiation medium which is

similar to mESC medium excluding LIF. On the inner side of the lid of 100 mm tissue culture dish (Iwaki), 50 to 60 droplets, 20 µl in volume containing 1000 cells per drop were kept. The dishes were filled with autoclaved Milli-Q water to avoid loss of nutrients through evaporation and the lid was placed so that the drops hang from the lid. After 72 h of incubation at 5% CO_2 and 37 °C, spherical EBs were formed (Fig. 1) and these 3-days old EBs were used for subsequent experiments.

2.1.3 Differentiation of ES cells to beating cardiomyocytes

EBs were collected and plated on 35 mm tissue culture dishes coated with 0.1% gelatin (Sigma). After attachment, EBs started growth and differentiation. Regular monitoring was done to observe for the initiation of beating. On the initiation of beating, beating videos were captured on day-8, day-10, day-11 and day-12 with a view to follow the beating tissue through the process of organization and maturation.

2.1.4 Drug Experiments

The effectiveness of the proposed image analysis method in monitoring the beating behavior of the differentiated cardiomyocytes was judged by subjecting the cells to three different chemicals *viz.* caffeine hydrate ($C_8H_{10}N_4O_2.H_2O$; Wako) at high concentration as negative inotropic agent, *p*-Hydroxyphenylacetamide ($C_8H_9NO_2$;Wako) as negative control, and calcium chloride dehydrate ($CaCl_2.H_2O$; Wako) as positive inotropic agent. In this experiment, the final concentrations of caffeine hydrate and calcium chloride dehydrate were

5 mM and for p-hydroxyphenylacetamide it was 1 mM. The stock solutions of all the three chemicals were made by dissolving them in autoclaved Milli-Q water, separately.

Caffeine hydrate is known for increasing the beat rate of cardiomyocytes at lower concentrations and for decreasing it and even stop it at high concentrations,[29-32] calcium chloride dehydrates can increase the heart rate[33] whereas heart rate remain indifferent to *p*-hyroxyphenylacetamide. For the experiment, after the prerecording of the beating video of differentiated cardiomyocytes on 35 mm dish, single drug was added to the medium to its final concentration, after 5 minutes of incubation the beating video was recorded again. The drug containing medium was then aspirated, cells were washed twice with fresh medium and incubated in fresh medium for 10 minutes to bring the cells back to the normal condition before subjecting them to other drugs in similar way.

2.1.5 Imaging of cardiomyocyte beating

A high-quality 8-bit video-rate digital color CCD camera (DP71, Olympus, Japan) (Olympus, DP71, JAPAN) was mounted on the inverted microscope (IX71, Olympus, JAPAN). The microscope was equipped with a stage top mini-incubator (TOKAI HIT, Japan) which maintained the temperature of culture dishes at 37 °C and CO_2 at 5% during imaging. The video was recorded with × 10 objective at 30 fps, 640 × 480 pixels (day-8) and at 15 fps, 720 × 480 pixels (other days) with 8 bit deepness in audio video interleave (.avi) format as sequential bright-field images. For day-8, the approximate total field of view in video images used for our analysis was 627 × 440 μm and for other days it was 877 × 657 μm. Imaging analysis was performed offline using an algorithm developed at our lab based on MATLAB.

2.1.6 Analysis of beating frequency

Video images of EB beating were pixel binned to quantify the intensity of video images at high-frame rate. The sequential image sets were decomposed from video image to extract derivative images for systolic and diastolic phases of beating (Fig 1 a, top panel).

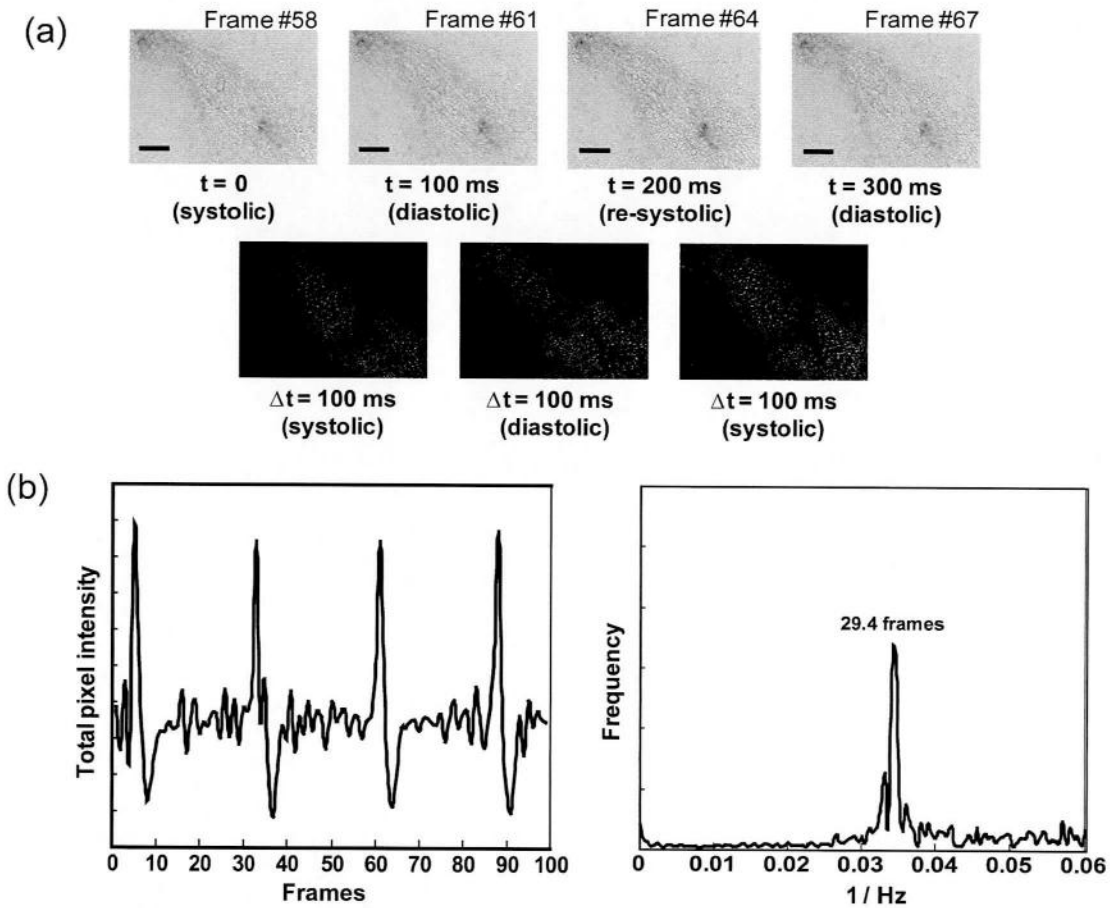

Figure 1 *The analytical method and representative instance of its application: (a) Derivative images were obtained by deducting pixel intensity of preceding frame from their subsequent frames, scale bar 100 μm. Original light microscopy video frames (upper panel) and derivative images (lower panel) representing systolic and diastolic phases of beating. The total pixel intensities were calculated based on these derivative images. (b) The resulting time domain (left) and the frequency domain (right) representation of pixel intensity (after FFT).*

The pixel intensity of each frame was differentiated by that of the next successive frame (Fig 1 a, bottom panel) and the intensity of all the pixels on each derivative image was summed up to attain the total intensity of each derivative frame, $dI_{x,y}(f)$ which is defined by:

$$dI_{x,y}^{(f)} = \sum_{x} \sum_{y} \frac{I_{x,y}^{f} - I_{x,y}^{f+1}}{dt}$$

Here, $I_{x,y}(f)$ is the pixel intensity of a frame (f) and dt is the time difference between two successive frames. The statistical analysis of the beating time was performed by computing the intervals between two successive local peaks. The threshold intensity for the local peaks were defined as the intensity in the range of 60 to 70% of maximum differentiated total pixel intensity, which was approximately 5 micro meter difference on still image. The maximum differentiated total pixel intensity was calculated under the signal to noise consideration. The algorithm for derivative imaging analysis and statistic interval analysis was developed at our laboratory using MATLAB (The MathWorks Inc., LA, USA). Fast Fourier Transform (FFT) analysis was carried out with commercialized scientific software (Igor Pro, USA) to obtain the power spectrum (Fig 1b). Since the FFT result of periodic function of spike data, in general, involves the several wave number domains, the result should be considered with the statistics of beating interval analysis.

2.2 Results

2.2.1 Beating periodicity and rhythm

As the 3-days old EBs were transferred to gelatin coated dishes, and LIF was removed from the growth medium, the cells from the EBs started proliferation and differentiation (Fig 2). Mesodermal cells of the EBs were differentiating towards cardiomyocytes which were

observed to beat on day-8. Due to the beating of cardiomyocytes, the time domain presentation of total pixel intensities showed the usual cyclic patterns of systolic and diastolic rhythms in beating cells (Fig 1b, left). From time domain of intensity variation, the regularity of intensity changes due to beating of cardiomyocytes was estimated. The patterns produced by this approach showed similarities, to some extent, to the beating patterns obtained through other recording methods, for example electrophysiological recording, patch-clamp measurement, Ca^{++} current recording etc.[34-40] The fast Fourier transformation yielded the frequency domain of beating, from which we calculated the time interval of beating and the major frequency or frequencies at which cells were synchronizing their beatings (Fig 2b, right). FFT graph showed major frequencies indicating the time interval of beating intensity maxima at about 29.4 frames. With 30 fps recordings, it gave the beating frequency of about 1 Hz i.e 60 beats per minute. This information was readily obtained using our method. Kojima et al [25, 41] reported a technique for the measurement spontaneous contraction rhythm of cultured cardiac myocytes by a phase contrast CCD video-image recording changes in the cross-sectional area of cardiac myocytes with beating followed by estimation of their beating frequency. Through further refining and investigation, this simple method will become useful, in some cases, as a valid alternative to complex, expensive, time consuming and expertise-oriented electrophysiological recordings.

2.2.2 Changes in cardiomyocyte beating with maturity

We recorded the video at the same beating location on day-8, day-10, day-11 and day-12 in order to monitor the changes in the beating pattern (Fig 3 second and third panels). The

time domain analysis presented non-uniform pixel intensity variation on day-8 and the frequency domain analysis showed the presence of several frequencies with low amplitudes.

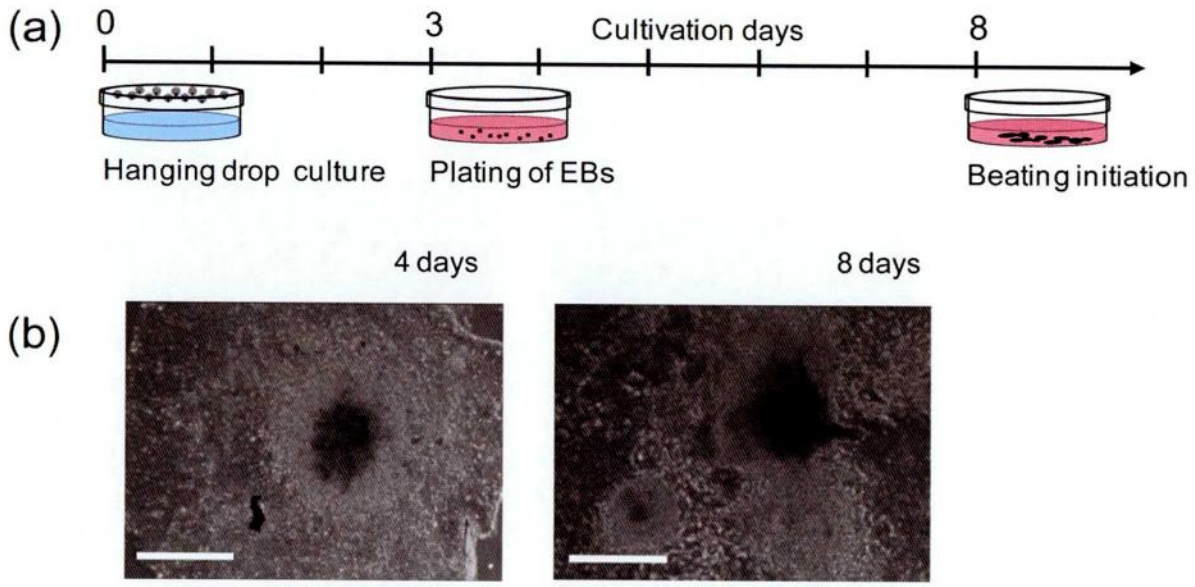

Figure 2 *The mESC differentiation into cardiac myocytes. (a) The time scale of cell and EB culture. (b) The growth of tissue from EB: 4- and 8-days after plating of EBs onto gelatin coated dishes, scale bar 200 μm.*

It was probably due to the initiation of beating in tiny patches of cells which were beating asynchronously each with its own unique frequency of beating. Based on this hypothesis, the number of beating patches at the location under observation was detected. On day-8, at the location we recorded gave six different frequencies on the FFT panel (Fig 3, third panel) indicating six distinct patches with definite beating frequencies.

From the amplitude of beating, one can estimate whether small or large numbers of cells are beating. From our recording, we observed small changes in the recorded intensities which indicated the presence of small number of beating cells in each patch. This assessment is an indicator of the efficiency of a differentiation protocol if the target cells are cardiomyocytes. On day-10, beating was much rhythmic and amplitude of pixel intensity was increased indicating the occurrence and progression of synchronization among the beating patches of cells. In FFT panel (Fig 3, third panel) for day-10, we located three distinct frequencies, which indicated better organization of beating tissue on the dish. On day-11, expectedly more organization happened and beating became faster, and the amplitude was more uniform. This result was also confirmed by FFT panel as it showed two distinct beating frequencies.

However, on day-12, though the beatings were distinctly visible, FFT graph was hazy but two peaks with one comprehensive frequency (Table 1) was obtained from the Gaussian fitting to the differential intensity distribution (Fig 3, fourth panel). This was either due to the growth of tissue over time which buried the beating cells underneath[42] or it was caused by the actual changes happened in the beating tissue after they crossed the optimal limit of growth and synchronization.[43, 44]

Table 1: Number of peaks from beating frequency histogram after Gaussian fit alongwith the number of comprehensive frequencies observed from FFT analysis.

	Day 8	Day 10	Day 11	Day 12
No. of peaks in beating histogram	N.A.	2 (250, 900)	2 (400, 750)	2 (740, 1250)
No. of comprehensive frequencies	1 (0.36)	4 (1.49, 0.84, 0.55, 0.42)	2 (0.58, 0.50)	1 (0.576)

2.2.3 Signal to noise ratio

We have tried to estimate the signal to noise ratio (SNR) of the signals we obtained (Fig 4). S/N ratio in the amplitude of positive peaks in the time domain presentation of the total pixel intensities indicated that on the day of initiation of beating, the noise level was high. We attributed it to the weak and patchy beating in the beginning which was interfered substantially by the background noise. As the beating tissue grown, more cells started beating and they became organized - giving more regular, rhythmic and strong beatings, SNR reached to almost six. Based on Rose criterion,[45] an SNR of five is considered good enough to distinguish image features at 100% certainty. Therefore, for evaluating rhythmic and stronger beating, on days after the initiation of beating, our method was proven efficient without implementation of any noise filtration algorithm.

2.2.4 Analysis of cardiomyocyte properties

In our analysis, the negative and positive total pixel intensities of the derivative images corresponded respectively to the systolic and diastolic phases of beating. The integration of the positive local peak corresponded to the size difference in systolic phase and that of the negative local peak intensity corresponded to the size difference in diastolic phase. Furthermore, the local peaks of small width with high intensities indicated the strong and well-synchronized beating. The distance from one systolic peak to another systolic peak indicated the beating interval and number of systolic peaks per unit time indicated the beating frequency. Based on our approach we analyzed beating properties - initiation of beating, beating frequency, strength of beating, number of distinctly beating patches etc.

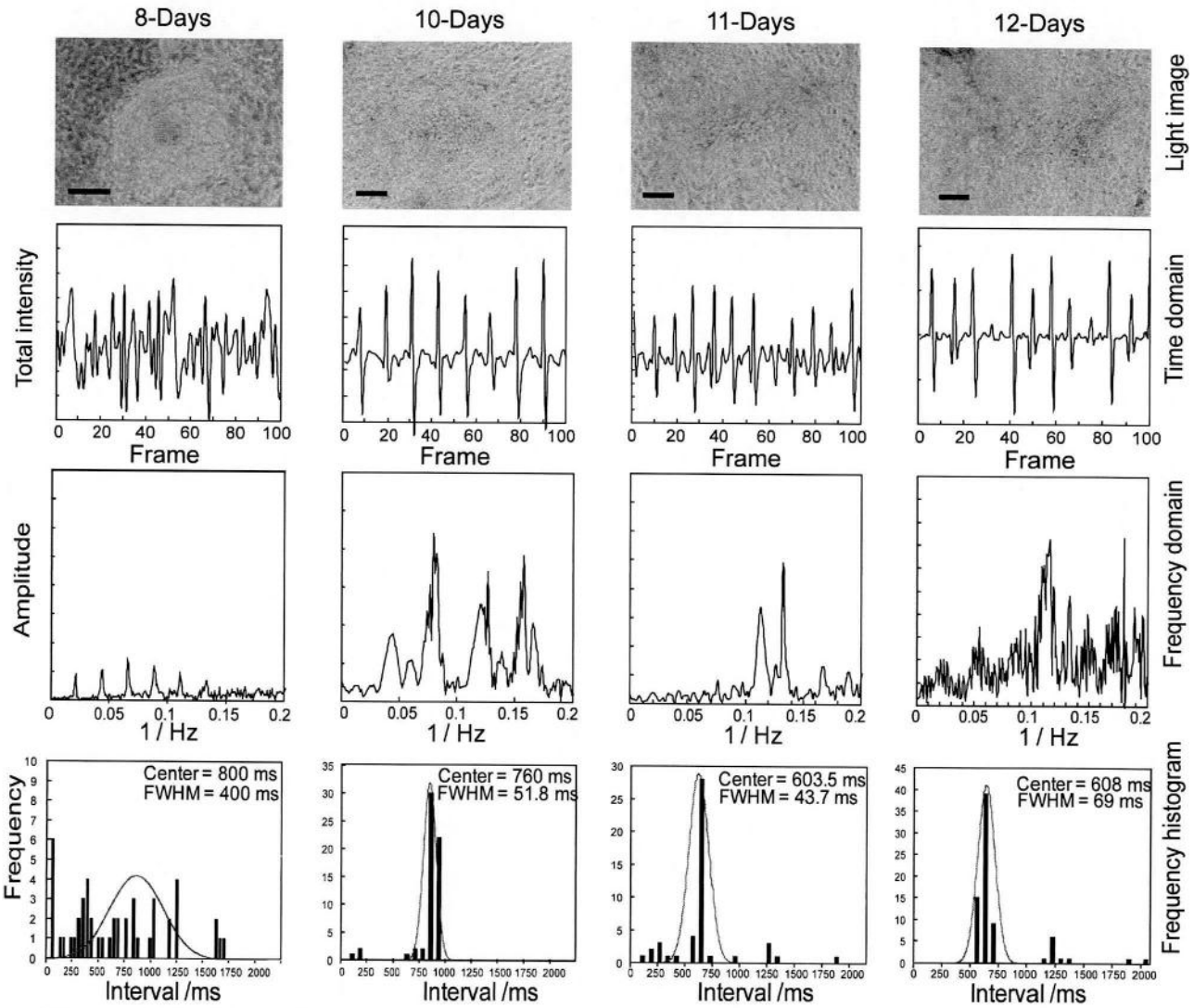

Figure 3 *Analysis of beating properties based on time and frequency domains. The top panel shows the growth of cells with days in culture, scale bar 100 μm. The second panel is time domain variation in beating intensity where the rhythmic pattern is visible. Beating interval and beating rhythm along with organization of cells is evident from it. The third panel shows the FFT analysis and gives the presence of major frequencies in the beating tissue and indicates number of places with distinct beating on the tissue. The last panel gives the frequency distribution of different time intervals at which there had been some rhythmic activities. After Gaussian fitting, we obtained the comprehensive number of frequencies present.*

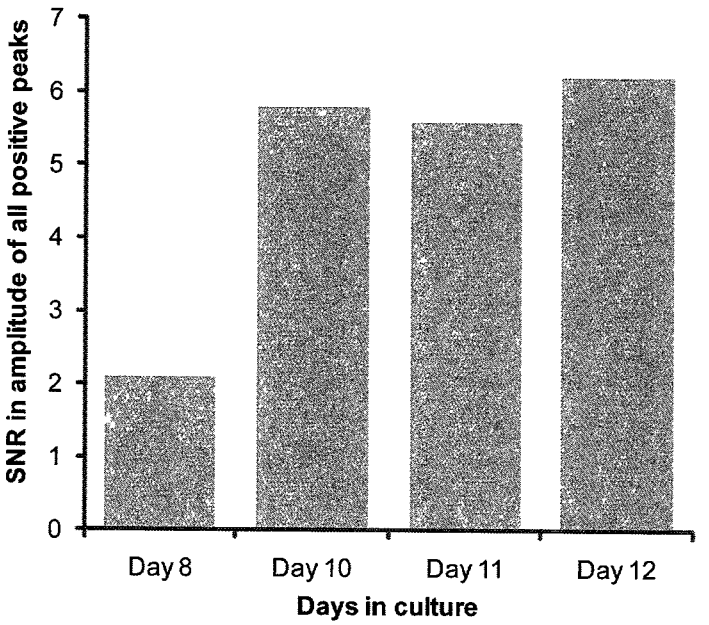

Figure 4 *Signal to noise ratio (SNR) in the amplitude of positive peaks and beating intervals. Improvement in SNR over time with progressive organization and maturity of beating cardiac myocytes.*

Estimation of these properties is fundamental to the characterization of differentiated cardiomyocytes along with their molecular and functional characterization. Initiation of beating was marked by the start of intensity fluctuation over the derivative frames from the video image. The strength of beating was indicated by the amplitude of the total pixel intensity and the rate of beating was calculated from the interval between the peaks on the time domain presentation of total pixel intensity. As evident from Fig 3 (second panel), the beating gained strength and became faster on the following day after the initiation of beating and with organization of beating tissue, the beating rate increased but the strength remained almost similar. The presence of couple or multiple peaks on the frequency domain presentation (Fig 3, third panel) and its confirmation from numerical analysis (Table 1) revealed the presence of differential beating within the tissue. The presence of sub-

populations of synchronizing contractile cardiomyocytes with distinct beating frequencies in the same patch of beating tissue was responsible for this observation.

2.2.5 Maturation of beating cardiomyocytes

The analytical method that we proposed here could follow the maturation of differentiating cardiac mycoytes into mature cardiac tissue. Maturity assessment is necessary to decide the right time for transplantation of in-vitro grown cardiac cells in the form of cell sheet or in any other means for regenerative therapy. We followed the changes in the pattern of beating from the time or frequency domain presentation (Fig 3). For the cultures we used in developing our method, we concluded that on day-3 following the initiation of beating, the beating cardiomyocytes consolidated their rhythm and strength. This, to our view, was the optimal performance of the beating cells *in vitro*; indicating their maturity and it also indicated that these cells are ready for being processed further. This time line varies from cell-to-cell, culture-to-culture and among different cell culture condition but our approach is suitable to follow the growth of ES derived beating cardiomyocytes towards the optimum maturity.

2.2.6 Response to drugs

In order to demonstrate the ability of our proposed image analysis method in evaluating the changes in beating behavior of differentiated cardiomyocytes to external stimulation, we subjected them to positive, neutral and negative inotropic drugs - high concentration of caffeine hydrate (5 mM), *p*-hydroxyacetamide and calcium chloride, respectively. As seen in

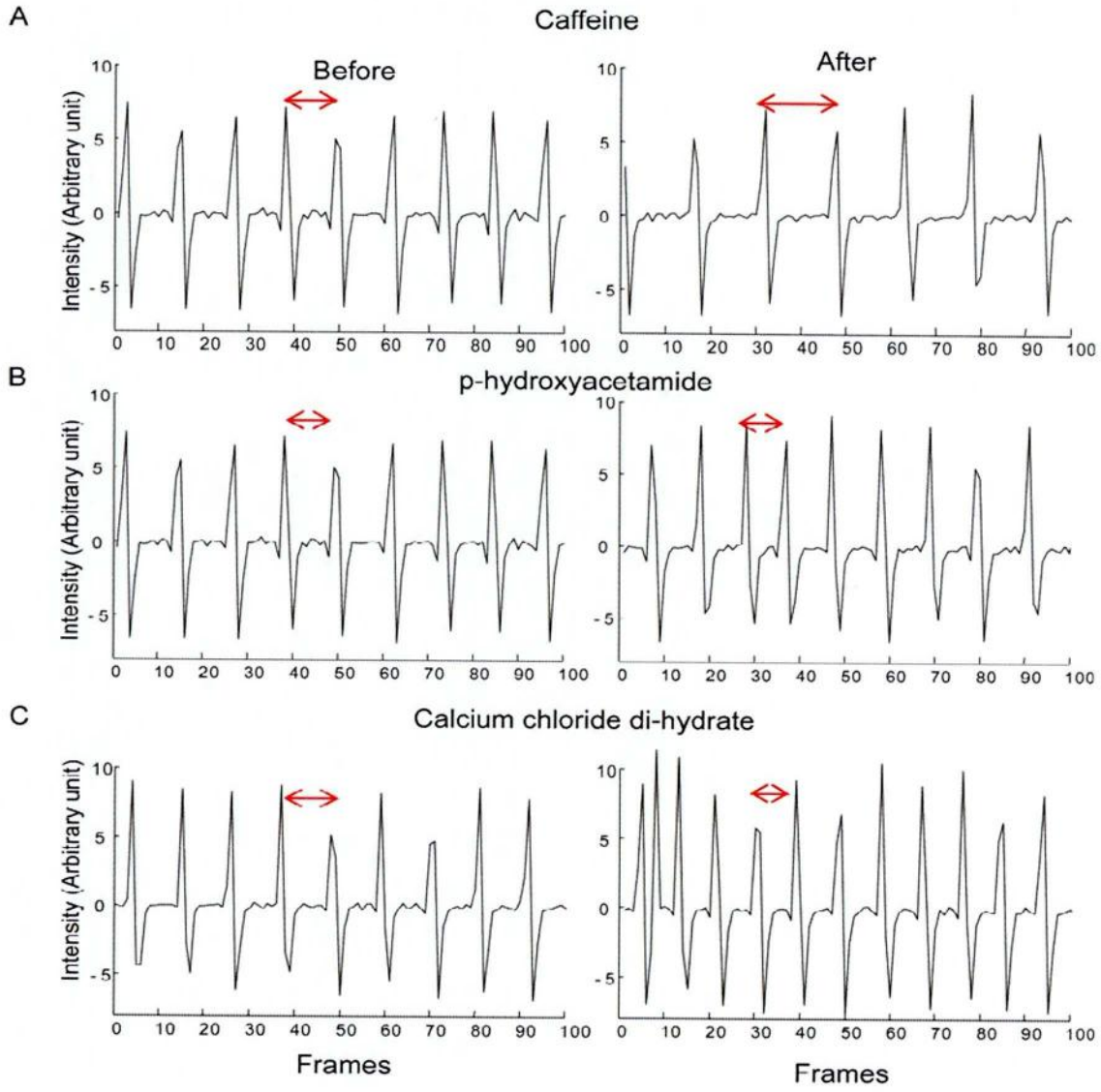

Figure 5 *Response of ES derived cardiomyocytes to inotropic substances. Reduction in beating frequency due to the exposure of cells to 5 mM of caffeine monohydrate which is negative inotropic substance at high concentration (a), non-inotrpic p-hydroxyacetamide did not alter the beating frequency or strength (b) and the presence of positive inotropic calcium chloride di-hydrate in the culture medium enhanced both the frequency and the strength of beating (c). Frequency is expressed by number of peaks in time domain intensity profile and the amplitude of total intensity in beating video images indicated the strength.*

Figure 5, on addition to the medium, expectedly, caffeine slowed the beating rate down from 81 beat per minute (BPM) to 54 beat per minute; *p*-hydroxyacetamide did not affect beating behavior and calcium chloride made the cells to beat faster (from 81 BPM to 108 BPM) and stronger. When we compared such results to the manual counting from beating video, we got conformity between manual counting and the image analysis methods. These results are promising in the sense that, this simple technique we propose is capable of being used for primary screening of inotropic substances.

2.3 Discussion

Extensive research is underway to enhance the differentiation efficiency of ES cells to cardiomyocytes which is at present in the range of 10% of the total differentiated cells.[46] With the advent of regenerative medicine for cardiac problems, clinical grade supply of well characterized cardiomyocytes obtained from the differentiation of ES or iPS cells, is becoming an important issue.[47] There are alternative and complementary approaches for characterization of which few are based on optical microscopic video image analysis. Here we reported a non-invasive video image based characterization method and applied it to evaluate the beating of mES derived cardiac mycoytes. A similar approach for cardiac beating analysis was reported earlier by Weisense et al.[25] But following the contraction of one or a few specific cardiac myocyte/s on layered in vitro tissue is difficult, which made these approaches unreliable and complex specifically if it is not in primary cardiac myocyte culture. Stummann et al[24] reported a video movie based beating analysis software where they considered certain points on the beating cardiomyocytes for monitoring based on pixel intensity variation due to beating unlike our approach of considering the whole beating patch for monitoring. Another video image based contraction measurement approach was also

reported by Wassermann and Mejail[26] which also followed the membrane contraction with beating to determine the frequency. Fink et al[48] also reported a frame brightness algorithm and changing pixel intensity algorithm based heartbeat parameter detection approach for drosophila, zebrafish and embryonic mouse.

Our approach is better fitted to in-vitro beating tissues obtained from either primary cardiomyocyte culture or from the differentiation of ES or iPS cells. As we used the method for characterizing differentiated cardiomyocytes form mESC where we do not have control over the number of cells in a beating area, we could not compare the ability of our approach in following the beating of very small number of contractile cells. But from our results, we predict that this approach can be used for small number of beating cells by improving the noise handling. In case of drug exposure, through our image analysis method, we observed the expected behavior for all the three chemicals to which we exposed cardiomyocytes. For high concentration of caffeine, we observed the cells to reduce beating rate which conform to similar results reported by Satoh et al[30] whereas for calcium chloride, as expected,[33] the beating became faster.

2.4 Conclusion

A non invasive image analysis method based on the temporal changes in the total intensity in video images of differentiated cardiomyocytes from mouse embryonic stem cells has been developed. The method was successfully applied in monitoring the initiation, propagation and maturation of beating of mESC derived cardiac muscle cells. Moreover, using our method - the beating frequency, the strength of beating, number of distinctly beating patches at a certain location on the culture dish could be obtained. Moreover, we used

our proposed method in evaluating the response of differentiated cells to positive and negative inotropic agents. All of these are important in evaluating stem cell derived cardiomyocytes for subsequent applications after differentiation. We hope this method will be adopted as a handy approach for the characterization of cardiomyocytes derived *in vitro* from the differentiation of ES or iPS.

2.5 References

[1] E. M. Jolicoeur, C. B. Granger, J. L. Fakunding, S. C. Mockrin, S. M. Grant, S. G. Ellis, R. D. Weisel and M. A. Goodell, *American Heart Journal*, 2007, **153**, 732-742.

[2] L. Liao and R. Chunhua Zhao, *Stem Cells and Development*, 2008, **17**, 613-618.

[3] A. Behfar, C. Perez-Terzic, R. S. Faustino, D. K. Arrell, D. M. Hodgson, S. Yamada, M. Puceat, N. Niederlander, A. E. Alekseev, L. V. Zingman and A. Terzic, *Journal of Experimental Medicine*, 2007, **204**, 405-420.

[4] K. Takahashi, K. Tanabe, M. Ohnuki, M. Narita, T. Ichisaka, K. Tomoda and S. Yamanaka, *Cell*, 2007.

[5] K. Okita, T. Ichisaka and S. Yamanaka, *Nature*, 2007, **448**, 313-317.

[6] C. Mauritz, K. Schwanke, M. Reppel, S. Neef, K. Katsirntaki, L. S. Maier, F. Nguemo, S. Menke, M. Haustein, J. Hescheler, G. Hasenfuss and U. Martin, *Circulation*, 2008, **118**, 507-517.

[7] Y. Ohno, S. Yuasa, T. Onizuka, T. Egashira, K. Shimoji, S. H. Yoon, T. Arai, J. Endo, T. Kageyama and H. Chen, *Circulation*, 2008, **118**.

[8] G. Narazaki, H. Uosaki, M. Teranishi, K. Okita, B. Kim, S. Matsuoka, S. Yamanaka and J. K. Yamashita, *Circulation*, 2008, **118**, 498-506.

[9] S. Nishikawa, R. A. Goldstein and C. R. Nierras, *Nature Reviews Molecular Cell Biology*, 2008.

[10] E. R. Andersson and U. Lendahl, *Journal of Internal Medicine*, 2009, **266**, 303-310.

[11] T. Yamada, M. Yoshikawa, M. Takaki, S. Torihashi, Y. Kato, Y. Nakajima, S. Ishizaka and Y. Tsunoda, *Stem Cells*, 2002, **20**, 41.

[12] J. E. Locke, Z. Sun, D. S. Warren, T. P. Sheets, H. Holzer, M. J. Shamblott, R. A. Montgomery and A. M. Cameron, *Annals of Surgery*, 2008, **248**, 487-493.

[13] C. E. Murry and G. Keller, *Cell*, 2008, **132**, 661-680.

[14] C. Mummery, D. Ward, C. E. Van den Brink, S. D. Bird, P. A. Doevendans, T. Opthof, A. B. de la Riviere, L. Tertoolen, M. van der Heyden and M. Pera, *Journal of Anatomy*, 2002, **200**, 233.

[15] K. Tashiro, M. Inamura, K. Kawabata, F. Sakurai, K. Yamanishi, T. Hayakawa and H. Mizuguchi, *Stem Cells*, 2009, **27**, 1802.

[16] S. M. Chambers, C. A. Fasano, E. P. Papapetrou, M. Tomishima, M. Sadelain and L. Studer, *Nature Biotechnology*, 2009, **27**, 275-280.

[17] D. Zhang, W. Jiang, M. Liu, X. Sui, X. Yin, S. Chen, Y. Shi and H. Deng, *Cell Research*, **19**, 429-438.

[18] J. B. Stephen, W. R. Robert, L. S. Anita, B. Meinrad, F. B. John and C. P. Andrew, *Differentiation*, 2007, **75**, 337-349.

[19] K. Strong, C. Mathers and R. Bonita, *The Lancet Neurology*, 2007, **6**, 182 - 187.

[20] T. J. Gardner, *Circulation*, 2009, **119**, 1838-1841.

[21] K. R. Boheler, J. Czyz, D. Tweedie, H. T. Yang, S. V. Anisimov and A. M. Wobus, *Circulation research*, 2002, **91**, 189.

[22] K. Jungling, K. Nagler, F. Pfrieger and K. Gottmann, *The FASEB Journal*, 2003, 301181.

[23] B. C. Heng, H. K. Haider, E. K.-W. Sim, T. Cao and S. C. Ng, *Cardiovascular Research*, 2004, **62**, 34-42.

[24] T. C. Stummann, M. Wronski, T. Sobanski, B. Kumpfmueller, L. Hareng, S. Bremer and M. P. Whelan, *ASSAY and Drug Development Technologies*, 2008, **6**, 375-385.

[25] D. Weisensee, J. Bereiter-Hahn, W. Schoeppe and I. Löw-Friedrich, *International Journal of Immunopharmacology*, 1993, **15**, 581-587.

[26] D. Wassermann and M. Mejail, in *Progress in Pattern Recognition, Image Analysis and Applications*, Editon edn., 2005, pp. 420-430.

[27] P. Sasse, J. Zhang, L. Cleemann, M. Morad, J. Hescheler and B. K. Fleischmann, *Journal of General Physiology*, 2007, **130**, 133.

[28] J. Gorelik, N. N. Ali, A. I. Shevchuk, M. Lab, C. Williamson, S. E. Harding and Y. E. Korchev, *Tissue Engineering*, 2006, **12**, 657-664.

[29] M. G. Myers, *Archives of Internal Medicine*, 1988, **148**, 1189-1193.

[30] H. Satoh, *General Pharmacology: The Vascular System*, 1993, **24**, 1223-1230.

[31] J. M. Cooper, *Circulation*, 2005, **112**, e299-301.

[32] K. Somei and W. Riker, *The Japanese Journal of Pharmacology*, 1991, **57**, 25-35.

[33] J. Lipman, I. Jardine, C. Roos and L. Dreosti, *Intensive Care Medicine*, 1982, **8**, 55-57.

[34] M. Doss, J. Winkler, S. Chen, R. Hippler-Altenburg, I. Sotiriadou, M. Halbach, K. Pfannkuche, H. Liang, H. Schulz, O. Hummel, N. Hubner, R. Rottscheidt, J. Hescheler and A. Sachinidis, *Genome Biology*, 2007, **8**, R56.

[35] J. Riistama, J. Vaisanen, S. Heinisuo, J. Lekkala and J. Kaihilahti, Engineering in Medicine and Biology Society, 2007. 29th Annual International Conference of the IEEE, 2007.

[36] M. Halbach, K. Pfannkuche, F. Pillekamp, A. Ziomka, T. Hannes, M. Reppel, J. Hescheler and J. Muller-Ehmsen, *Circulation Research*, 2007, **101**, 484-492.

[37] M. H. Malone, N. Sciaky, L. Stalheim, K. M. Hahn, E. Linney and G. L. Johnson, *BMC biotechnology*, 2007, **7**, 40.

[38] B. Fleischmann, Y. Duan, Y. Fan, T. Schoneberg, A. Ehlich, N. Lenka, S. Viatchenko-Karpinski, L. Pott, J. Hescheler and B. Fakler, *Journal of Clinical Investigation*, 2004, **114**, 994-1001.

[39] A. Verkerk, R. Wilders, M. van Borren and H. Tan, *International Journal of Biological Sciences*, 2009, **5**, 201.

[40] C. Herr, N. Smyth, S. Ullrich, F. Yun, P. Sasse, J. Hescheler, B. Fleischmann, K. Lasek, K. Brixius, R. H. G. Schwinger, R. Fassler, R. Schroder and A. A. Noegel, *Molecular and Cellular Biology*, 2001, **21**, 4119-4128.

[41] K. Kojima, T. Kaneko and K. Yasuda, *Journal of Nanobiotechnology*, 2005, **3**, 4.

[42] N. Ali, X. Xu, M. Brito-Martins, P. Poole-Wilson, S. Harding and S. Fuller, *Basic Research in Cardiology*, 2004, **99**, 382-391.

[43] F. E. Kapucu, M. Pekkanen-Mattila, V. Kujala, J. Viik, K. Aalto-Setelä, E. Kerkelä, J. M. A. Tanskanen and J. Hyttinen, in *4th European Conference of the International Federation for Medical and Biological Engineering*, Editon edn., 2009, pp. 8-11.

[44] C. Kim, M. Majdi, P. Xia, K. Wei, M. Talantova, S. Spiering, B. Nelson, M. Mercola and H.-s. V. Chen, *Stem Cells and Development*, **0**.

[45] J. Bushberg, J. Seibert, E. Leidholdt Jr, J. Boone and E. Goldschmidt Jr, *Medical Physics*, 2003, **30**, 1936.

[46] M. Muller, B. Fleischmann, S. Selbert, G. Ji, E. Endl, G. Middeler, O. Muller, P. Schlenke, S. Frese and A. Wobus, *The FASEB Journal*, 2000, **14**, 2540.

[47] D. C. Kirouac and P. W. Zandstra, 2008, **3**, 369-381.

[48] M. Fink, C. Callol-Massot, A. Chu, P. Ruiz-Lozano, J. C. I. Belmonte, W. Giles, R. Bodmer and K. Ocorr, *BioTechniques*, 2009, **46**, 101–113.

Chapter: 3

Effects of the exposure to functionalized multiwalled carbon nanotubes on embryoid body formation from mouse embryonic stem cells, their subsequent growth and cardiomyogenic differentiation

Chapter summary

Among the directed differentiation strategies for embryonic stem cells, hanging drop embryoid body (EB) formation - as the first step of stem cell organization into the three germ layers - has become widely accepted. On the other hand, meso-scale materials such as carbon nanotubes are considered as potential effecter in guiding ES cells differentiation. We have tried to combine these two approaches by exposing the cells to purified and carboxylate functionalized MWCNTs (f-MWCNT) during EB formation. Two different dispersants - Milli-Q water and 0.1% gelatin solution were used to prepare 0.3 mg of f-MWCNT per ml of dispersion, referred to as W-CNT and G-CNT, respectively. The mouse ES cell suspensions with desired cell density was supplemented with 1.5, 3, 7.5, 15 and 30 $\mu g\ ml^{-1}$ of G-CNt and W-CNT separately and kept for hanging drop EB formation. Short and long term toxicities to such exposure were measured by MTS assay and EBs were analyzed for their morphology. We observed that CNT exposed EBs were bigger and more spherical and we did not observe cytotoxic role of CNT on EBs. Upon plating, EBs showed normal growth and in TEM observation after one week of growth, negative effect of CNT on the grown tissue was not seen, traces of CNT like structures were found in or at the edges of secondary lysozomes, prominently in W-CNT EBs. EB formation dynamics by continuous video monitoring exhibited relatively quicker EB formation in f-MWCNT EB without any visible toxic effect. The tissue growth and cystic body formation were normal.. Beating initiated earlier in f-MWCNT EBs compared to control and they showed lower beating rates with stronger beating. Some glia like cells were also evident. Between two dispersants, gelatin was better for EB health and the subsequent cell growth. Our results on CNT nonmaterial and ES cell interaction elucidates the usability of f-MWCNT for similar applications with the necessity of further investigations.

3.0 Introduction

Guided differentiation of embryonic stem cells (ESC) and recently introduced induced pluripotent stem cells (iPSC) [1-3] into desired terminal cell types, for instance - cardiomyocytes, neurons, pancreatic beta cells etc., is one of the prime challenges in stem cell research [4] for making practical therapeutic interventions of stem cells in the emerging field of regenerative medicine [5-7]. Several approaches towards controlling the epigenetic events for guiding the pluripotent cells into desired lineage have been reported [8-11]. However, aggregation of ESC or iPSC into three dimensional spherical embryoid bodies (EB) consisting of three germ layers akin to the primary gastrulation stages of in-vivo embryo development has become a common protocol to this end [12-14]. There is remarkable diversity in platforms for hanging drop based EB formation [15-18] but classical hanging drop culture on the inner surface of the lids of tissue culture dishes has remained the most widely adopted alternative.

On the other hand, some researchers are trying small molecule or meso-scale nanomaterials in modulating the epigenetic fate of ES or iPS cells with limited success [19-21]. We also believe that, nanomaterial interaction with pluripotent cells worth exploring in stem cell research. Metallic and non-metallic, organic and inorganic nanoparticles have been tried in the field of cellular biology for different purposes [22-28]. In this regard functionalized carbon nanotubes (CNT) worth special attentions owing to the exceptional properties they possess - the high aspect ratio with unique mechanical strength which helps CNTs in nano-scale mechanical modification of growth environments, the metal like conductivity of CNTs makes them favorable for being used in stem cell differentiation studies where electro-active cardiac muscle cells or neuronal cells are the targeted terminal cells. There is still widespread concern about the toxicity of carbon nanotubes [29, 30] to cells and tissues and their biodegradability but the current spree of reports [31-39]

are easing those concerns and help in augmenting the interest in purified and functionalized CNTs for varied purposes involving living cells [37, 40]. Moreover, it has also been suggested that, in the long run – functionalized CNTs are amenable to enzymatic degradations which involves peroxidases, for example, myeloperoxidase [41].

In response to recent findings regarding CNT biocompatibility, we have decided to investigate the role of carboxylate functionalized multiwall carbon nanotubes (f-MWCNTs) in the formation of embryoid bodies from mouse embryonic stem (mES) cells during classical hanging drop culture. For this we have supplemented the mES cell suspended in differentiation medium with f-MWCNT dispersions in gelatin and in water which will henceforth be called G-CNT and W-CNT, respectively. The cells in medium containing f-MWCNT supplements were used for the formation of embryoid bodies (EB) in traditional hanging drop culture on the inner lid of the polystyrene tissue culture dishes. We investigated the toxicity of f-MWCNT on embryoid bodies, the dynamics of EB formation by continuous monitoring along with the analysis of the morphology of formed EBs. The subsequent growth of cells from such EBs were investigated and after one week of growth TEM analysis was done to confirm the effect of f-MWCNT at the developmental stages of tissue from such EBs. We observed that instead of being toxic, f-MWCNTs favored the formations of more spherical and bigger embryoid bodies. Moreover, we confirmed the uptake and intracellular localization of f-MWCNT from TEM micrographs taken after prolonged culture of f-MWCNT EBs on tissue culture dishes. We expected that electrical conductivity of f-MWCNT fibrous structures embodied into the EBs may promote differentiation into cardimyogenic or neuronal lineages. We observed synchronously beating functional cardiomyocytes from such EBs which has been confirmed by method we reported earlier [42]. This, to the best of our knowledge, is the first report on the role of f-

MWCNTs in mES cell aggregation and their subsequent differentiation and this will promote deeper investigations into the interaction between functionalized CNTs in different dispersing agents with embryonic and non-embryonic stem cells.

3.1 Materials and methods

3.1.1 Purification and functionalization of MWCNT

MWCNT (Wako, Japan) samples were purified and functionalized according to method described elsewhere [43] with little modifications. In brief, MWCNTs dispersion in 5M HNO_3 was heated at 180°C in hot oil bath under refluxing condition for 48 hours till all the acids were vaporized. This purified the CNTs from other carbon allotrops and removed the metallic catalyst residues while at the same time oxidation by strong acid generated surface functional group (-COOH) on MWCNT surface. Carboxylate modified CNTs are reported to be more amenable to enzymatic degradation by peroxidases [41] and ensure better distribution in dispersion medium. The surface functionalization of MWCNTs was confirmed by Fourier transform infrared (FT-IR) spectroscopy. Surface-oxidized MWCNT was collected by repeated washes using Milli-Q water and filtering them through 0.65 μm Durapore membrane (Millipore) using KG-47 vacuum filtration apparatus (Adventec, Japan) till a neutral pH was obtained. The f-MWCNT sample was dried in vacuum for 24 hours before use.

3.1.2 Preparation of MWCNT dispersion in gelatin

Dispersions of purified f-MWCNTs were prepared in two different dispersant medium – in Milli-Q water (W-CNT) and in 0.1% (w/v) gelatin solution in ultrapure water followed by autoclaving of the dispersions at 120°C for 20 minutes. In both the cases, 0.3 mg of f-MWCNT

per ml of water or gelatin solution was dispersed by prolonged sonication at 35 kHz in UT-205HS sonicator (Sharp, Japan). In case of W-CNT, f-MWNT remained well dispersed for almost a day while in case of G-CNT, CNT remained well dispersed throughout.

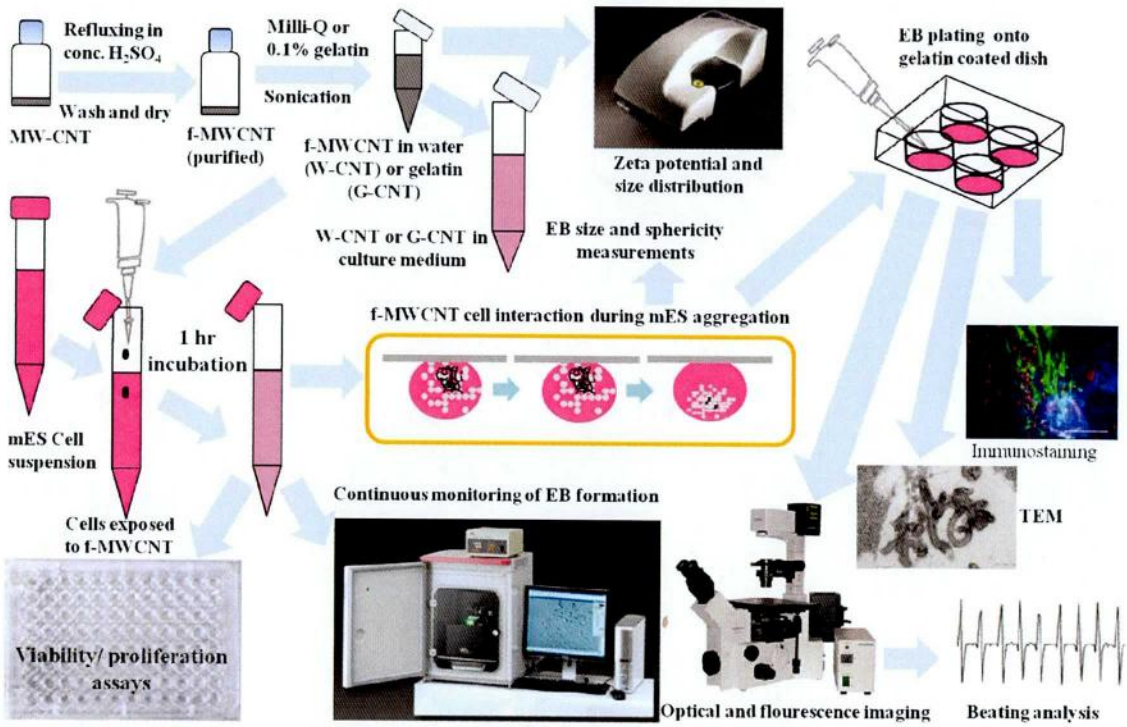

Scheme 1 The methodology of the research in schematic presentation.

3.1.3 Size distribution and zeta potential measurement

We measured the size distribution and the zeta potential (ζ) of the G-CNT and W-CNT dispersions by Zetasizer Nano ZS (Malvern, Worcestershire, UK) equipped with Dispersion Technology Software (DTS) version 5.2. The f-MWCNT dispersion in water and 0.1% gelatin were sonicated before loading the samples into separate disposable capillary cell (DTS1060) for the measurement.

3.1.4 ES cell culture

ES cells were grown according to protocol established protocol [42], in brief, 10% FBS (Gibco), 2 mM L-glutamine (Invitrogen), 50 U ml^{-1} penicillin with 50 μg ml^{-1} streptomycin (Invitrogen) supplemented DMEM high glucose (Nacalai Tesque) was used to culture STO (ECACC) cells at 37°C and 5% CO_2 in humidified incubator, media was changed daily. STO cells, at confluence stage, were exposed to 10 µg ml^{-1} Mitomycin C (Wako) for 2.15 h, trypsinized, washed in PBS and plated at 75000 cells/cm^2 as feeder layer onto gelatin-coated tissue culture dishes and incubated overnight before plating ES cells. Mouse ES cells (B6G2, Riken cell bank) were cultured on mitomycin C-treated STO (ECACC) feeders in medium containing DMEM high glucose (Nacalai Tesque) supplemented with 15% FBS (Gibco), 0.1 mM nonessential amino acids (NEAA, Invitrogen), 2 mM L-glutamine (Invitrogen), 50 U/ml penicillin and 50 μg/ml streptomycin (Invitrogen), 0.1 μM β-mercaptoethanol (Invitrogen), and 1000 U/ml recombinant Leukemia inhibitory factor (LIF, Chemicon). Dishes were incubated in humidified incubator at 5% CO_2 and 37 °C with daily replenishment of fresh medium. B6G2 cells express green fluorescent protein (GFP) ubiquitously under beta-actin promoter and helps monitoring the growth of tissue from such cells by their characteristic green fluorescence [44].

3.1.5 MTS assay

In order to assess the toxicity of W-CNT and G-CNT on mES cells used for the formation of EBs, cells treated with 3 and 15 µg of W-CNT and G-CNT dispersions per milliliter of cell suspension were incubated for one hour. The cell viability and cell proliferation were studied in 96-well plate using CellTiter 96® AQ_{ueous} One Solution (Promega, WI, USA) according to the manufacturer's instructions. In this assay, metabolically active cells reduce MTS tetrazolium

compound into colored and medium soluble formazan through NADPH or NADH produced by mitochondrial dehydrogenase enzymes. The concentration of formazan which is directly proportional to the number of viable cells was measured from the absorbance at 490 nm using a 96-well microplate reader (SH-1000, Corona Electronics, Ibaraki, Japan). In case of viability assay, after one hour of incubation with CNT, we added 20 µl of MTS reagent per well of 96-well plate and measured the formazan absorbance each hour for four hours. The absorbances were normalized with respect to the blank medium and expressed as the percentages of absorbance from cells not exposed to f-MWCNT *i.e.* control. On the other hand, cell proliferation was studied by addition of MTS reagent to f-MWCNT exposed cells on day 0, day 1, day 2 and day 3 after exposure. For each day, after one hour of incubation with the assay reagent, absorbances were measured, normalized with respect to blank medium and expressed as the percentages of day 0 measurements.

3.1.6 Hanging drop EB formation in medium supplemented with CNT dispersion in gelatin

Mouse ES cell monolayer on feeder cells were trypsinized (0.05% Trypsin-EDTA, Invitrogen) after 2 days in culture to prepare single cell suspension, cell number was counted. Hanging-drop cultures to form mES cell aggregates popularly known as embryoid bodies (EB) was then done using the single cell suspension in differentiation medium i.e. mESC medium excluding LIF. Before putting the cells for hanging drop, cells were exposed to W-CNT and G-CNT at five different concentrations *viz* 5, 10, 25, 50 and 100 µl of CNT dispersion per milliliter of cell suspension and incubation was done at 37°C for one hour at 37°C in humidified incubator with 5% CO_2. The final concentration of f–MWCNT in the cell suspensions became 1.5, 3, 7.5, 15 and 30 µg of f-MWCNT per ml of cell suspension, respectively. After f-MWCNT exposure

and incubation, 50 to 60 hanging drops, each with 20 µl of cell suspension containing 1000 cells per drop were kept on the inner side of the lid of 100 mm tissue culture dish (Iwaki). The dishes were filled with autoclaved Milli-Q water to avoid evaporation induced reduction of droplet volume. After 96 h of incubation in humidified incubator at 5% CO_2 and 37 °C, EBs formed.

3.1.7 Continuous monitoring of EB formation

The dynamics of EB formation in presence of f-MWCNT in the cell suspension was investigated by continuous monitoring using cultured cell monitoring system CCM1.4XYZ/CO_2 (Astec, Fukoka, Japan) on a round bottom ultra low attachment 96-well plate (no. MS-9096U, Sumitomo Bakelite, Akita, Japan) using a × 10 objective lens, images were taken at the centre of the wells at an interval of five minutes for 36 hrs. The illumination was done by an LED light source which minimized the effect of repeated exposure of cells to illumination. In this continuous monitoring experiment, we exposed mES cells suspension to 50 µl of W-CNT which was equivalent to 15 µg of f-MWCNT per ml of cell suspension. We have used 2000 cells per well in 100 ml of LIF free medium. In case of hanging drop cultures were 20 µl droplets were used, the evaporation was taken care of by the water on the dish whereas in the continuous monitoring experiment, we optimized the amount of cell culture medium to 100 µl in order to minimize evaporation from wells of the round bottom 96-well plate while keeping the volume optimum for cell aggregation.

3.1.8 EB characterization

Images of EBs, formed without nanomaterials (*i.e.* control) or with different concentrations of the nanomaterials *viz* 1.5, 3, 7.5, 15 and 30 µg ml^{-1} of G-CNT and W-CNT per ml of cell suspension, were taken with × 10 objective lens using the IX70 light microscope (Olympus Co.,

Tokyo, Japan) where each hanging drop, for EB formation, contained 1000 cells per 20 µl of cell suspension. The algorithm for image analysis was developed at our laboratory using MATLAB (The MathWorks Inc., LA, USA). Images were analyzed to obtain the EB size distribution in terms of average EB diameter. Based on the fitting of EB outlines to elliptical shape, we obtained the semi-major (a) and semi-minor axes (b) of the EBs and then Wadell's formula (Ref Khademhosseini paper) was employed to calculate the sphercity (Ψ) as

$$\Psi\ (sphericity) = \frac{2\sqrt[3]{ab^2}}{a + \frac{b^2}{\sqrt{a^2+b^2}} \ln\left(\frac{a+\sqrt{a^2-b^2}}{b}\right)}$$

3.1.9 EB growth and differentiation

After four days in hanging drop culture, f-MWCNT containing EBs were plated onto 0.1% gelatin (w/v) coated dishes. The subsequent growth, formation of cystic body structures and the differentiation were monitored on a IX70 light microscope (Olympus Co., Tokyo, Japan). After the initiation of beating, video images were recorded to yield the beating pattern following the method reported earlier [42]. In brief, the pixel intensities in the video images were quantified by pixel binning at high frame which gave total pixel intensities of individual frames. The differential pixel intensities of successive frames were obtained and the total intensities of the derivative images were plotted against time to obtain the systolic and diastolic intensity variations *i.e.* the beating pattern. In this report we did not use any filtering to cancel out the apparent noise as the peaks were clearly discernible. In the beating pattern obtained, the number of peaks over time gave the rate of beating and the amplitude gave the strength of beating.

3.1.10 TEM

Five days old EBs formed from cell suspensions supplemented with G-CNT and W-CNT at a concentration of 15 µg per milliliter of cell suspension were transferred to gelatin coated dishes and grown for another seven days in 4-well tissue culture dish (Nunc, Japan). Glutaraldehyde (2.5%, v/v) dissolved in 0.1 M sodium phosphate buffer (pH 7.0) was used for the fixation of grown tissue by 30 min incubation at room temperature. After three washes using 0.1 M phosphate buffer containing 8% sucrose, post fixation was carried out for 45 min at room temperature with 2% (w/v) Osmium tetroxide in sucrose-phosphate buffer. This was followed by washing with sucrose-phosphate buffer and sequential complete dehydration of the specimen in a series of increasing ethanol concentrations (60 to 100%). The samples were then infiltrated by and embedded into epoxy resin and 80 nm thin sections were cut using a diamond knife parallel to the bottom of the culture dish. The specimen sections were supported on TEM copper grids before post staining with 2% aqueous Uranyl acetate followed by lead citrate following Sato's method [45]. The TEM images were acquired with iTEM (Olympus SIS, Germany) software at an accelerating voltage of 80 kV using JEOL 1200 EX transmission electron microscope (JEOL, Tokyo, Japan) equipped with digital CCD camera (Morada, Olympus SIS, Germany).

3.2 Results and discussion

3.2.1 Surface functionalization of MWCNT

The purification and carboxylate functionalization of MWCNTs into f-MWCNTs by acid treatment were confirmed by FTIR study. The FTIR spectra (Fig. 1a) with an absorbance band at about 1,300 cm^{-1} for O–H bending deformation and the broad peak at around 3300 cm^{-1} for O–H

stretching vibration from carboxyl groups confirmed the presence of carboxyl groups on f-MWCNT surface [46]. The peak around 1200 cm^{-1} could be attributed to O-H group from ambient moisture bound to MWCNTs [47]. On the other hand, the absence of characteristic peaks from metallic catalyst and other adulterants confirmed the purification of MWCNT.

3.2.2 Hydrodynamic radius and zeta potential of G-CNT and W-CNT

The size distribution measured in terms of hydrodynamic radius by dynamic light scattering does not approximate the exact sizes of f-MWCNTs as they are high aspect ratio (>10^3) laser absorptive materials [48]. However, the data gave a comparison of the size distributions in terms of the hydrodynamic radius between G-CNT and W-CNT samples. G-CNT showed (Fig. 1b) bigger size with an average of 313.5 nm when compared to W-CNT the average hydrodynamic radius was 184.6 nm. We assume this was due to two reasons – firstly, the stretching of normally folded MWCNTs in gelatin [49] and secondly, due to the hydrophobic interaction between the hydrophobic amino acids of zwitterionic gelatin structure and the hydrophobic wall of the single or aggregated MWCNTs [50]. However, when mixed with LIF free culture medium containing FCS, we did not see any significant changes in hydrodynamic radius for G-CNT while for W-CNT the average hydrodynamic radius increased to 242.6 nm. This was due to the adsorption of protein onto MWCNTs [51] which were not already gelatin coated in case of W-CNT. On the other hand, the zeta potential for G-CNT was -1.14 mV compared to -31.9 mV for W-CNTs (Fig 1c) which when dispersed in the LIF free culture medium containing FCS, fell down to -1.78 mV in case of G-CNT but increased to -10.3 mV for W-CNT. This was also related to the presence of gelatin coating on MWCNTs in case of GCNT. Both the size distribution and the zeta potential measurements indicated the different modes of interactions of f-MWCNTs with water and

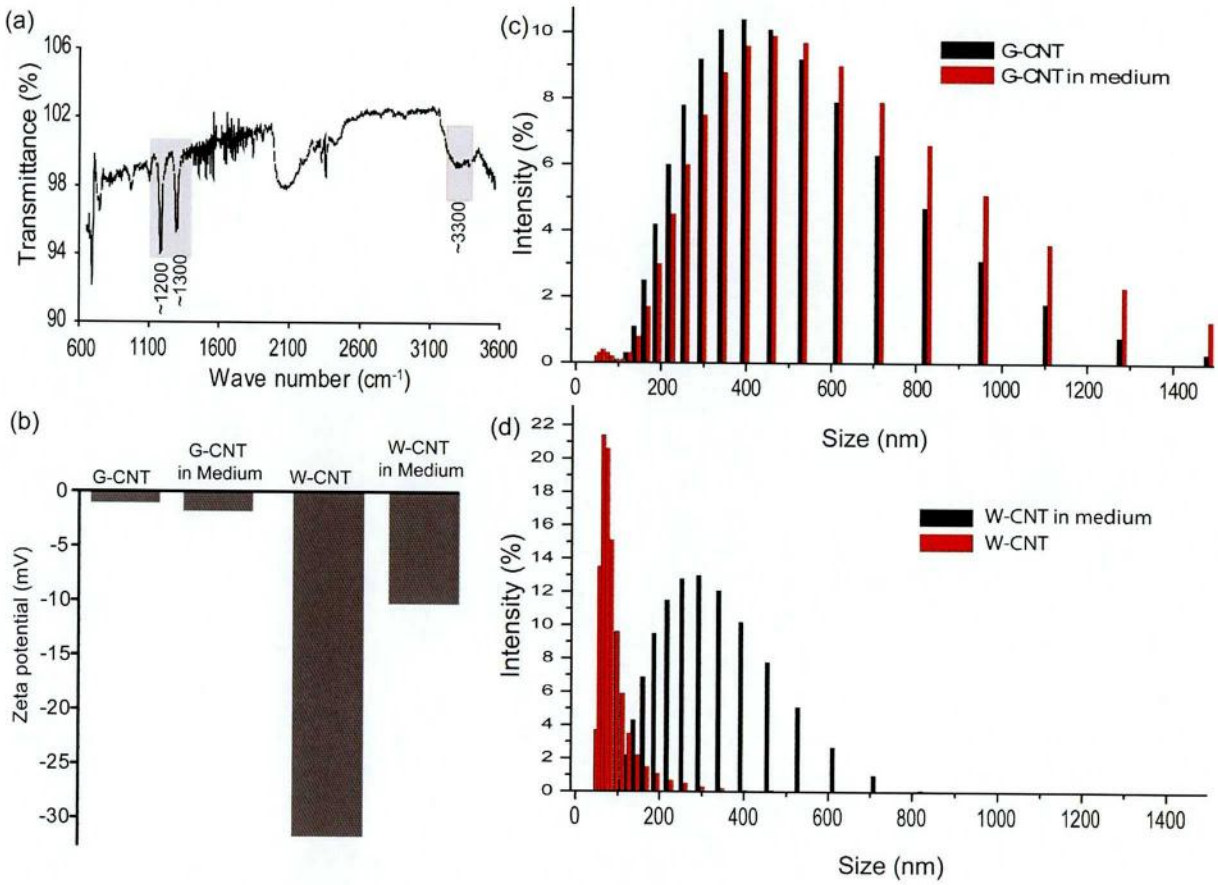

Figure 1 *FTIR spectra, zeta potential and size (hydrodynamic radius) distribution of G-CNT and W-CNT dispersions. (a) FTIR spectra shows characteristic peaks at 1300 cm^{-1} for bending deformation of O–H and another peak at 3300 cm^{-1} for O–H stretching vibration from carboxyl groups. (b) The zeta potential of G-CNT was not affected much by medium but W-CNT interacted with medium which brought down its zeta potential significantly. (c) The hydrodynamic radius of G-CNT was bigger compared to W-CNT and it remained almost unchanged after sample was added to the medium. (d) W-CNT showed a smaller hydrodynamic radius and it became almost double in the medium, owing probably to the interaction of bare f-MWCNTs with proteins from FCS in the medium.*

gelatin respectively in G-CNT and W-CNT and such interaction was affected by the protein rich culture medium.

3.2.3 f-MWCNT cytotoxicity by MTS assay

We studied the cytotoxicity of water and gelatin dispersed f-MWCNTs, *i.e.* W-CNT and G-CNT, respectively by exposing the cells to these dispersions. The cell viability or f-MWCNT toxicity over a period of 24 hrs showed that cell viability was not affected in the short term (Fig. 2a) by W-CNT or G-CNT at higher (15 $\mu g\ ml^{-1}$) or lower concentrations (3 $\mu g\ ml^{-1}$). As the absorbances from control samples *i.e.* cells without f-MWCNTs were considered as 100%, we could make out that both types of CNT treatments gave higher absorbances, which we confirmed was associated with the presence of f-MWCNTs. We observed a gradual increase of absorbance over a period of four hours indicating that the cells were viable and metabolically active, here also W-CNT readings were higher than G-CNT samples ($P<0.05$). In G-CNT, we speculated that, f-MWCNTs were better dispersed into gelatin and were coated by gelatin which reduced their role in the enhancement of absorbance compared to W-CNT. On the other hand, in case of proliferation studies, we subjected cells exposed to G-CNT and W-CNT to MTS assay on day 0, day 1, day 2 and day 3 (Fig. 2a). This gave us a better insight into the effect of long term exposure of cells to CNT as cells need longer incubation for hanging drop EB formation. W-CNT initially slowed down the proliferation of cells but the cells regained their proliferation potential and reached almost to the same level of proliferation to that of G-CNT. We did not observed dose dependent variations in cytotoxicity in terms of viability and proliferation. Zhu et al reported mESC DNA damage by CNT [52] but in their study the cells were treated with much higher doses of non-functionalized MWCNTs (100 $\mu g\ ml^{-1}$). Zhang et al [53] reported the inhibition of growth and proliferation of primary osteoblast in dose dependent manner which we

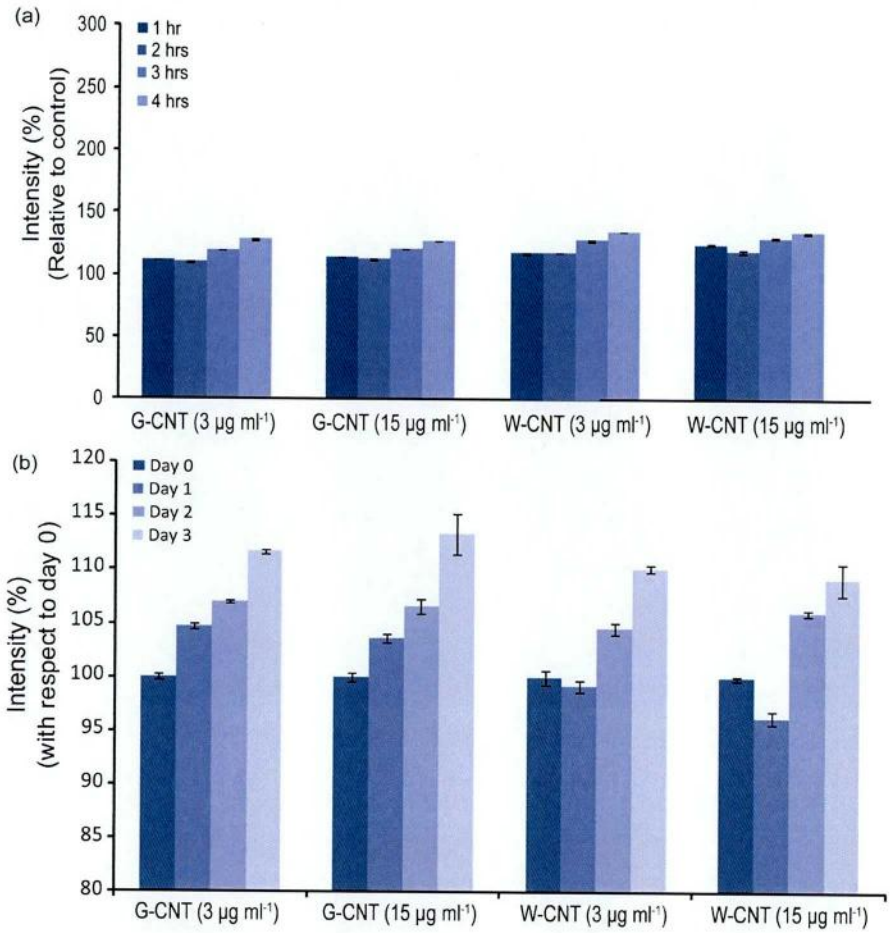

Figure 2 *Cell viability and proliferation assays for CNT toxicity evaluation. (a) The viability of cells followed by measuring MTS derived formazan absorbance (Mean±SE of at least three measurements) from cells samples exposed to 3 µg and 15 µg of W-CNT and G-CNT per ml of cell suspension; measurements were taken after one hour of incubation with MTS reagent and absorbances was normalized with respect to blank medium and expressed as percentage of the control i.e. cells without CNTs. (b) The proliferation of cells from upon exposure to f-MWCNTs were measured by MTS assay using day 0, day 1, day 2 and day 3 cells; absorbances after 1 hour of incubation with MTS reagent were taken, normalized with respect blank medium and expressed as the percentage of day 0 measurements.*

think was cell type specific [54, 55] and also at lower concentrations the effect on viability and proliferation was less. However, in this report f-MWCNTs were carboxylate functionalized and were humanized by dispersing especially into gelatin. Moreover, ES cells were exposed to CNT at lower concentrations at the cell aggregation stage. The long term viability results (Fig 2b) gave us the indication that we can keep mES cells with G-CNT or W-CNT supplements for hanging drop EB formation even for the duration of four days.

Some recent reports suggested the enzymatic degradation of carboxylate functionalized CNTs by peroxidases, for example, by plant derived horseradish peroxidases (HRPs) or human neutrophil myeloperoxidase [41]. In our observations (Fig. 2), we saw greater absorbance due to enzymatic breakdown of MTS into formazan in case of G-CNT and W-CNT samples compared to control samples. Since the production of medium soluble color formazan compound is mediated by mitochondrial dehydrogenase enzymes, these results suggested us that, the mitochondrial dehydrogenase activity in f-MWCNT exposed cells might be elevated in CNT exposed samples. In line with the recent results on enzymatic degradation of CNTs, we concluded that, cells released higher quantities of dehydrogenase enzymes in response to the exposure to nanomaterials. The enzymatic responses of cells to f-MWCNTs need further investigations.

3.2.4 Dynamics of EB formation by continuous monitoring

The formation of stem cell aggregate is a dynamic and a conserved process. Though ES cells form aggregates even in monolayer cultures, for better subsequent differentiations from such aggregates, we need spherical cell aggregates or embryoid bodies with three distinctly organized germ layers containing lineage committed precursor cells. In our continuous monitoring

experiments (Fig. 3), we followed the dynamics of EB formation in real time in the presence and absence of nanomaterials where we did not observe negative effect whatsoever of f-MWCNT presence on the formation of EBs. As compared to cell aggregation in the absence of f-MWCNTs, any unusual changes in cell morphology or cell behavior was not evident and the occurrence of cell death during aggregation was not seen. The EB formation dynamics was comparable to the control but interestingly, cells exposed to f-MWCNT tend to aggregate faster compared to control, which needs further investigation. We speculated that the interaction of extracellular matrix proteins with CNTs might have made the aggregation process faster in case of f-MWCNT containing cells.

3.2.5 EB characteristics: Size and sphericity

The role of nanomaterials on the morphology of the formed EBs was assessed by comparing the sizes (Fig. 4) and sphericity (Fig. 5) of EBs formed from W-CNT and G-CNT exposed EBs to those from control EBs. The representative EB images from different CNT treatments (Fig. 6) also elucidated the effects on sizes and shapes. To our surprise, we observed that G-CNT EBs were significantly bigger in size ($P<0.05$) compared to control EBs and W-CNT EBs. On the other hand, W-CNT EBs, though larger in general than control EBs, the difference was not significant statistically. We did not observe any dose-dependent pattern in EB size in case of W-CNT while the EBs from 7.5 and 30 $\mu g\ ml^{-1}$ G-CNT containing suspensions were bigger in size (Fig. 4). The CNT-gelatin composites may have marginal contribution to the overall EB volume but we think the nanomaterials positively influenced the proliferation of cells during EB formation stages. On the other hand, in terms of sphericity, W-CNT EBs were the most spherical compared to control and G-CNT EBs ($P<0.05$) while such trend was not clear between G-CNT and control EBs which was also interesting (Fig. 5). We believe that the cells were influenced by

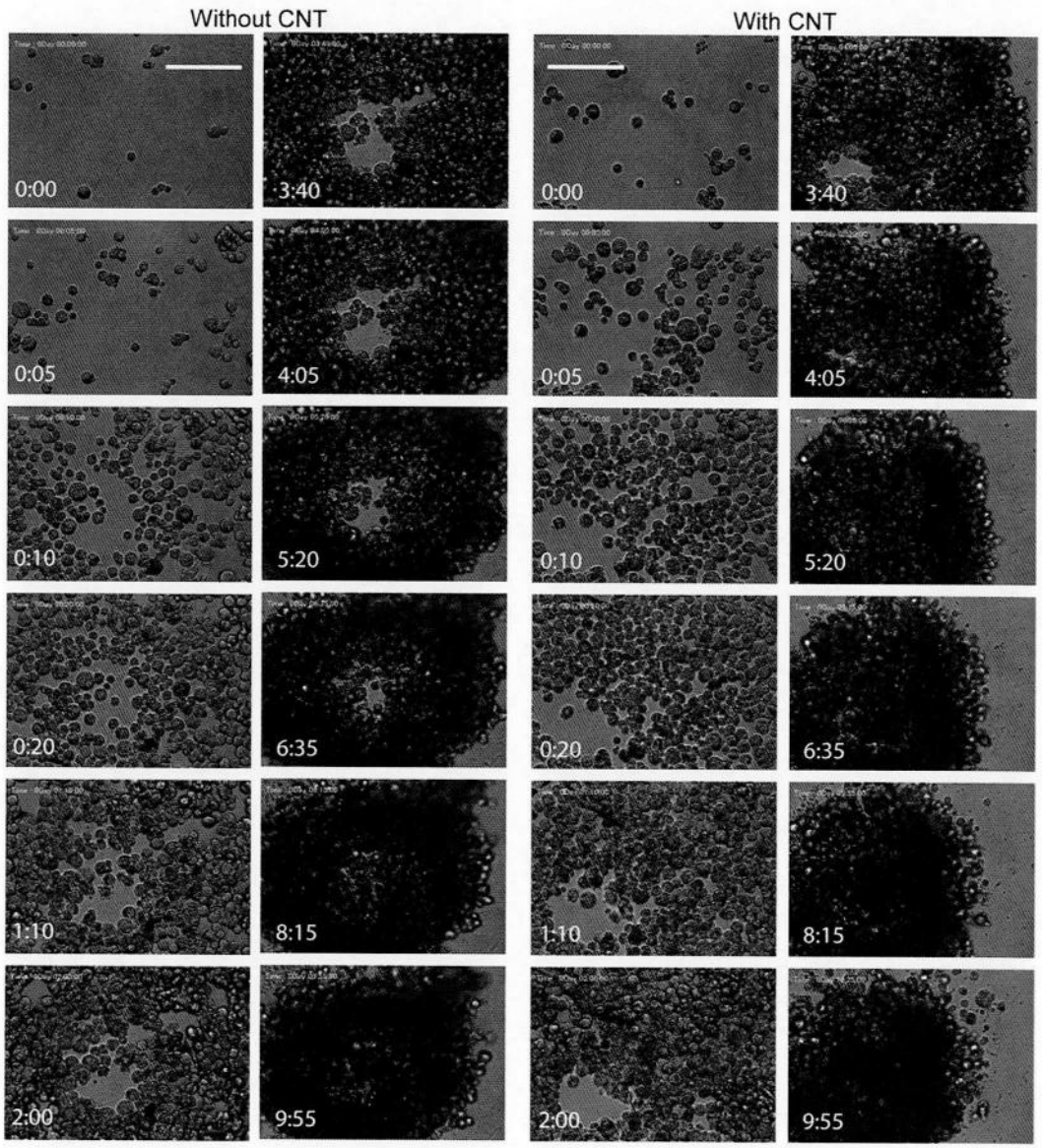

Figure 3 *Dynamics of EB formation in the presence and in the absence of f-MWCNT dispersion in water by ASTEC's cultured cell monitoring system (CCM-1.4XYZ/CO_2). EBs were formed from in round bottom 96-well plates with 2000 cells in 100 µl of f-MWCNT supplemented medium per well. As evident f-MWCNT exposed EBs showed relatively quicker aggregation, bigger and more compact EBs with more spherical morphology. Visual evidence of cell death or other unusual events were not evident. Scale bar 100 µm and time indicates hh:mm.*

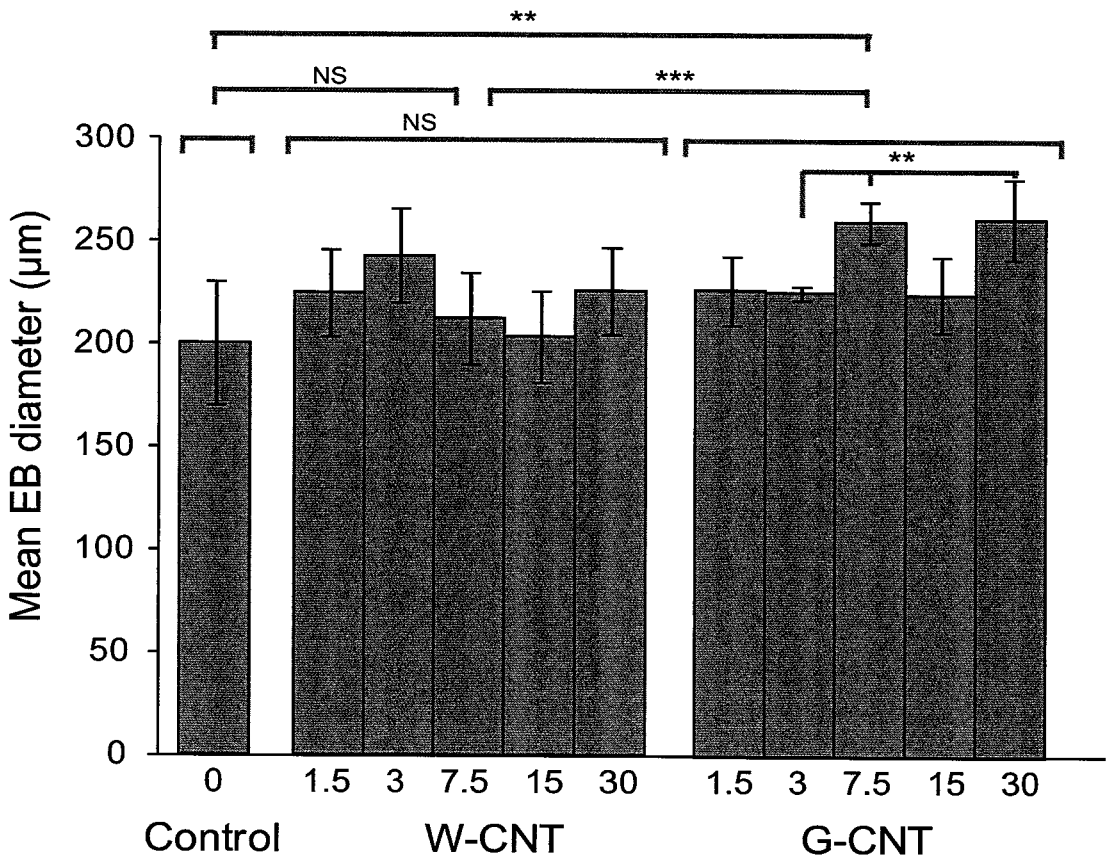

Figure 4 *The diameter distribution of f-MWCNT containing EBs with respect to control EBs in relation to different concentrations of water dispersed CNT (W-CNT) and gelatin dispersed CNT (G-CNT). In general, CNT containing EBs were bigger in diameter than control EBs while W-CNT EBs were smaller than G-CNT EBs. The diameter differences between control EBs and W-CNT EBs was statistically insignificant but it was significant for G-CNT EBs. In case of W-CNT there had been no significant variation in EB diameter due to varied concentrations. However, in case of G-CNT, higher concentrations lead to bigger EBs except for cells exposed to 15 µg of G-CNT per ml of cell suspension. Non significant (NS), significant at P<0.01 (***) and significant at P<0.05 (**) are indicated at the top. Each bar indicates Mean ±SE of 15~20 EBs.*

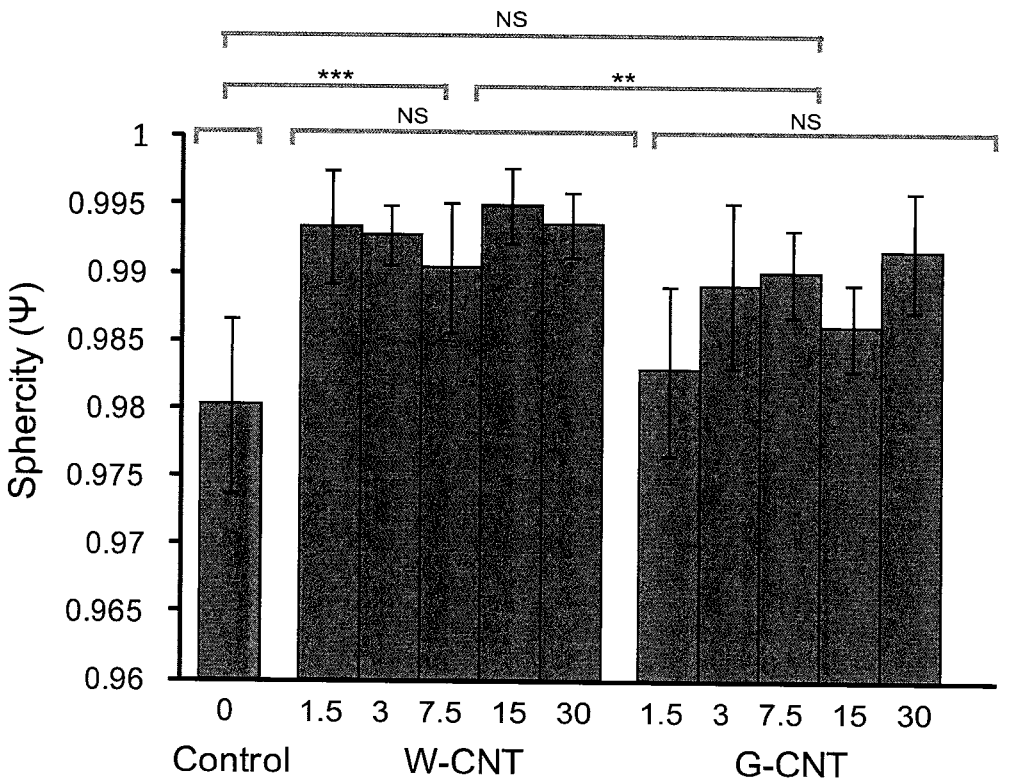

Figure 5 *The sphericity of f-MWCNT containing EBs with respect to control EBs in relation to different concentrations of water dispersed CNT (W-CNT) and gelatin dispersed CNT (G-CNT). CNT containing EBs were more spherical compared to control EBs and W-CNT EBs exhibited higher sphericity than G-CNT EBs. Compared to control EBs, the difference in sphericity was statistically significant for both W-CNT and G-CNT EBs. Both for W-CNT and G-CNT, there had been no significant variation in EB diameter due to varied CNT concentrations. Non significant (NS), significant at P<0.01 (***) and significant at P<0.05 (**) are indicated at the top.*

G-CNT and W-CNT differently. A clue for the probable explanation to this difference might be in the uniformity of dispersion of stretched out f-MWCNT in gelatin which we assumed from the findings of Kim et al [49] who reported the role of gelatin in the prevention of SWCNT

aggregation. This observation was also supported by the marked differences in sizes and zeta potentials of G-CNT and W-CNT samples (Fig 1). This was probably the reason for which, compared to water dispersion, gelatin modification led to the uniform uptake of f-MWCNT by EB forming cells in G-CNT EBs. Moreover, the culture medium containing FBS also enhanced dispersion in case of W-CNT [56] and contributed to the bigger W-CNT EBs than control. In general, the aggregation of mES cells (Fig. 3) into bigger sizes of EBs owing to nanomaterials exposure could be explained by the presence of carboxylate groups on f-MWCNT walls which made possible the adhesion of extracellular matrix proteins [57] onto CNTs and enhanced the aggregation of cells (Video in the Supplementary).

3.2.6 Role of Gelatin versus water as dispersion medium on CNT aggregation inside EBs

As we can see from Fig 6, the presence of f-MWCNTs was not clearly visible in case of G-CNT EBs even in the fluorescence images which were similar to the control EBs. But the presence of CNT aggregates was clearly visible in the case of W-CNT EBs especially in the fluorescent images and the higher prevalence was evident with increased concentrations. This was due to the formation of fine dispersion of f-MWCNTs in gelatin which inhibited the formation of CNT aggregates while in case of water f-MWCNTs produced aggregates which were visible. The better dispersion in gelatin necessarily ensured the uniform distribution of f-MWCNTs in the cell suspension and we assumed the uniform uptake by cells as well which was not necessarily the case with W-CNT where accumulation of CNT in cells was preferential depending on the location of the presence of f-MWCNT aggregates.

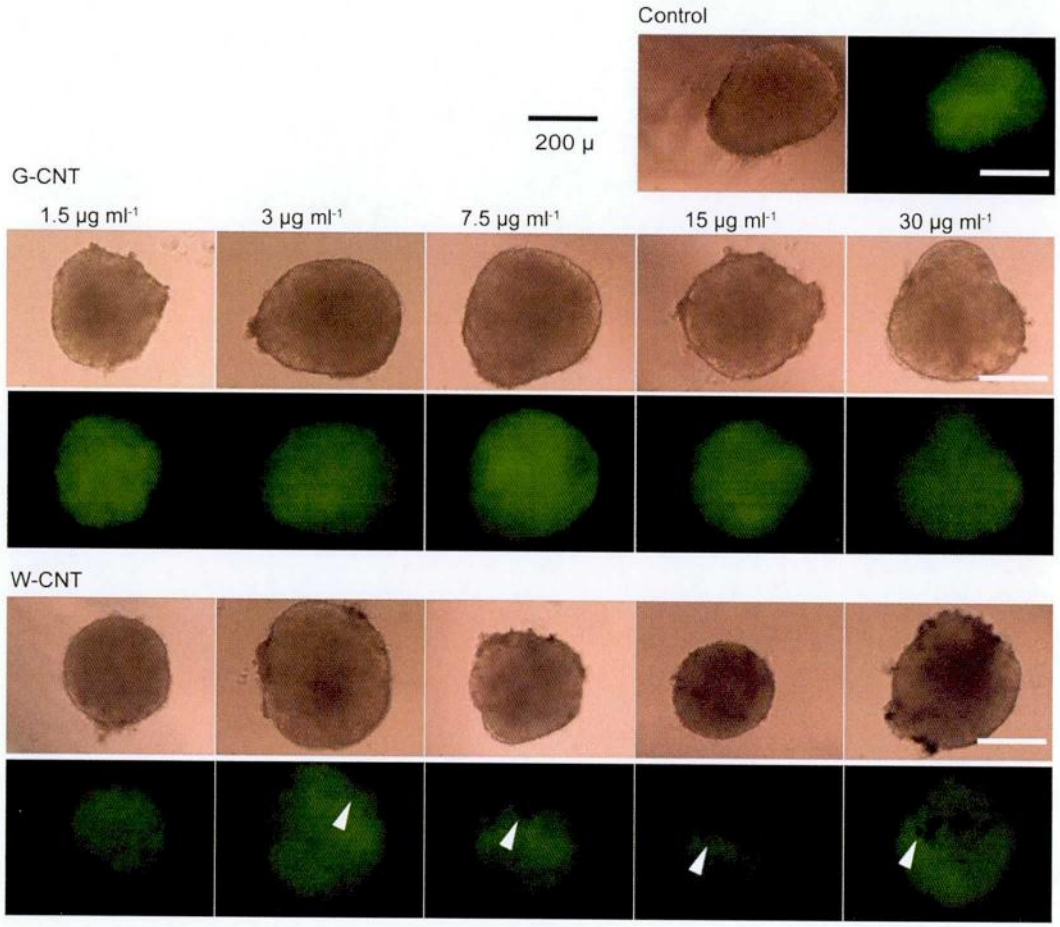

Figure 6 *Embryoid bodies formed under the influence of f-MWNT dispersions in water (W-CNT) and gelatin (G-CNT) at various concentrations. In case of GCNT, EBs were bigger and more spherical. CNT aggregates inside the cells were visible in fluorescence images (white arrows) in case of W-CNT except for very low concentration of CNT, while in case of G-CNT due to better dispersion CNT aggregates were not visible in optical or fluorescence images.*

3.2.7 Growth of EBs after plating and their cardiomyogenic differentiation with some clue of neurogenesis

As shown in Fig 7a, for the proliferating G-CNT EBs, 4 days after plating onto 0.1% gelatin coated 4-well plates, CNT aggregates were merely visible only in case of EBs from suspension

containing 30 μg ml^{-1} of G-CNT. Specs of CNT aggregates were visible throughout with greater number of specs for higher W-CNT concentrations. But W-CNT and G-CNT EBs got attached to gelatin coated dishes normally and no visible effect of G-CNT or W-CNT was seen on the outgrowth of the tissue from plated EBs. This again proved the viability of cells upon exposure to such concentrations of MWCNT dispersions in water and gelatin and exhibited that gelatin dispersion was better in dispersing f-MWCNT for cell applications.

Synchronously beating cardiomyocytes appeared from 7-days onward in the plated EBs (Fig 8d), and the initiation of beating was, in general, earlier for the f-MWCNT exposed EBs both in the cases of G-CNT and W-CNT. On the other hand, as we studied the beating profiles (Fig 8a-c), we could see that the beating in the control EB considered was ~100 beats per min which was faster than both the G-CNT and W-CNT EBs which respectively showed beating rates of 48 and 60 beats per minute. We also observed neuronal cells in the fluorescent microscopy (Fig 10). But the numbers of glia-like cells were not as abundant and they were seen in the culture three to four weeks after transferring the EBs.

3.2.8 TEM

TEM images showed traces of f-MWCNTs inside the cells which were less prominent in TEM micrographs from G-CNT exposed cells (Fig 9 a-c) than W-CNT exposed ones (Fig 9 d-f). In case of G-CNT samples some traces of f-MWCNTs were seen in the cytosol and secondary lysozomes whereas in case of W-CNTs, presence of f-MWCNTs was predominantly inside or at the boundary of secondary lysozomes. As the lysozomes are cell organelle filled with hydrolytic enzymes for breaking down the unwanted materials entered into cells, we think that the W-CNT exposed cells exhibited activity for processing the f-MWCNTs entered into the cells. In Fig 9e,

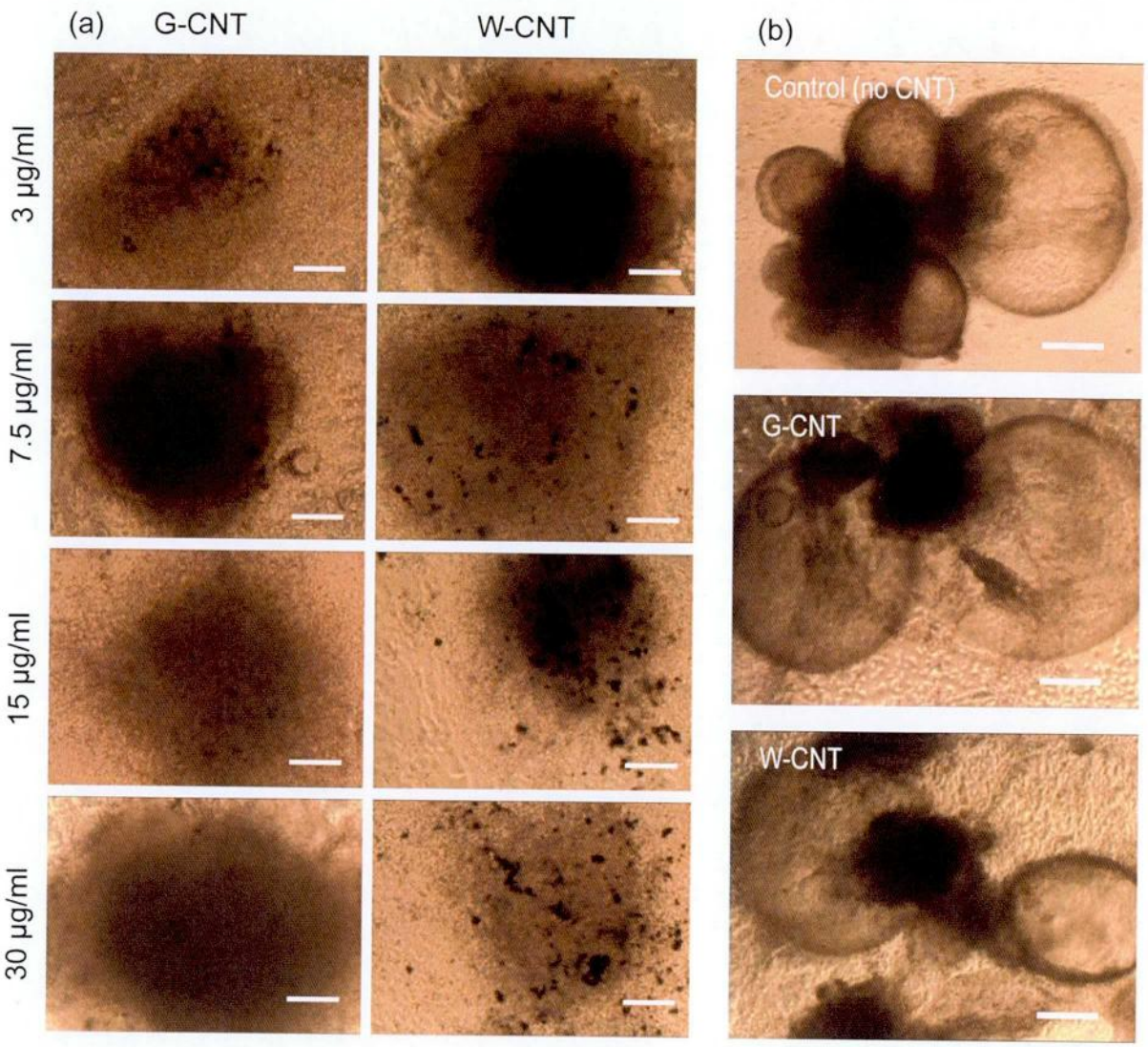

Figure 7 *The comparison of the after-plating growth of G-CNT and W-CNT EBs on 0.1% gelatin coated 4-well polystyrene tissue culture plates and the formation of cystic bodies. (a) No observable damage to growing cells is evident either in G-CNT or W-CNT EB growths. No specs of CNTs were visible for any concentration of G-CNT whereas in W-CNT EBs the specs of CNT aggregates were visible in a dose dependent manner but they did not affect the cells and we believe those CNTs, owing to their sizes did not localized into the cells. (b) The formation of cystic bodies in CNT treated EBs were comparable to control EBs which reflected the progression of normal cellular organization during EB growth after plating. Scale bar 100 µm.*

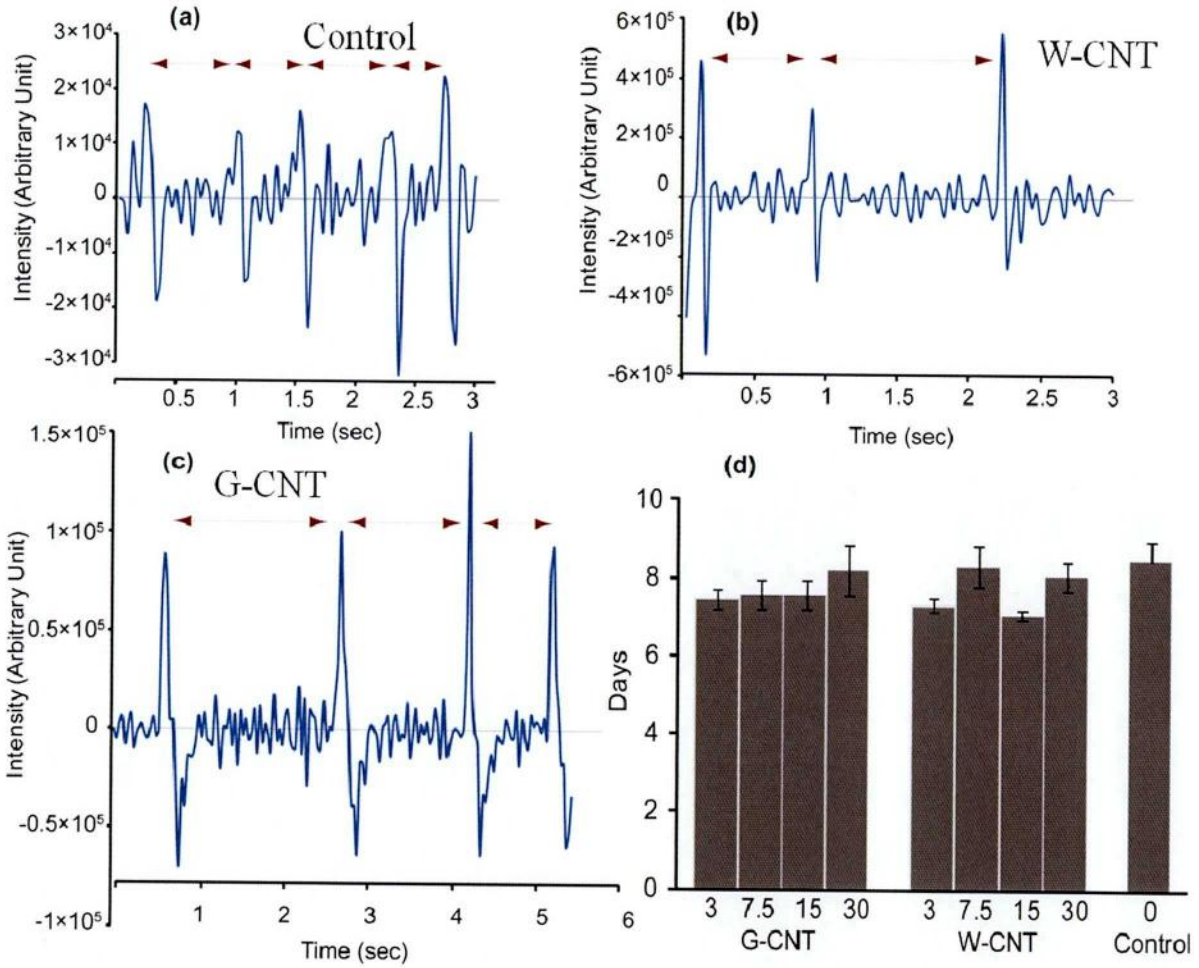

Figure 8 *Beating profiles of cardiomyocytes from G-CNTand W-CNT exposed EBs compared to control as obtained from the analysis of optical video taken two weeks after plating. (a) Beating profile of cardiomyocytes from control EB showing faster but weak beating. (b) Beating profile of cardiomyocytes from W-CNT EB showing slower but very strong beat. (c) Beating profile of cardiomyocytes from G-CNT EB showing slower but stronger beat than control EB. (d) Onset of beating was earlier in tissue from f-MWCNT exposed EBs compared to control EBs (mean±SE from 8~10 EBs after plating onto gelatin coated plates).*

we observed the presence of pseudopods in the proximity of f-MWCNT containing secondary lysozomes which was in line with the widely accepted view that cells uptook CNTs by

phagocytosis [55, 58]. This was in line with our consideration that gelatin modification rendered CNTs more humanized for cells. However, in the TEM images the ultrastructural organization of cells did not show toxicity from f-MWCNTs in the form of apoptotic cells or necrotic zones.

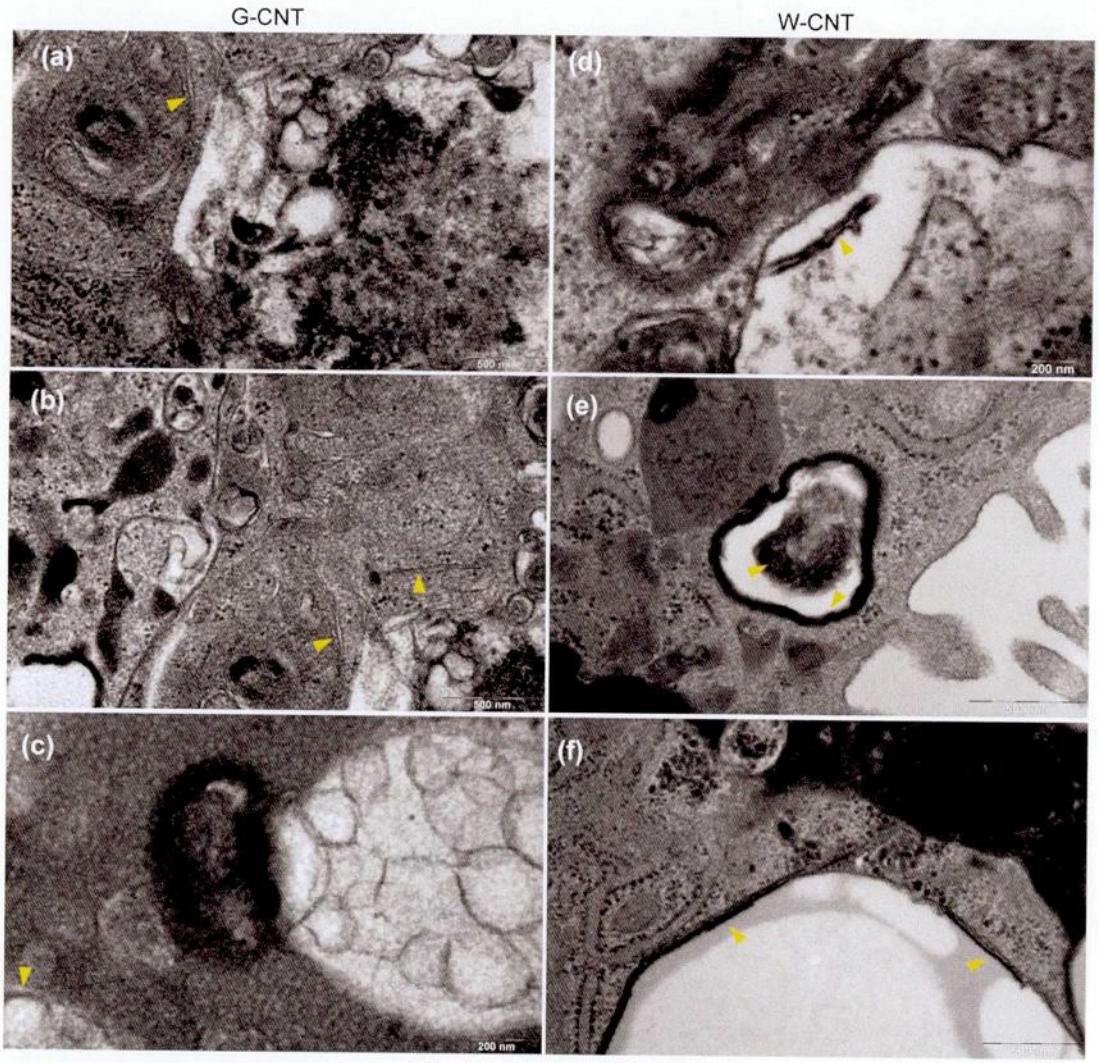

Figure 9 *TEM micrograph from tissue derived from EBs formed from cell suspension supplemented with f-MWNT dispersion in water and gelatin. In case of G-CNT (a, b, c), the presence of CNT in grown tissue was barely visible as indicated by yellow arrow heads and f-MWCNTs were also seen in the cytosol. But in case of W-CNT (d,e,f) CNTs were more prominent (yellow arrowheads) mainly in the secondary lysozomes especially towards the edge of them.*

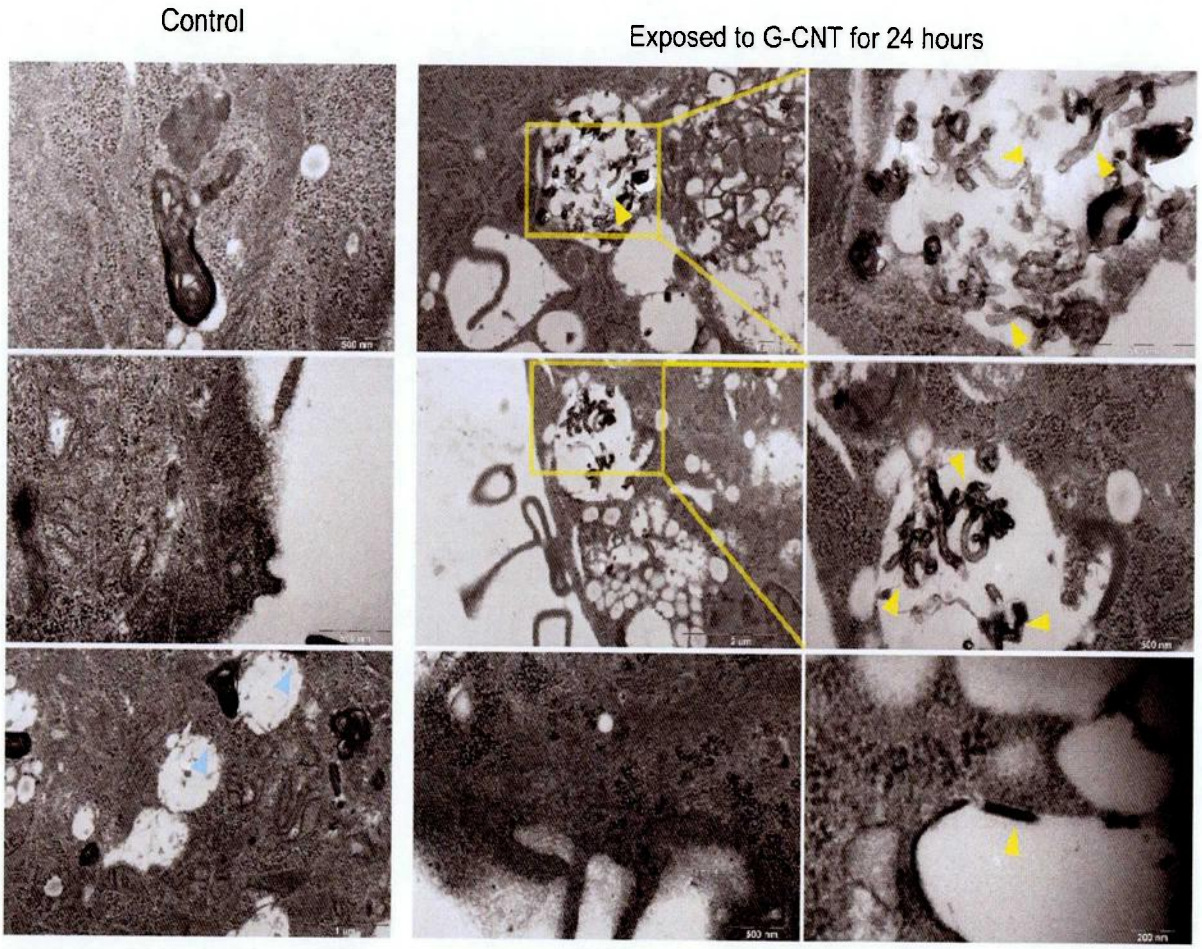

Figure 10 *TEM micrograph from of cells exposed to f-MWNT dispersion in gelatin for 24 hours with respect to control i.e. cells not exposed to f-MWCNTs. In case of CNT exposed cells (Right columns), the presence of CNT in secondary lysozomes were visible as indicated by yellow arrow heads. The presence of CNT can be confirmed by comparison with TEM images from cells unexposed to CNTs. The edges of lysozomes were clean in CNT unexposed cells which led us to conclude that the blackish edges of secondary lysozomes in CNT exposed cells are CNTs. The low magnification and high magnifications are indicated by yellow box. In presence of CNTs cells did not look affected or unhealthy.*

3.2.9 Cystic body formation

Cystic body formation is reportedly [59-61] related to the organization of the cells during the proliferation of lineage committed cells from EBs after plating onto dishes at the initial stage of differentiation process. This process is not well understood but thought to be crucial to the

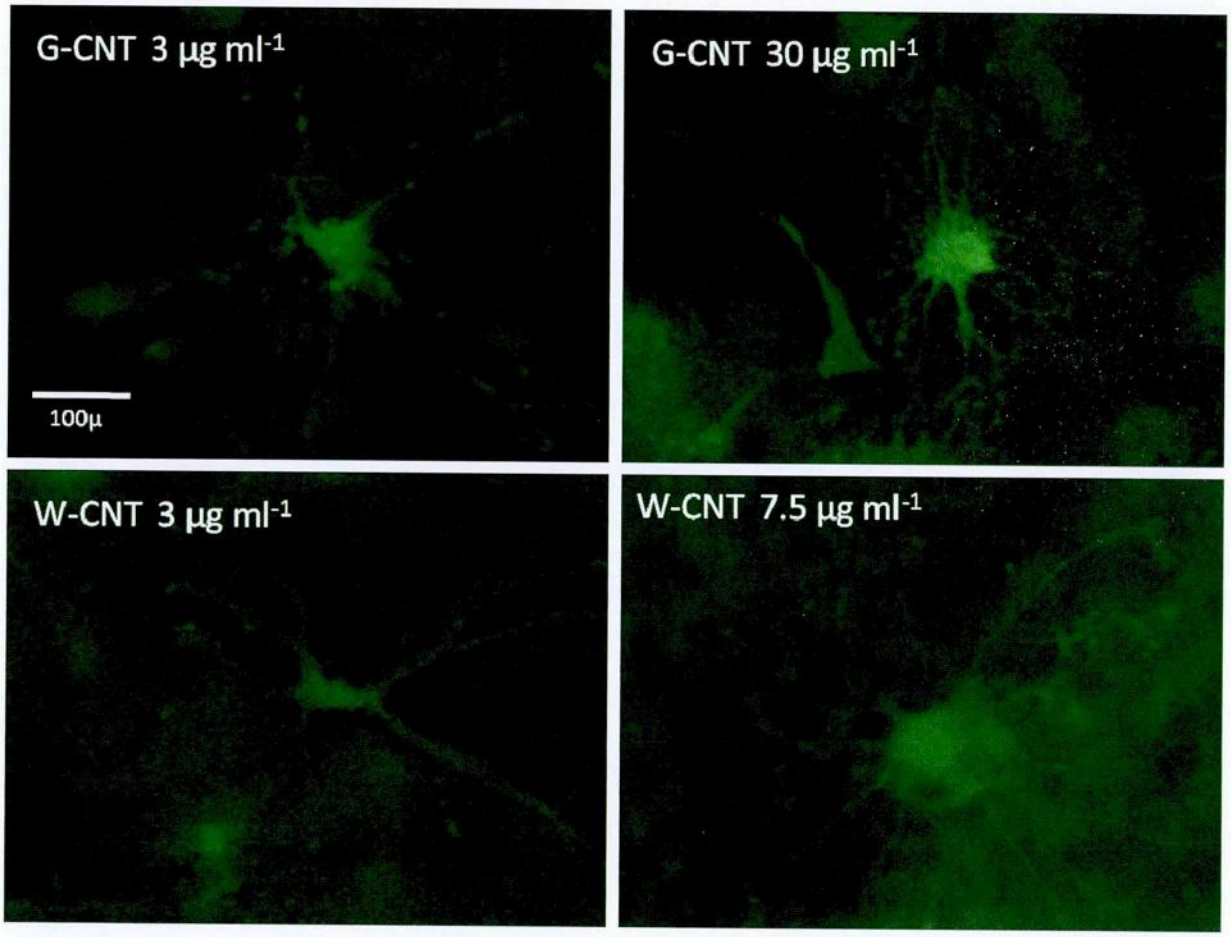

Figure 11 *Glia like neuronal cells were visible in f-MWCNT containing dishes. Cells were with bigger cell bodies and many axon processes were clearly visible in the fluorescence images. Upper panel shows such cells from G-CNT samples and the lower panel shows cells from W-CNT samples. These cells were visible in all the dishes containing f-MWCNT exposed EBs, irrespective of the CNT concentrations.*

epigenetic determination of cell lineage through cell death mediated by the production of reactive oxygen species (ROS) and other radicals mediating programmed cell elimination for tissue organization. This is a crucial stage in ES cell proliferation after plating the EBs. In case of EBs derived from f-MWCNT interaction with mES cells, both in the cases of W-CNT and G-CNT, on plating, we observed the formation of cystic bodies (Fig 7b) on day 3 onward of plating. The formation varied from EB to EB but we did not observe any visible differences between control and nanomaterial-exposed EBs in this regard that worth mention. This indicated that, nanomaterials did not affect the normal functioning of mES cells in terms of tissue organization at the initial stage of cell growth.

3.2.10 Proposed Mechanism of f-MWCNT-ES cell interaction

It is difficult to understand the exact mechanism that promoted the relatively quicker formation of EBs of better sizes and sphericity in f-MWCNT exposed ES cells compared to control with our current level of CNT-Cell interactions. But based on the observations, we are proposing a scheme (Fig 12) of such interaction that may help explaining the possible role of f-MWCNTs in augmenting the aggregation of mES cells. The Zeta potential measurement clearly showed the interaction of gelatin, an extracellular matrix (ECM) protein which is important for cell adhesion, with f-MWCNT. When f-MWCNTs were dispersed in 0.1% gelatin, the clear changes in size distribution indicated that the surface of the f-MWCNT attracted the gelatin and promoted the formation of a gelatin coating onto itself. On the other hand, the mES cell aggregation during hanging drop culture is accomplished through the release of different types of ECM proteins by ES cells at the initial stage of aggregation which is further consolidated through the formation of cell adhesion protein molecules onto the cell surfaces connecting the neighboring cells.

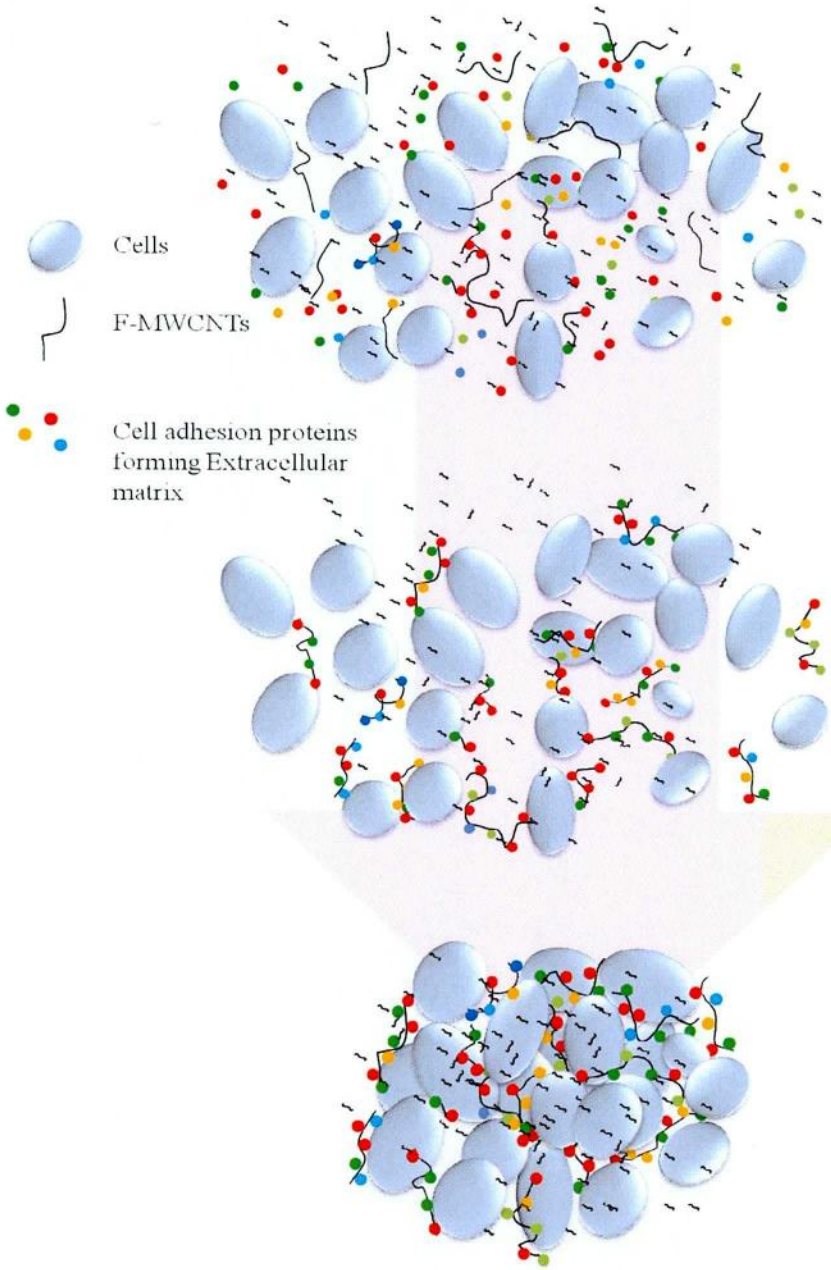

Figure 12 *The scheme of probable interaction among cell adhesion molecules, mainly extracellular matrix proteins, ES cells and f-MWCNTS. f-MWCNTs in the cell suspension provided a favorable surface for the adsorption of cell adhesion proteins and promoted quicker aggregation of mES cells into bigger and more spherical shaped EBs. Presence of ECM coated f-MWCNTs might also affected the differentiation behavior of such EBs.*

In presence of f-MWCNT in the cell suspension, we speculate that, the mES excreted ECM proteins were adsorbed on f-MWCNTs surfaces and this adsorption promoted the formation of mES-CNT bonding where f-MWCNT acts as a promoter for enhancement of EB formation and also being incorporated into the EB itself, such ECM protein containing CNTs might have contributed to the size and sphericity of the formed EBs. Moreover, the localization of some f-MWCNTs into the cell through endocytotic or phagocytotic means promoted the complex interactions among mES cell-ECM-cell junction molecules-CNTs.

In combination, such interactions, made the aggregation process faster while the inclusion of ECM adsorbed f-MWCNTs into the EBs lead to the formation of bigger EBs with better sphericity. The presence of ECM adsorbed f-MWCNTs both in the cytosol and in the extracellular space of the EBs might have modulated the differentiation trajectory and promoted better adhesion surface to promote cardiomyocyte differentiation with stronger beating while at the same time the conductive f-MWCNTs might have contributed to augment the neurogenic differentiation to some extent. This model is a speculative one as we do not have very clear evidences and studies on the interaction between f-MWCNTs and different ECM proteins, further research into this field will be quite interesting and will definitely augment our understanding of the probable role of f-MWCNTs on the dynamics of EB formation.

3.3 Conclusion

In this report we have demonstrated, to the best of our knowledge, for the first time that MWCNT based functionalized multiwalled carbon nanotubes can interact with mES cells especially in serum rich medium at the aggregation stage favorably towards the formation of mES cells aggregates or embryoid bodies. We systematically exposed the single mES cell

suspension to different concentrations of carboxylate functionalized MWCNTs in the forms of their dispersion in water and gelatin, keeping the maximum concentration at 30 μg ml^{-1} of cell suspension. In our investigations with mES EBs formed by hanging drop method, each hanging drop contained 1000 cells in 20 μl of cell suspension. The functionalized and well dispersed MWCNTs did not show any short term or long term toxicities against cell proliferation or viability rather we found formation of bigger and more spherical EBs in shorter time in general but prominently for G-CNT EBs. Gelatin dispersed f-MWCNT well and we did not see any CNT aggregates in G-CNT EBs or in tissue obtained thereof unlike W-CNT EBs where upon plating CNT aggregates were visible in light and fluorescence images though they did not exert any visible effect on EB growth. The formation of cystic bodies confirmed the normal organization of ES cells from EBs upon plating. TEM analysis of tissue grown from such EBs did not show much prevalence of CNTs in the cell ultrastructure, however, some traces could be seen inside or at the edges of secondary lysozomes. Moreover, we saw earlier onset of beating cardiomyocytes from the tissue grown off these EBs with some glia like neuronal cells, which provided the preliminary proof of concept that f-MWCNTS can promote the mES cell differentiation towards electroactive cell lineages. Undoubtedly, f-MWCNTs have a lot to offer in stem cell research especially in differentiation and regenerative applications. But it requires the detailed understanding of the interaction of f-MWCNTs with cells at EB formation stage from molecular and genetic perspectives. The long term effect of such exposures will be interesting and necessary. Moreover, the uptake and processing of f-MWCNTs from dispersion phase are to be addressed more comprehensively as no widely accepted model for this has yet been developed.

3.4 References

[1] Takahashi, K.; Yamanaka, S. *Cell* **2006,** 126, (4), 663-676.

[2] Takahashi, K.; Tanabe, K.; Ohnuki, M.; Narita, M.; Ichisaka, T.; Tomoda, K.; Yamanaka, S. *Cell* **2007,** 131, (5), 861-872.

[3] Nakagawa, M.; Koyanagi, M.; Tanabe, K.; Takahashi, K.; Ichisaka, T.; Aoi, T.; Okita, K.; Mochiduki, Y.; Takizawa, N.; Yamanaka, S. *Nature Biotechnology* **2007,** 26, (1), 101-106.

[4] Hogan, B. In *Summary: Present and Future Challenges for Stem Cell Research*, 2008; Cold Spring Harbor Laboratory Press: 2008.

[5] Chien, K. *Nature* **2008,** 453, (7193), 302-305.

[6] Yamashita, J. *Experimental Cell Research* **2010**.

[7] Lengner, C. J. *Annals of the New York Academy of Sciences* **2010,** 1192, (Skeletal Biology and Medicine), 38-44.

[8] Boheler, K. *Expert Review of Cardiovascular Therapy* **2009,** 7, (1), 1-4.

[9] Reubinoff, B.; Itsykson, P.; Turetsky, T.; Pera, M.; Reinhartz, E.; Itzik, A.; Ben-Hur, T. *Nature Biotechnology* **2001,** 19, (12), 1134-1140.

[10] Wichterle, H.; Lieberam, I.; Porter, J.; Jessell, T. *Cell* **2002,** 110, (3), 385-397.

[11] Collas, P. *Biochimica et Biophysica Acta (BBA)-General Subjects* **2009,** 1790, (9), 900-905.

[12] Kleinsmith, L.; Pierce Jr, G. *Cancer Research* **1964,** 24, (9), 1544.

[13] Risau, W.; Sariola, H.; Zerwes, H.; Sasse, J.; Ekblom, P.; Kemler, R.; Doetschman, T. *Development* **1988,** 102, (3), 471.

[14] Desbaillets, I.; Ziegler, U.; Groscurth, P.; Gassmann, M. *Experimental Physiology* **2001,** 85, (06), 645-651.

[15] Carpenedo, R.; Sargent, C.; McDevitt, T. *Stem Cells* **2007,** 25, (9), 2224-2234.

[16] Kurosawa, H. *Journal of Bioscience and Bioengineering* **2007,** 103, (5), 389-398.

[17] Ezekiel, U.; Muthuchamy, M.; Ryerse, J.; Heuertz, R. *Electronic Journal of Biotechnology* **2007,** 10, 328-335.

[18] Choi, Y.; Chung, B.; Lee, D.; Khademhosseini, A.; Kim, J.; Lee, S. *Biomaterials* **2010,** 31, (15), 4296-4303.

[19] Murtuza, B.; Nichol, J. W.; Khademhosseini, A. *Tissue Engineering Part B: Reviews* **2009,** 15, (4), 443-454.

[20] Gelain, F. *International Journal of Nanomedicine* **2008,** 3, (4), 415.

[21] Malafaya, P. B.; Silva, G. A.; Reis, R. L. *Advanced Drug Delivery Reviews* **2007,** 59, (4-5), 207-233.

[22] Harrison, B.; Atala, A. *Biomaterials* **2007,** 28, (2), 344-353.

[23] Xu, Z.; Zeng, Q.; Lu, G.; Yu, A. *Chemical Engineering Science* **2006,** 61, (3), 1027-1040.

[24] Lin, Y.; Tsai, C.; Huang, H.; Kuo, C.; Hung, Y.; Huang, D.; Chen, Y.; Mou, C. *Chemical Materials* **2005,** 17, (18), 4570-4573.

[25] Jiang, W.; Kim, B.; Rutka, J.; Chan, W. *Nature Nanotechnology* **2008,** 3, (3), 145-150.

[26] Faraji, A.; Wipf, P. *Bioorganic & Medicinal Chemistry* **2009,** 17, (8), 2950-2962.

[27] Kam, N.; Jan, E.; Kotov, N. *Nano Letters* **2009,** 9, (1), 273-278.

[28] Jan, E.; Kotov, N. *Nano Letters* **2007,** 7, (5), 1123-1128.

[29] Kostarelos, K. *Nature Biotechnology* **2008,** 26, (7), 774-776.

[30] Simeonova, P. *Nanomedicine* **2009,** 4, (4), 373-375.

[31] Wörle-Knirsch, J. M.; Pulskamp, K.; Krug, H. F. *Nano Letters* **2006,** 6, (6), 1261-1268.

[32] Elgrabli, D.; Abella-Gallart, S.; Aguerre-Chariol, O.; LACROIX, G. *Nanotoxicology* **2007,** 1, (4), 266-278.

[33] Pulskamp, K.; Diabaté, S.; Krug, H. F. *Toxicology Letters* **2007,** 168, (1), 58-74.

[34] Bardi, G.; Tognini, P.; Ciofani, G.; Raffa, V.; Costa, M.; Pizzorusso, T. *Nanomedicine: Nanotechnology, Biology and Medicine* **2009,** 5, (1), 96-104.

[35] Dong, L.; Joseph, K.; Witkowski, C.; Craig, M. *Nanotechnology* **2008,** 19, 255702.

[36] Vittorio, O.; Raffa, V.; Cuschieri, A. *Nanomedicine: Nanotechnology, Biology and Medicine* **2009**.

[37] Kaiser, J.-P.; Krug, H. F.; Wick, P. *Nanomedicine* **2009,** 4, (1), 57-63.

[38] Huczko, A.; Lange, H. *Fullerene Science and Technology* **2001,** 9, (2), 247 - 250.

[39] Bakota, E. L.; Aulisa, L.; Tsyboulski, D. A.; Weisman, R. B.; Hartgerink, J. D. *Biomacromolecules* **2009,** 10, (8), 2201-2206.

[40] Mooney, E.; Dockery, P.; Greiser, U.; Murphy, M.; Barron, V. *Nano Letters* **2008,** 8, (8), 2137-2143.

[41] Kagan, V. E.; Konduru, N. V.; Feng, W.; Allen, B. L.; Conroy, J.; Volkov, Y.; Vlasova, I. I.; Belikova, N. A.; Yanamala, N.; Kapralov, A.; Tyurina, Y. Y.; Shi, J.; Kisin, E. R.; Murray, A. R.; Franks, J.; Stolz, D.; Gou, P.; Klein-Seetharaman, J.; Fadeel, B.; Star, A.; Shvedova, A. A. *Nature Nanotechnology* **2010,** 5, (5), 354-359.

[42] Hossain, M.; Shimizu, E.; Saito, M.; Rao, S.; Yamaguchi, Y.; Tamiya, E. *Analyst* **2010**, 135, 1624 - 1630.

[43] Hoa, L. Q.; Sugano, Y.; Yoshikawa, H.; Saito, M.; Tamiya, E. *Biosensors and Bioelectronics* **2010,** 25, (11), 2509-2514.

[44] Okabe, M.; Ikawa, M.; Kominami, K.; Nakanishi, T.; Nishimune, Y. *FEBS letters* **1997,** 407, (3), 313-319.

[45] Sato, T. *Journal of Electron Microscopy* **1968,** 17, (2), 158.

[46] Kan, K.; Xia, T.; Yang, Y.; Bi, H.; Fu, H.; Shi, K. *Journal of Applied Electrochemistry* **2009,** 40, (3), 593-599.

[47] Haldorai, Y.; Lyoo, W.; Shim, J.-J. *Colloid & Polymer Science* **2009,** 287, (11), 1273-1280.

[48] Li, Z.; Luo, G.; Zhou, W.; Wei, F.; Xiang, R.; Liu, Y. *Nanotechnology* **2006,** 17, 3692.

[49] Kim, Y.; Minami, N.; Kazaoui, S. *Applied Physics Letters* **2005,** 86, 073103.

[50] Zheng, W.; Zheng, Y. F. *Electrochemistry Communications* **2007,** 9, (7), 1619-1623.

[51] Salvador-Morales, C.; Flahaut, E.; Sim, E.; Sloan, *Journal of Molecular immunology* **2006,** 43, (3), 193-201.

[52] Zhu, L.; Chang, D. W.; Dai, L.; Hong, Y. *Nano Letters* **2007,** 7, (12), 3592-3597.

[53] Zhang, D.; Yi, C.; Zhang, J.; Chen, Y.; Yao, X.; Yang, M. *Nanotechnology* **2007,** 18, 475102.

[54] Hussain, M. A.; Kabir, M. A.; Sood, A. K. *Current Science* **2009,** 96, (5), 664-673.

[55] Kostarelos, K.; Lacerda, L.; Pastorin, G.; Wu, W.; WieckowskiSebastien; Luangsivilay, J.; Godefroy, S.; Pantarotto, D.; Briand, J.-P.; Muller, S.; Prato, M.; Bianco, A. *Nature Nanotechnology* **2007,** 2, (2), 108-113.

[56] Casey, A.; Davoren, M.; Herzog, E.; Lyng, F.; Byrne, H.; Chambers, G. *Carbon* **2007,** 45, (1), 34-40.

[57] Yang, W.; Thordarson, P.; Gooding, J.; Ringer, S.; Braet, F. *Nanotechnology* **2007,** 18, 412001.

[58] Czajkowska, B.; Baewicz, M. *Biomaterials* **1997,** 18, (1), 69-74.

[59] Hernández-García, D.; Castro-Obregón, S.; Gomez-Lopez, S.; Valencia, C.; Covarrubias, L. *Experimental Cell Research* **2008,** 314, (10), 2090-2099.

[60] ten Berge, D.; Koole, W.; Fuerer, C.; Fish, M.; Eroglu, E.; Nusse, R. *Cell Stem Cell* **2008,** 3, (5), 508-518.

[61] Boyd, S.; Hooper, M.; Wyllie, A. *Development* **1984,** 80, (1), 63.

Chapter: 4

Carboxylate functionalized Multiwalled Carbon nanotube modified gelatin substrate enhances cardiac differentiation and promote neuronal differentiation of mouse embryonic stem cells

Chapter Summary

There is a growing interest on the nanomaterials interactions with living cells and carbon nanotubes are versatile material with unique properties to that end. Mesoscale nano-materials have special interactions with cells due to complex and varied interactions which can modulate the behavior of cells functionally and structurally and we tried to use nanomaterials for Mesoscale culture surface modification to study the behavior of mouse embryonic stem (mES) on such surfaces. In this work, purified and carboxylate functionalized multiwalled carbon nanotubes (f-MWCNTs) dispersed in 0.01% gelatin was used to coat the polystyrene culture dishes in order to assess such composite substrate in guiding the epigenetic events to differentiate mES cells towards electro-active cardiac and neuronal lineages. We adequately characterize the substrate using FTIR and Raman spectroscopy which indicated the presence of f-MWCNTs in the modified substrates. Scanning electron microscopy (SEM) and atomic force micrsocopy (AFM) showed the embedment of f-MWCNTs into the gelatin substrate. Differentiation of mES cells was initiated by making ES cell aggregate *i.e.* embryoid body by keeping 20 µl hanging drops containing 1000 cells in leukemia inhibitory factor (LIF) free medium. These EBs were plated onto the modified culture substrates. The toxicity of CNT-gelatin matrix to cells was evaluated by MTS assay, PI staining and GFP tracking which revealed that such composites are not detrimental for normal growth and differentiation of mES cells. TEM study also exhibited that f-MWCNTs did not damage the cells. Cultures were routinely investigated for subsequent growth and differentiation through optical imaging and finally immunostaining was done to confirm the concurrent differentiation of mES cells into cardiac and neuronal lineages. We believe, embryonic and induced pluripotent stem (iPS) cell differentiation needs physical, chemical and biological clues – where this work may contribute.

4.0 Introduction

Stem cells from embryonic and non-embryonic sources are promising the advent of the era of regenerative medicine[1-4] which has further been augmented by the creation of embryonic stem (ES) cell like induced pluripotent stem (iPS) cells through cellular reprogramming.[5,6] But real hurdles in regenerative therapeutic applications of stem cells lies in achieving a comprehensive understanding of the factors involved with multi-lineage differentiations of these cells and finding out clues to control the differentiation machineries to direct these cells towards a desired lineage to produce clinical grade terminally differentiated cells with all their *in-vivo* properties.[7-9] The control of differentiation towards a particular lineage have so far been achieved with limited success for limited number of lineages with approaches ranging from culture medium optimization,[10,11] modification of cell growth and attachment substrates,[12,13] provision of physical and chemical induction factors,[14,15] creation of three dimensional *in-vivo* like growth environment[16] etc. As we know, in their natural niches, stem cells grows in special environments that provides them, firstly with a unique surface to stick to and then a practically inimitable surrounding to get the chemical and physical clues from, for initiating and directing differentiation as needed. ES and iPS cells are known to differentiate into spontaneously beating cardiac muscle cells and neuronal cells upon exposure to different chemicals[17-19] or if grown on special substrates[20,21]. So far, suggest that, any particular environment and factor favors only a particular lineage commitment. We, however, speculated that, though there are differences in their mode of action potential generation, neurons and cardiomyocytes have following things in common – both are electro-active in nature and both prefer elastic surfaces, soft matrix by neurons and rigid matrix by cardiomyocytes,[13] with conductive properties. For this reason, it might be possible to direct ES and iPS cells to commit towards cardiomogenic and neurogenic paths by providing them a substrate which will support their normal growth and proliferation and will

favor their commitment towards electro-active lineages over other types of cells. It had been reported that carbon nanotube (CNT) favors neurogenic differentiation[22-24] but there are reservations against the toxic role of CNT towards cells,[25,26] for which, in any scheme of using CNT for cellular differentiation, the direct exposure to cells should be kept to a minimum so that the toxicity of CNT, if any, will not affect the cells. Moreover, Gelatin, in one hand, is very good substrate for adherent culture of ES cells in vitro, while on the other hand, it is known to be a very good dispersant of CNT[27]. CNTs are materials of very high aspect ratio and posses metal-like electrical properties. These made CNT a material of choice when we wanted composite materials with modified electrical properties and elastic behavior both of which can define lineage commitment of stem cells. CNT dispersion in gelatin, mixed with cell culture media, proved the non-toxic nature of such dispersion to different types of cells including cardiomyocytes,[28] neurons,[29] mesenchymal stem cells[30] etc.

Consequently, in this work, we used CNT dispersed in 0.01% gelatin to coat the polystyrene culture dishes and we grew the ES cell derived embryoid bodies to see the lineage defining role of this composite substrate towards electro-active cardiac and neuronal lineages. This composite substrate material was non-toxic and biocompatible for the growth and differentiation of murine embryonic stem cells and directed the ES cells towards concurrent differentiation towards cardiomyocytes and neuronal cells. This is, as far our knowledge goes, the first report on directing ES cells differentiation concurrently towards two different lineages using the cell adherence surface modification. Though, on successful differentiation, the removal of residual CNTs may become a concern for the therapeutic applications of generated cells, but the high biocompatibility of the generated tissue to CNT and gradually decreasing concentration of CNTs in the cells due to successive cell divisions allowed us to ignore, for the time being, the CNT removal issue. We agree that this will be a major focus of research in CNT based stem cell differentiation for therapeutic purpose.

4.1 Materials and methods

4.1.1 Purification and fictionalization of MWCNTs

Arc produced multiwalled carbon nanotube (MWCNT, Wako, Japan), 40-70nm in diameter, were oxidized in 5M HNO_3 in a hot oil bath at 180°C under reflux to remove impurities and metal catalyst residues. After 48 hours, reflux was stopped and the residual acid was allowed to evaporate. Pure and functionalized MWCNT sample was collected by repeated washing and filtration using ultrapure Milli-Q water till neutral pH was reached. The pure and functionalized CNT (f-MWCNT) were the collected, dried in the convection oven to remove the excess moisture and preserved at room temperature for further use. Acid treatment generated surface functional –COOH groups on MWCNT. The presence of –COOH functional groups on CNTs was confirmed through analysis of the functionalized MWCNT by Fourier transform infrared (FT-IR) spectrometer as well as by using micro raman spectroscopy.

4.1.3 Preparation of CNT-Gelatin substrate

In the beginning, 0.1% gelatin solution was prepared in Milli-Q water and the solution was autoclaved. In our study we added 0.3 mg of the purified and functionalized CNT per ml of 0.1% gelatin solution. It was then sonicated for three hours to ensure complete dispersion of CNT into the gelatin solution. The mixture was then autoclaved again to ensure that the CNT dispersion is sterilized for use in cell culture experiments. The CNT dispersion in 0.1% gelatin was then added to polystyrene tissue culture dishes and incubated overnight at 4°C to create the gelatin embedded CNT coating for subsequent use. Before putting the cells and embryoid bodies, the CNT-gelatin dispersion was removed, fresh warm media was added to the dishes and cells or EBs were placed onto the dishes.

4.1.4 Size distribution and zeta potential measurement

We measured the size distribution of the f-MWCNT dispersions in gelatin by Zetasizer Nano ZS (Malvern, Worcestershire, UK) equipped with Dispersion Technology Software (DTS) version 5.2. After sonication of the f-MWCNT dispersion for half an hour the sample was loaded into disposable capillary cell (DTS1060) for the measurement. The dynamic light scattering (DLS) based measurements of f-MWCNT samples dispersed in water and in 0.1% gelatin solution, gave the size distribution of f-MWCNT in both the types of dispersions while at the same time we could get the zeta potential of the samples which also gives an idea about the quality of dispersion of CNTs into these two dispersants.

4.1.5 Characterization of CNT gelatin substrate

For surface characterization of the functionalized CNT modified gelatin substrates, the bottom of the treated tissue culture dishes were cut and used for tapping mode atomic force microscopy (AFM, SPA400, Seiko, Chiba, Japan), Scanning Electron Microscopic (SEM, FEI-Phillips, Hillsboro, OR) analysis fourier transform infrared microscopy (FTIR), micro raman spectroscopy and four point probe conductivity measurements. Polystyrene tissue culture dishes (35 mm, IWAKI, Japan) were coated overnight with f-MWCNT containing gelatin. The dishes were then cleaned, dried and the substrates were cut for FTIR and Raman spectroscopy. Samples prepared in the similar manner were used in atomic force microscopy. For SEM imaging, the samples were coated with osmium in an osmium coater.

4.1.6 ES cell culture

Mouse ES cells B6G2 (Riken cell bank) were cultured according to established protocol, in brief, cells were seeded onto at 5% CO_2 and 37 °C on mitomycin C-treated STO (ECACC) feeder cells. The DMEM high glucose (Nacalai Tesque) was supplemented with

15% FBS (Gibco), 0.1 mM nonessential amino acids (NEAA, Invitrogen), 1 mM L-glutamine (Invitrogen), 50 U ml^{-1} penicillin and 50 μg ml^{-1} streptomycin (Invitrogen), 0.1 μM β-mercaptoethanol (Invitrogen), and 1000 U ml^{-1} recombinant Leukemia inhibitory factor (LIF, Chemicon) with daily replenishment of fresh medium. STO cells (ECACC) were grown at 5% CO_2 and 37 °C in the medium containing DMEM high glucose (Nacalai Tesque) supplemented with 10% FBS (Gibco), 2mM L-Glutamine (Invitrogen), 50 U ml^{-1} penicillin

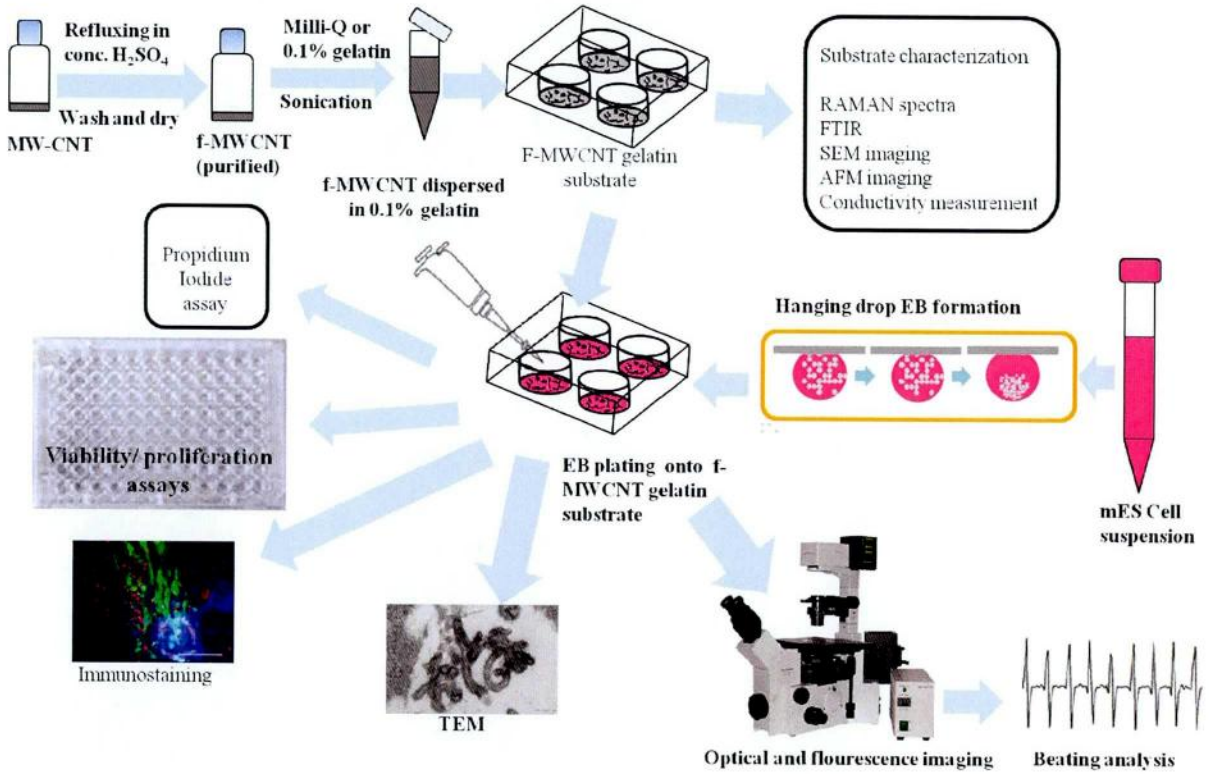

Scheme 1 *The methodology of the research at a glance in the schematic presentation – from purification and functionalization of MWCNTs to preparation and characterization of f-MWCNT modified gelatin substrate to EB plating, tissue growth and differentiation.*

with 50 μg ml^{-1} streptomycin (Invitrogen) with daily media replenishment. As they reached confluent stage, STO cells were exposed to 10 µg ml^{-1} Mitomycin C (Wako) for 2.15 h. The mitomycin C-treated MEF cells were washed in PBS and plated at 75000 cells cm^{-2} in 0.1%

gelatin-coated tissue culture dishes to form the feeder layer. Feeder cells were incubated overnight before plating ES cells.

4.1.7 Hanging drop culture for EB formation

mESC colonies formed on the feeder cells and after 2-3 days of growth the cells were trypsinized (0.05% Trypsin-EDTA, Invitrogen) and washed in fresh medium to prepare single cell suspension. The cell number was counted and the suspension containing desired cell density was used for hanging-drop cultures to form mES cell aggregates popularly known as embryoid bodies (EB) in differentiation medium which was similar to mESC medium but without LIF. On the inner side of the lid of 100 mm tissue culture dishes (Iwaki), 50 to 60 droplets each containing 20 µl of cell suspension with 1000 cells per droplet were kept. The dishes were filled with autoclaved Milli-Q water to avoid loss of nutrients through evaporation and the lid was placed so that the drops remain hanging from the lid. After 72 h of incubation at 5% CO_2 and 37 °C, spherical EBs were formed.

4.1.8 MTS assay

The toxicity f-MWCNT modified gelatin substrates mES cells and mES cell derived EBs were asseduring the formation of EBs, cells treated with 10 and 50 µl W-CNT and G-CNT dispersions per milliliter of cell suspension were kept for hanging drop EB formation. After 96 hrs of hanging drop culture the formed EBs were collected trypsinized down to single cell suspension. The cell viability and cell proliferation study was done in 96-well plate using Cell-Titer 96 Aqueous One solution Cell proliferation Assay kit (Promega, USA) according to the manufacturer's instructions. In this assay, metabolically active cells reduce MTS tetrazolium compound into colored and soluble formazan through NADPH or NADH produced from mitochondrial dehydrogenase enzymes.** The concentration of formazan which is directly proportional to the number of variable cells is measured by the absorbance

at 490nm using a 96-well plate reader (SH-100, Corona electronics, Ibaraki, Japan). We took the cell suspensions on day 0, after breaking the EBs and plated them on 96-well plates. After incubation for 2 hours, Cell-Titer 96 Aqueous One solution was added and absorbance was measured at 1, 2, 3, 4, 24 and 48 hrs to assess the viability of cells by normalizing the absorbance with respect to the control. Proliferation was studied by addition of Cell-Titer 96 Aqueous One solution to cells on day 0, day 1, day 2 and day 3 and normalizing the absorbance with respect to day 1 measurement.

4.1.9 Differentiation studies: Immunostaining

For immunostaining of the samples, we took the differentiated cells in 4-well culture dishes (Nunc, Japan), the wells were washed three times with Ca^{++} and Mg^{++} free PBS followed by the fixation of cells in 4% paraformaldehyde (Wako) solution in PBS. After fixations, the samples were washed thrice with PBS once again and cells were permeabilized with 0.2% triton X-100 (ICN biomedics) in PBS for 30 minutes. After three times PBS wash to remove the residual surfactant, the samples were blocked with bovine serum albumin (BSA, Sigma) for 2 hours. Primary monloclonal antibodies, dissolved in PBS, were α-Actinin (1:500, Sigma), ANP (1:100, Santa Cruz), Troponin (1:100, Santa Cruz), NeuN (1:200; Chemicom), Neurofilament 160KDa (1:300, Sigma). Among these α-Actinin, Troponin and ANP were used as cardiac specific markers while NeuN and Neurofilaments 160KDa were used as neuron specific markers. The secondary antibodies were Goat anti-mouse IgG-R (1:200 to 1:400, Santa Cruz) for α-actinin, NeuN and Neurofilament and Donkey anti-goat IgG-R (1:200 to 1:400, Santa Cruz) for ANP and Troponin. α-Actinin, ANP and Troponin were used for staining differentiated cardiomyocytes whereas NeuN and Neurofilaments were intended for differentiated neuronal cells. Images of immunistained samples were acquired using the BioRevo-9000 flourescence imaging system (Keyence, Osaka, Japan).

4.2 Results and discussion

4.2.1 CNT-Gelatin substrate

4.2.1.1 FTIR, Raman spectra with size distribution

We confirmed the purification of the commercial MWCNT samples and its concurrent functionalization into f-MWCNT in the form of the formation of carboxylate (-COOH) group

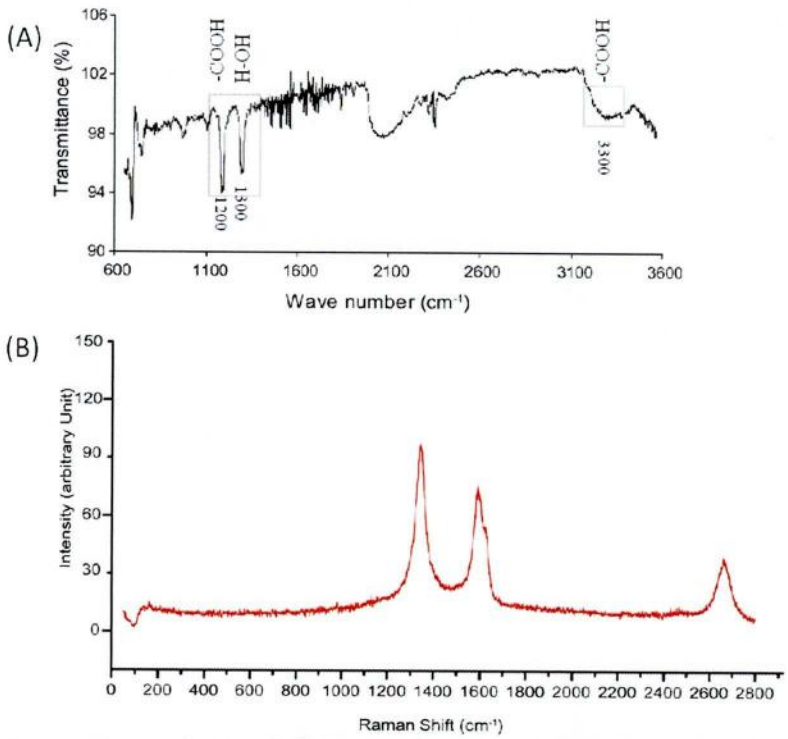

Figure 1 *Spectroscopic analysis of CNT purification and CNT modified substrate. (A) FTIR confirmed the purification of MWCNT samples and their carboxylate functionalization. (B) Raman spectra showing the differences between CNT dispersions in water and in Gelatin. The presence of radial D, D' and G bands confirmed the presence of f-MW CNTs in the CNT modified gelatin substrates*

on the side wall and ends of MWCNTs by FTIR study. There was no characteristic peak from metallic catalyst and other adulterants indicated the purification of MWCNTs. We have

observed an absorbance band at about 1,300 cm^{-1} for O–H bending deformation and the broad peak at around 3300 cm^{-1} for O–H stretching vibration from carboxyl groups in the FTIR spectra (Fig. 1A).[32] Another peak was seen at around 1200 cm^{-1} and O-H group from ambient moisture bound to MWCNTs.[33]

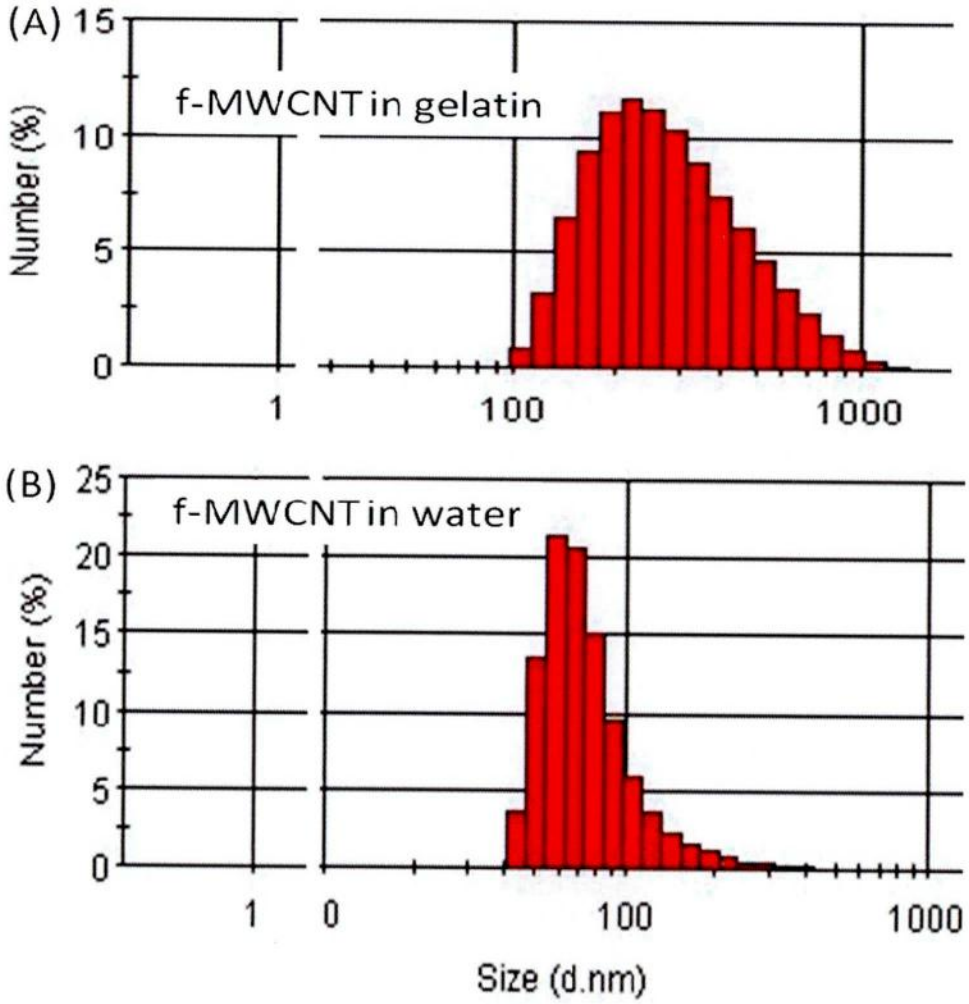

Figure 2 *The size distribution of f-MWCNT dispersed in gelatin compared to water. The size indicates the hydrodynamic radius of CNTs and the higher value of that in case of gelatin dispersion indicated straightening of CNTs in gelatin dispersion and the that CNT disperses better in gelatin.*

On the other hand, Raman spectra (Fig 1B) confirmed the presence of CNT in the gelatin-CNT substrate by exhibiting the presence of G, D and D' bands in the spectra typical to MWCNTs. On the other hand, as we assessed the size distribution (Fig 2) of these dispersions in terms of hydrodynamic radius, we saw that gelatin dispersed samples had bigger size than water dispersed ones. We assume this was due to two reasons – firstly, the stretching of normally folded MWCNTs in gelatin[34] and secondly, due to the hydrophobic interaction between the hydrophobic amino acids of zwitterionic gelatin structure and the hydrophobic wall of the single or aggregated MWCNTs.[35]

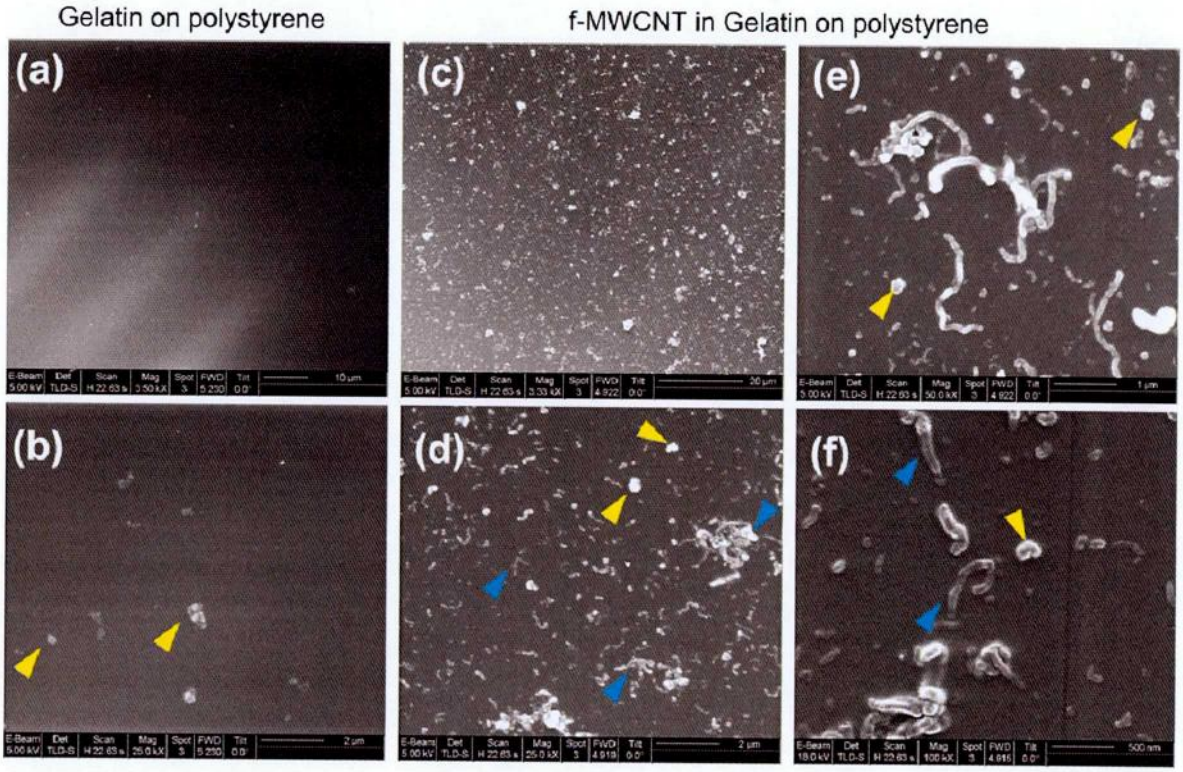

Figure: 3 *The SEM image of the f-MWCNT modified gelatin substrate showing almost uniform distribution (c, d) of CNTs in gelatin and only gelatin coated substrates (a, b) were clean with some specs of gelatin seen at high magnification (yellow arrowheads. High magnification images (e, f) show that CNTs are partially or completely embedded into gelatin coating. Moreover there was no indication of the formation of a continuous conductive mesh by CNTs.*

4.2.1.2 SEM of the substrate

SEM images (Fig 3) showed the presence of f-MWCNTs on the surface of gelatin coated substrate. The MWCNTs were partially or completely embedded into the gelatin coating layer. There was relatively uniform distribution of MWCNTs on the culture substrate but they did not show any continuous mesh of MWCNTs which explained why we did not find any conductivity of the composite substrate when we tried to measure the conductivity using four point probe. Our results indicated that the probable interaction of such embedded CNTs with cells will be anchorage dependent and there is possibility of local connectivity initiation among the electro active cardiac or neuronal cells.

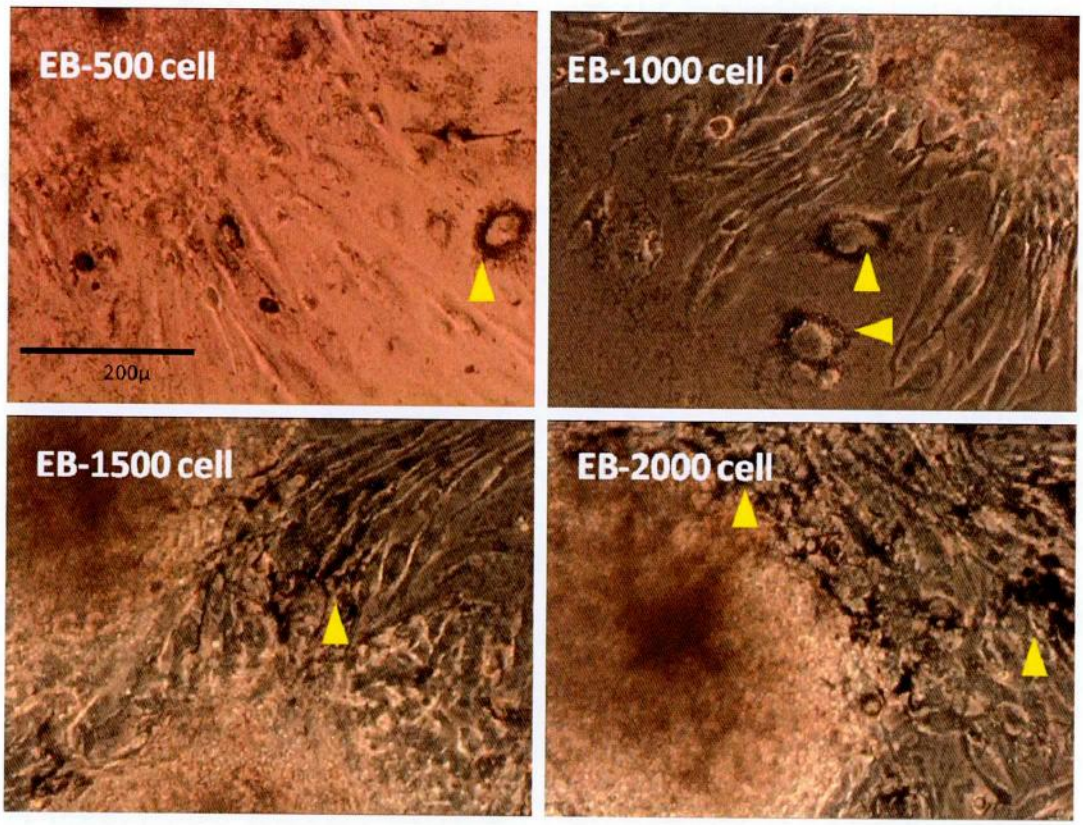

Figure 5 *The aggregates of CNTs (yellow arrowheads) which may have been uptaken by some cells outgrowing from plated EBs created from different cell numbers.*

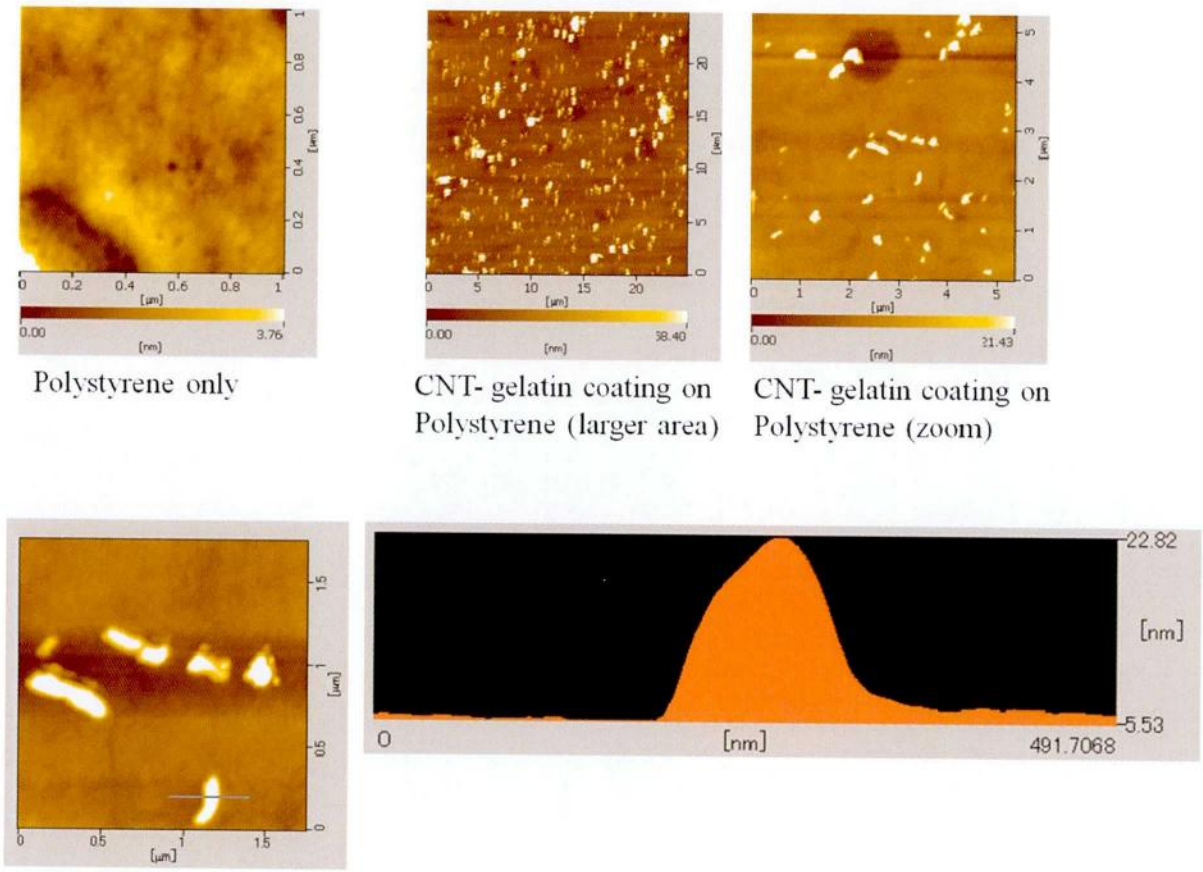

Figure 4 *The AFM micrograph showed the uniform layer of gelatin embedded f-MWCNTs on the culture substrate. The height measurements (lower panel) from AFM also agreed with our conclusion that CNTS were not on the surface of the gelatin coating; rather they were embedded into the gelatin layer.*

4.2.1.3 AFM

AFM imaging (Fig 4) also revealed the presence of uniformly distributed f-MWCNTs on the surface of gelatin coated substrate when compared to only gelatin coated substrate. The MWNT diameter was in the range of 30-50 nm and if we compare that with the 22 nm height of one nanotube on the substrate, we can conclude that f-MWCNTs were embedded into gelatin.

4.2.2 Uptake of MW-CNT by cells

As we can see from Fig 5, as the EBs were plated onto CNT-gelatin substrate, some of the cells were loaded with CNTs and those were visible in light micrographs, due probably to the aggregate formation of CNTs. As the cells move onto the culture surface continuously during the outgrowth of EBs, some of the loosely bonded f-MWCNTs might have detouched and subsequently uptaken by cells. But the sizes of the f-MWCNT aggregates as visible in the optical micorgraphs, led us to consider another probability that after getting detached from the substrates those big aggregates of CNTs were not taken up by cells, rather they were buried under the mass of cells or such aggregates were present in the intercellular spaces within the grown tissue. But we speculate that all such scenarios were happening simultaneously.

4.2.3 Toxic effect of CNT substrate on cells

The MTS assay (Fig 6) showed that the f-MWCNT modified culture substrates are not deleterious for the initial viability of the cells on such substrates subsequent to the plating of mES derived embryoid bodies as compared to the non-CNT control substrates. Moreover as we studied the long term proliferation of cells from plated EBs onto CNT-Gelatin composite substrate, we observed that, the cell proliferation, in the long run, were not also affected by the presence of f-MWCNTs on the culture substrate.

On the other hand, when we did the the actual counting of cells after growth of EBs for Day 1, day 2 and day 3, we observed showed almost similar proliferation pattern with control substrate i.e. substrate with only gelatin coating. Live dead assay using propidium iodide, which stains the dead cell nucleus to red, we could see that CNT modified surface supported almost similar growth of cells as in gelatin.

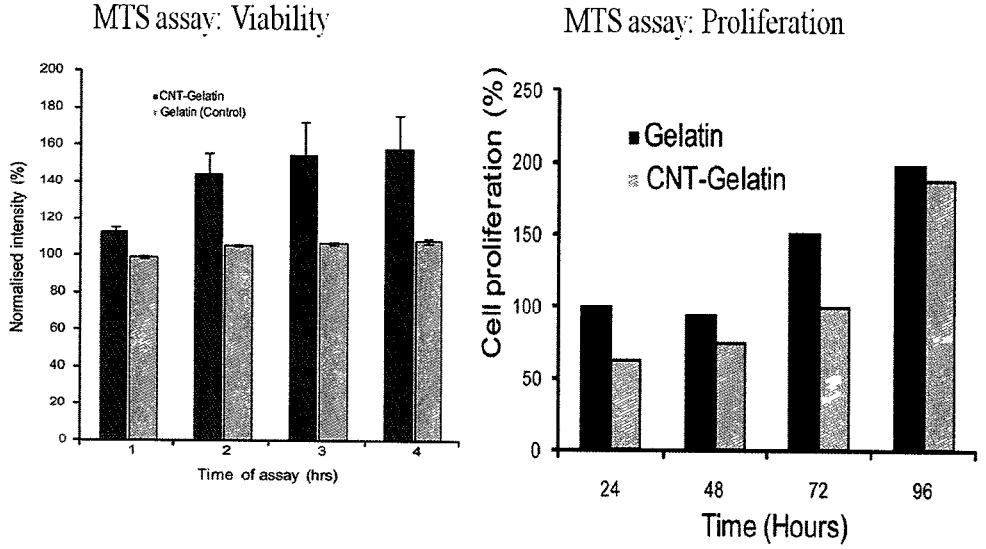

Figure 6 *MTS assay showing viability (Left) of cells after initial exposure to the CNT modified gelatin substrate and the proliferation of cells from EBs on CNT modified gelatin substrates. In the first three days cell proliferation was less but on day for it almost became equal to control plates.*

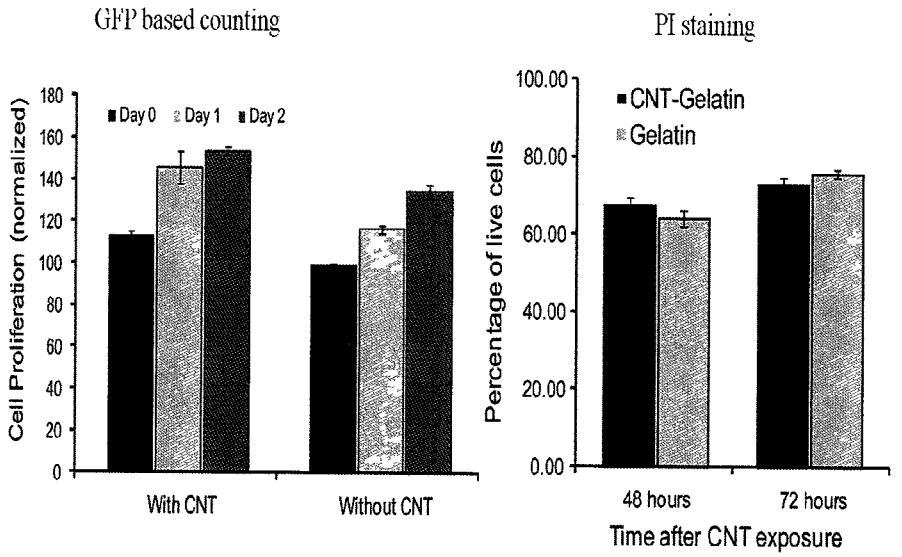

Figure 7 *Actual counting of cells (based on the green fluorescence from the mouse ES cells line) grown EBs with the progression of culture on day 0, day 1 (Left) and the live dead assay using propidium iodide assay (Right). Both approaches showed that cell proliferation and the percentage of live cells present were not affected to a mentionable extent by the presence of CNTs in gelatin.*

4.2.4 Cardiac Differentiation

The differentiation of cells into cardiomyocytes on the CNT-gelatin coated substrate was observed and confirmed by our video image analysis method and immunostaining. The beating zones showed bright green fluorescence from organized cardiac tissue in fluorescence microscopy. The organization of beating tissue was quite different and it looked better in CNT containing culture surface than in only gelatin coated surfaces as evident from immunostaining images (Fig 9).

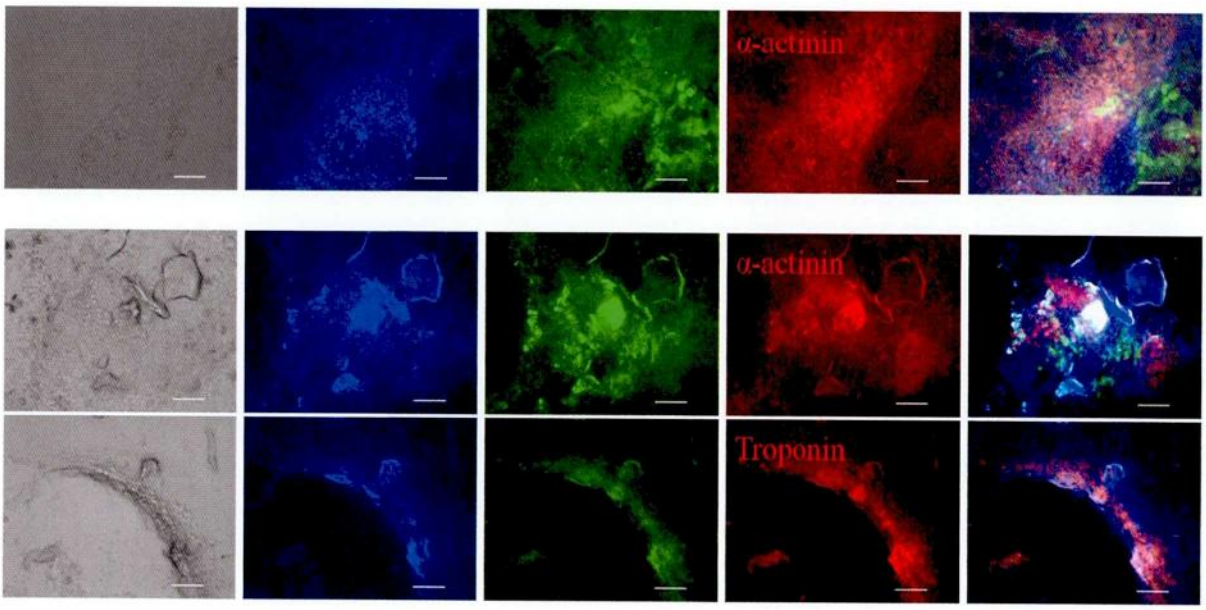

Figure 9 *Immunostaining of grown and differentiated tissue on the f-MWCNT modified culture substrate. Upper panel shows cardiomyocytes from control substrate (only gelatin) and the lower panels show the presence of better organized and more prominent cardiomyocytes on CNT modified substrate.*

4.2.5 Neural differentiation

Usually, one particular environment favors one particular kind of cells with exceptions. In our study, we have found the concurrent differentiation of mouse ES cells into beating

cardiomyocytes and glia like neuronal cells. The presence of neuronal cells was confirmed by fluorescence imaging and form immunostaining using neuronal nuclear marker Neu-N.

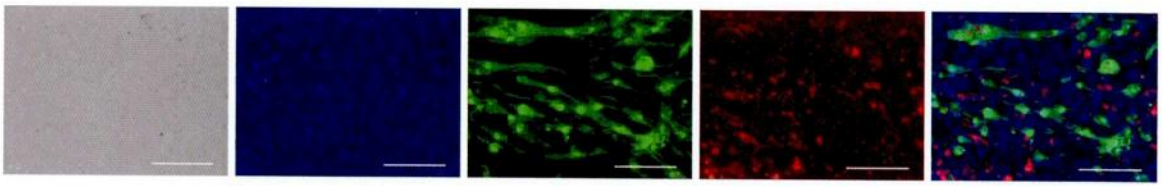

Figure 10 *Immunostaining of grown and differentiated tissue on the f-MWCNT modified culture substrate. Upper panel shows cardiomyocytes from control substrate (only gelatin) and the lower panels show the presence of better organized and more prominent cardiomyocytes on CNT modified substrate.*

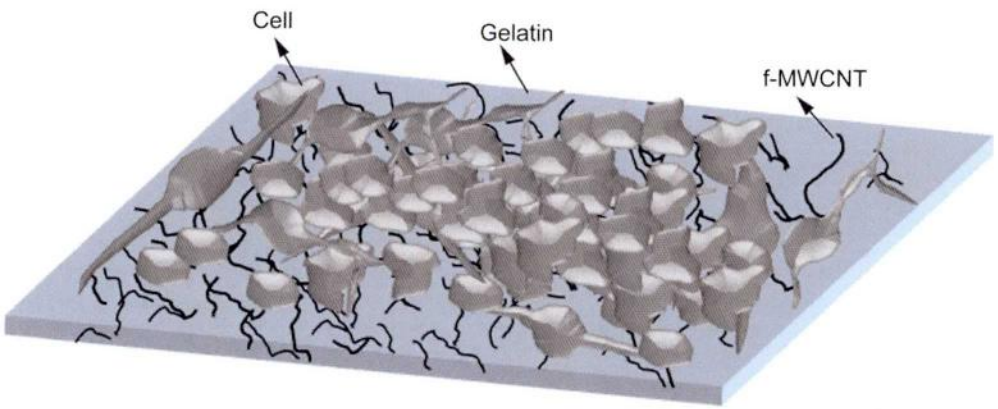

Scheme 2 *Schematic presentation of ES cell proliferation and differentiation of gelatin substrate modified with carboxylate functionalized multiwalled carbon nanotubes (f-MWCNTs). CNTs do not form any continuous rather a disjoin mesh with portion embedded into gelatin and portion protruded out of the gelatin substrate. Such inclusion changes the substrate physical properties, and help better cell anchorage while provides some local connectivity between electro-active cells.*

The co-differentiation of mES cells into neuronal and cardiac cells can be viewed in terms of the scheme 1, where we have shown that the f-MWCNTs sporadically embedded into the gelatin coating can create an environment which promoted local connectivity among the electro active cells, *i.e.* neurons and cardiomyocytes. Such local electrical connectivity may have promoted enhanced differentiation of such cells from the progenitor cells, which in absence of such substrate may not mature into cells of electroactive lineage.

4.3 Conclusion

In this work, purified and carboxylate functionalized multiwalled carbon nanotubes (f-MWCNTs) dispersed in 0.01% gelatin was used to coat the polystyrene culture dishes in order to assess such composite substrate in guiding the epigenetic events to differentiate mES cells towards electro-active cardiac and neuronal lineages. We adequately characterize the substrate using FTIR and Raman spectroscopy which indicated the presence of f-MWCNTs in the modified substrates. Scanning electron microscopy (SEM) and atomic force micrsocopy (AFM) showed the embedment of f-MWCNTs into the gelatin substrate. Differentiation of mES cells was initiated by making ES cell aggregate *i.e.* embryoid body by keeping 20 µl hanging drops containing 1000 cells in leukemia inhibitory factor (LIF) free medium. These EBs were plated onto the modified culture substrates. The toxicity of CNT-gelatin matrix to cells was evaluated by MTS assay, PI staining and GFP tracking which revealed that such composites are not detrimental for normal growth and differentiation of mES cells. TEM study also exhibited that f-MWCNTs did not damage the cells. Cultures were routinely investigated for subsequent growth and differentiation through optical imaging and finally immunostaining was done to confirm the concurrent differentiation of mES cells into cardiac and neuronal lineages. The differentiated cardiomyocyte properties have also been analyzed using our novel intensity variation based video image analysis method. We

believe, embryonic and induced pluripotent stem (iPS) cell differentiation needs physical, chemical and biological clues – where this work may contribute.

4.4 References

[1] Christou, Y. A.; Moore, H. D.; Shaw, P. J.; Monk, P. N. *Neuropathology and Applied Neurobiology* **2007**, *33*, 485–498.

[2] Amabile, G.; Meissner, A. *Trends in Molecular Medicine* **2009**, *15*, 59–68.

[3] Gurtner, G. C.; Callaghan, M. J.; Longaker, M. T. **2007**.

[4] Mimeault, M.; Hauke, R.; Batra, S. K. *Clinical Pharmacology & Therapeutics* **2007**, *82*, 252–264.

[5] Okita, K.; Nakagawa, M.; Hyenjong, H.; Ichisaka, T.; Yamanaka, S. *Science* **2008**, *322*, 949.

[6] Takahashi, K.; Tanabe, K.; Ohnuki, M.; Narita, M.; Ichisaka, T.; Tomoda, K.; Yamanaka, S. *Cell* **2007**, *131*, 861–872.

[7] Hwang, N. S.; Varghese, S.; Elisseeff, J. *Advanced Drug Delivery Reviews* **2008**, *60*, 199–214.

[8] Graf, T.; Enver, T. *Nature* **2009**, *462*, 587–594.

[9] Mantalaris, A.; Randle, W. L.; Polak, J. M. *Stem Cell Repair and Regeneration* **2008**, 45.

[10] Gong, Z.; Calkins, G.; Cheng, E.; Krause, D.; Niklason, L. E. *Tissue Engineering Part A* **2008**, *15*, 319–330.

[11] Shi, X. L.; Mao, L.; Xu, B. Y.; Xie, T.; Zhu, Z. H.; Chen, J. H.; Li, L.; Ding, Y. T. *Cell Biology International* **2008**, *32*, 959–965.

[12] Dawson, E.; Mapili, G.; Erickson, K.; Taqvi, S.; Roy, K. *Advanced Drug Delivery Reviews* **2008**, *60*, 215–228.

[13] Engler, A. J.; Sen, S.; Sweeney, H. L.; Discher, D. E. *Cell* **2006**, *126*, 677–689.

[14] Borowiak, M.; Maehr, R.; Chen, S.; Chen, A. E.; Tang, W.; Fox, J. L.; Schreiber, S. L.; Melton, D. A. *Cell Stem Cell* **2009**, *4*, 348–358.

[15] Schugar, R. C.; Robbins, P. D.; Deasy, B. M. *Gene Therapy* **2007**, *15*, 126–135.

[16] Ferreira, L. S.; Gerecht, S.; Fuller, J.; Shieh, H. F.; Vunjak-Novakovic, G.; Langer, R. *Biomaterials* **2007**, *28*, 2706–2717.

[17] Willems, E.; Bushway, P. J.; Mercola, M. *Pediatric Cardiology* **2009**, *30*, 635–642.

[18] Xu, Y.; Shi, Y.; Ding, S. *Nature* **2008**, *453*, 338–344.

[19] Greco, S. J.; Rameshwar, P. *Molecular BioSystems* **2010**, *6*, 324–328.

[20] Horton, R. E.; Millman, J. R.; Colton, C. K.; Auguste, D. T. *Regenerative Medicine* **2009**, *4*, 721–732.

[21] Reilly, G. C.; Engler, A. J. *Journal of Biomechanics* **2009**.

[22] Lee, W.; Parpura, V. *Progress in Brain Research* **2009**, 110–125.

[23] Chao, T. I.; Xiang, S.; Chen, C. S.; Chin, W. C.; Nelson, A. J.; Wang, C.; Lu, J. *Biochemical and Biophysical Research Communications* **2009**.

[24] Jan, E.; Kotov, N. A. *Nano Letters* **2007**, *7*, 1123–1128.

[25] Firme III, C. P.; Bandaru, P. R. *Nanomedicine: Nanotechnology, Biology and Medicine* **2009**.

[26] Inoue, K.; Yanagisawa, R.; Koike, E.; Nishikawa, M.; Takano, H. *Free Radical Biology and Medicine* **2010**.

[27] Kim, Y.; Minami, N.; Kazaoui, S. *Applied Physics Letters* **2005**, *86*, 073103.

[28] Krajcik, R.; Jung, A.; Hirsch, A.; Neuhuber, W.; Zolk, O. *Biochemical and Biophysical Research Communications* **2008**, *369*, 595–602.

[29] Sucapane, A.; Cellot, G.; Prato, M.; Giugliano, M.; Parpura, V.; Ballerini, L. *Journal of Nanoneuroscience* **2009**, *1*, 10.

[30] Mooney, E.; Dockery, P.; Greiser, U.; Murphy, M.; Barron, V. *Nano Letters* **2008**, *8*, 2137–2143.

[31] Sato, T. *J Electron Microsc (Tokyo)* **1968**, *17*, 158-159.

[32] Kan, K.; Xia, T.; Yang, Y.; Bi, H.; Fu, H.; Shi, K. *Journal of Applied Electrochemistry* **2010**, *40*, 593-599.

[33] Haldorai, Y.; Lyoo, W.; Shim, J. *Colloid & Polymer Science* **2009**, *287*, 1273-1280.

[34] Kim, Y.; Minami, N.; Kazaoui, S. *Applied Physics Letters* **2005**, *86*, 073103.

[35] Zheng, W.; Zheng, Y. *Electrochemistry Communications* **2007**, *9*, 1619-1623.

Chapter: 5

Microfluidic hanging drop chip for the formation of embryoid body with from mouse ES and iPS cells under medium replenishment for long term culture

Chapter summary

The advent of induced pluripotent stem cells (iPSC) has augmented our overall interest in embryonic stem (ES) cells and non-embryonic pluripotent cell research especially with a view to control the differentiation of such cells to clinically relevant lineages for applications in regenerative medicine. In the differentiation studies, the common means for the onset of differentiation is to create stem cell embryoid bodies (EBs) – the three dimensional spherical aggregates of ES or iPS cells where cells spontaneously onset the epigenetic changes and arranged themselves into three germ layers containing different precursor cells for different organ system. Of a large number of methods developed, hanging drop culture proved to be efficient in EB formation with limitations of medium deprivation, lack of long term culture capabilities, necessity of repeated manual interventions and disturbances at different stages. In this research we tried to develop gravity and centrifugation based microfluidic chips for cell aggregation and we are reporting the successful gravity based microfluidic hanging drop chips. The chip, made of PDMS from SU-8 molds on Si-wafer, was bonded to glass through oxygen plasma treatment. We kept the chips glued to the upper lid of conventional tissue culture dishes to form hanging drops. The chip successfully demonstrated its applicability for ES and iPS cell aggregation. The EBs formed from the chips showed comparable growth to control EBs from traditional hanging drop cultures. As we supplemented the culture medium with cardiac differentiation enhancer GSK3β inhibitor, cardiac differentiation came from chip derived EBs. The chips were designed in such a way that in the future, by the addition of a second layer for cell culture at the bottom of hanging drop chip will enable these chips to do aggregation, differentiation and further investigations on an integrated single platform which may open up new windows of microfluidic based stem cell research.

5.0 Introduction

Embryoid bodies (EB) are three dimensional cell aggregates, preferably spherical in shape, derived spontaneously from suspension culture or hanging drop culture of embryonic stem cells or induced pluripotent stem (iPS) cells in the absence of the feeder cells and anti-differentiation factors such as Leukemia Inhibitory Factor (LIF). Embryoid bodies are capable of emulating the phases of early gastrulation as seen in the development of an embryo, at least to some extent, for which there is rising interest in EBs as a model for studying early embryogenesis.[1] Moreover, EBs are important in the investigations involving drug screening, the cell fate determination,[2] the production of terminally differentiated cells like cardiomyocytes,[3] neurons,[4,5] pancreatic islets cells for regenerative medicine, are few examples. The mean to generate EBs are several, for example, suspension culture in bacterial grade dishes, methylcellulose culture (MC culture), hanging drop culture (HD culture) on inverted cell culture ware lids, suspension culture in low-adherence well plates, and spinner flask and bioreactor techniques for scalable production.[6] Each of these methods has intrinsic limitations. Suspension culture do not produce uniform size EBs and EBs formed are not spherical. Hanging drop culture produces EBs of uniform in size and spherical shape and the cells are aggregated at the bottom of the spherical hanging drops under the force of gravity which keeps them in an environment of favorable gaseous exchange. The main drawback of traditional hanging drop method is the nutrient deprivation suffered by EBs since media replenishment is impossible without disturbing the EBs under formation over a usual three to four days culture regime. Methylecellulose culture is more preferable as a mean to preserve already formed EBs than for EB formation itself. Formation of EBs from single cell clones in methylecellulose culture is reported, but there is always a mechanical pressure against

expanding EB sphere due to high viscosity of methyl cellulose media. Moreover, replenishing medium is also cumbersome in this method.

We are still in a quest for a simple and more efficient mechanism for high throughput production uniform and spherical EBs. On the other hand, microfluidic is an emerging technology offering greater control over fluid manipulation at micron scale. A few microfluidic approaches[7, 8, 9, 10] have been reported but these also did not put attention to medium exchange for long term EB culture and did not designed the chip for future integration into stand alone S cell differentiation chips. Moreover, the EBs were either put under shear stress from the flowing liquid inside the micro channels which, expectedly, come to play negatively with the ES/iPS cell organization into embryoid bodies.

In this article, we are proposing a simple microfluidic platform that ensures production of EBs of sizes and shapes in numbers. In this paper, we have reported a microfluidic platform for the hanging drop gravity based embryoid body formation. After trying to use gravity and centrifugal forces for cell aggregation on microfluidic devices, due to the problem associated with bubble formation in centrifugal devices, we opted to use gravity based hanging drop chips for cell aggregation. The chips were fabricated using PDMS based photolithography method. The chips of various designs and different throughputs were investigated and the optimum designs were selected based on optimization studies. Our chips successfully created ES and iPS EBs after three to four days of hanging drop culture. The chip derived EBs showed comparable in size and shape to traditional hanging drop EBs and were successfully grown and differentiated into contractile cardiomyocytes upon addition of cardiomyogenic enhancer GSK3β inhibitor to the cell culture medium. The chip has the potential for medium supplementing for long term EB culture and for being appended into an integrated EB and differentiation platform in the future.

5.1 Materials methods

5.1.1 Fabrication and characterization of the chip

We thought of using centrifugal force or gravitational force for the aggregation of ES/iPS cells. The chips of different designs have been thought of in the beginning. The masks were prepared from designs made by using Adobe Illustrator (CS2) software. The masks (Fig 1 and Fig 2) were printed on plastic transparency sheets and later trimmed into desired sizes. The SU-8 mold was prepared on Si-wafer by spin coating on the IH-D7 spin coater (Mikasa, Japan) the SU-8 100 (microchem) onto the wafer surface to get the desired thickness. The SU-8 layer was prebaked on a digital hot plate (DP-2S, AsOne, Japan) before exposing it to UV light through the mask using a mask aligner (Mikasa, Japan). Then it was post backed and developed in SU-8 developer solution which removed the unexposed SU-8 leaving the pattern of the chips onto the Si-wafer. The mask was adequately cleaned and dried using N_2 gas blow using ethanol and acetone to remove traces of unbound SU-8.

5.1.2 ES/iPS Cell culture

ES/iPS cells were grown according to protocol established protocol,[11] in brief, 10% FBS (Gibco), 2 mM L-glutamine (Invitrogen), 50 U ml^{-1} penicillin with 50 μg ml^{-1} streptomycin (Invitrogen) supplemented DMEM high glucose (Nacalai Tesque) was used to culture STO (ECACC) cells at 37°C and 5% CO_2 in humidified incubator, media was changed daily. STO cells, at confluence stage, were exposed to 10 µg ml^{-1} Mitomycin C (Wako) for 2.15 h, trypsinized, washed in PBS and plated at 75000 cells/cm^2 as feeder layer onto gelatin-coated tissue culture dishes and incubated overnight before plating ES cells. Mouse ES cells (B6G2, Riken cell bank) were cultured on mitomycin C-treated STO (ECACC) feeders in medium

containing DMEM high glucose (Nacalai Tesque) supplemented with 15% FBS (Gibco), 0.1 mM nonessential amino acids (NEAA, Invitrogen), 2 mM L-glutamine (Invitrogen), 50 U/ml

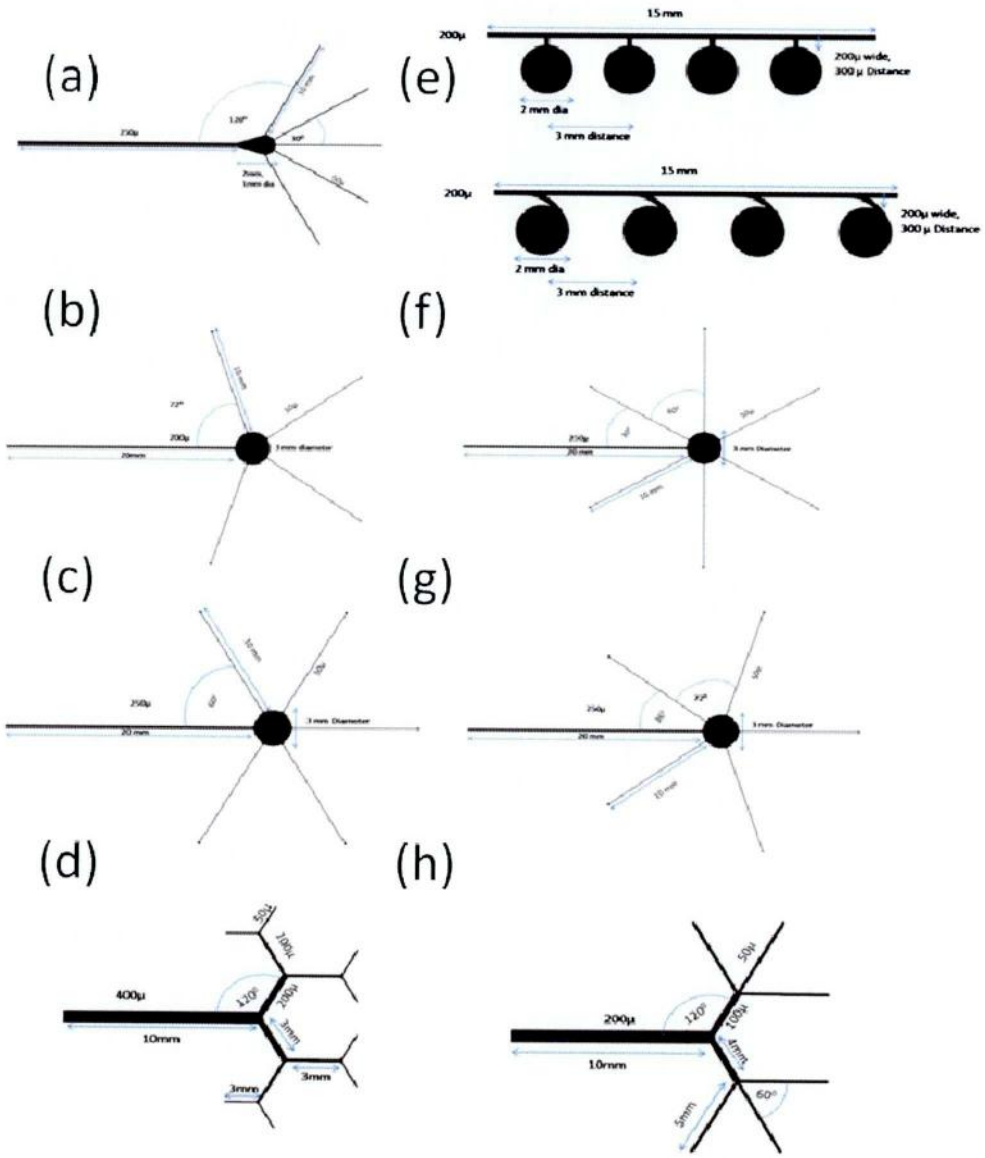

Figure 1 *Designs of low throughput microfluidic hanging drop chips for EB formation. After fabrication and trial with all these designs we found designs b, c, f, g works well and we conducted our further rworks based on design f, containing four outlest leading to the formation of four EBs in a run.*

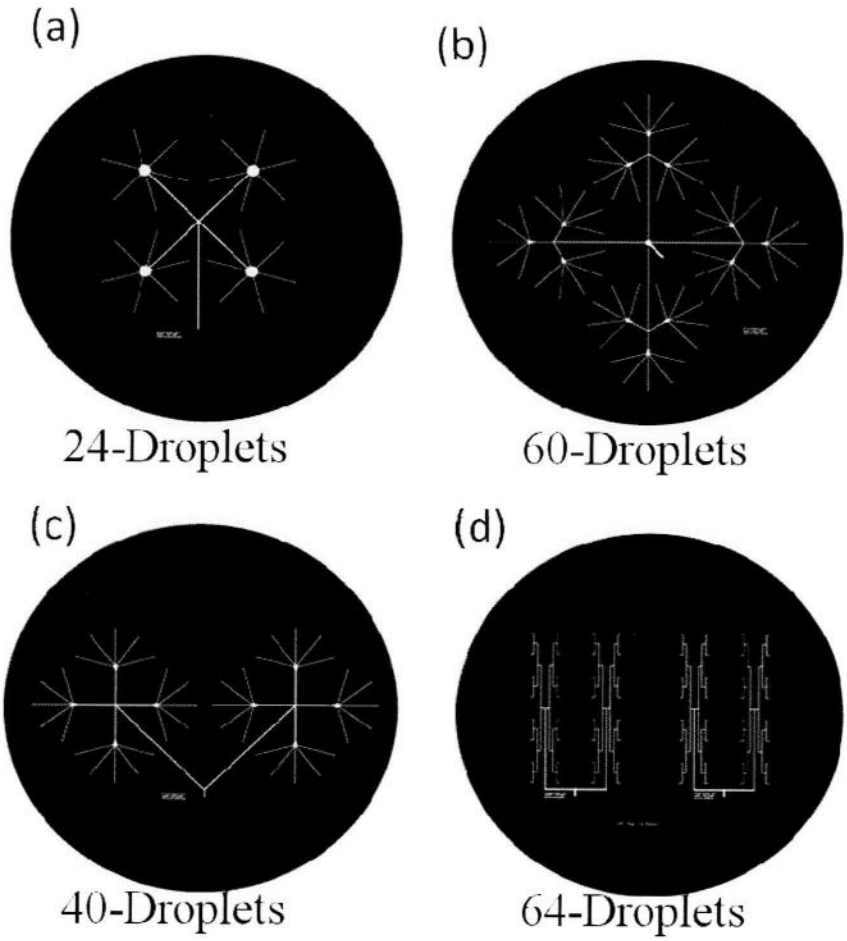

Figure 2 *High throughput designs of the microfluidic hanging drop chips. Designs a and d worked better and in other two the droplets were very close to each others.*

penicillin and 50 μg/ml streptomycin (Invitrogen), 0.1 μM β-mercaptoethanol (Invitrogen), and 1000 U/ml recombinant Leukemia inhibitory factor (LIF, Chemicon). Dishes were incubated in humidified incubator at 5% CO_2 and 37 °C with daily replenishment of fresh medium. B6G2 cells express green fluorescent protein (GFP) ubiquitously under beta-actin promoter and helps monitoring the growth of tissue from such cells by their characteristic green fluorescence. On the other hand iPS cells (Received from Professor Sawa group, Medical faculty, Osaka University)

expresses DSRed based red fluorescence that helped monitoring the growth of tissue from such cells.

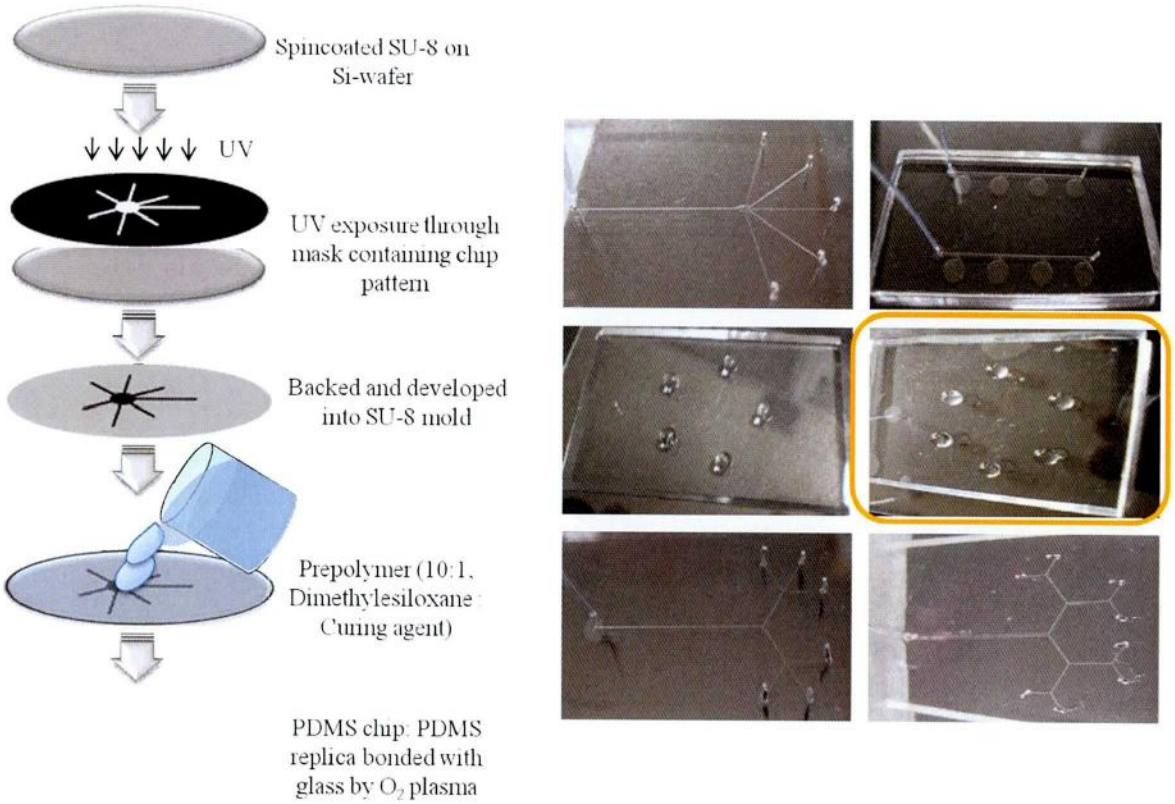

Figure 3 *Fabrication procedure of the microfluidic devices (left column) and the finalized chips (right columns). The chip marked yellow were the optimum one and we used this chip for further investigations.*

5.1.3 Preparation of iPS cells for Embryoid Body formation on chip

mES cell or iPS cell monolayer on feeder cells were trypsinized (0.05% Trypsin-EDTA, Invitrogen) after 2 to 3-days of culture, to prepare single cell suspension and the cell number was counted. The suspension was used for hanging-drop cultures to form mES cell aggregates popularly known as embryoid bodies (EB) in differentiation medium which is similar to

mES/iPS medium excluding LIF. On the inner side of the lid of 100 mm tissue culture dish (Iwaki), 50 to 60 droplets, 20 µl in volume containing 1000 cells per drop were kept. These were used as control as this is the widely adopted protocol for EB formation. The dishes were filled with autoclaved Milli-Q water to avoid loss of nutrients through evaporation and the lid was placed so that the drops hang from the lid. After 72 h of incubation at 5% CO_2 and 37 °C, spherical EBs were formed (Fig. 1).

5.1.4 Sterilization of chips

The chips were attached with tape to the upper lid of the tissue culture dishes. Chips and all other materials used were autoclaved. For chips three steps sterilization was done. Firstly, absolute ethanol was pumped through the channels followed by repeated washing with sterile Milli-Q water. It was then followed by dry sterilization in a convectionoven at 180°C for an hour. The chips were then kept under UV exposure for 30 minutes before use for surface sterilization.

5.1.5 Hanging drop cell culture of iPS cells on chip

The same cell suspension was introduced into the chips manually for the formation of droplets of desired sizes (20 to 30 µl in volumes) containing desired number of cells (500, 1000, 1500 or 2000 cells). The pumping, in these experiment were done manually after taking the amount of cell suspension needed to the droplet formation into the syringe, but in ultimate use of the chip these pumping can be easily automated with the help of a syringe pump or can be integrated into the chip by using valve controls. After the formation of droplets, chip containing lid was kept on the lower part of the tissue culture dish in order to form hanging drops. The

lower dish was filled with sterile Milli-Q water to check evaporation. In the future designs, the measures for controlling evaporation can be incorporated into the stand alone chips.

5.1.6 Formation of EBs on chip

The dishes were then kept in an incubator at 37°C in a 5% CO_2 environment for three to four days before taking them out for transferring the formed EBs. In three days satisfactory cell aggregation was observed. The EBs were transferred from the chips using a pipette under a light microscope in order to avoid damage to EBs.

5.1.6 Evaluation of EBs

The transferred EBs were evaluated by optical imaging and analysis of their size and shape in comparison with the control EBs. Moreover, such EBs were plated in 0.1% gelatin coated tissue culture dishes and the control EBs were also plated alongside in separate dishes. The attachment of EBs to dishes and their subsequent growth and proliferation were observed to assess the quality of chip derived EBs.

5.1.9 Generation of cardiomyocytes from EBs by adherent culture

During the EB formation, the LIF free differentiation medium we used were supplemented with GSK3β inhibitor which is known as an agent to enhance cardiogenesis from ES and iPS cells. Upon plating and subsequent tissue growth, the chip derived EBs formed beating contractile colonies of cardiomyocytes which were assessed by video monitoring under optical and fluorescence microscopy (IX70, Olympus, Japan). The functionality of these contractile EBs were also assessed by measuring the Ca^{++} dynamics by using fluo-4 assay.

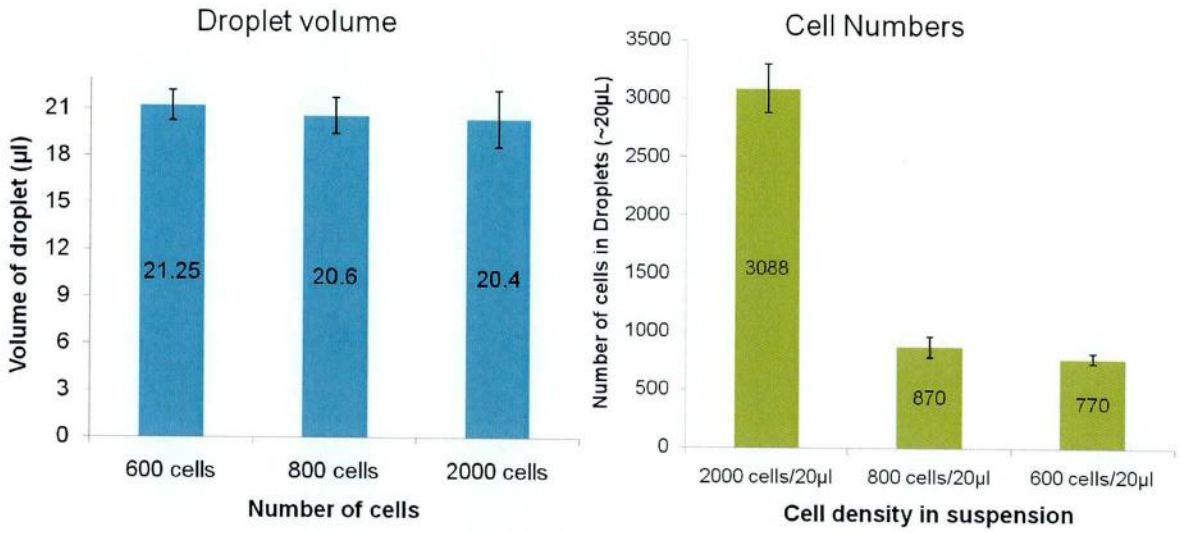

Figure 4 *The volume distribution of droplet in the low throughput chips (Left column) and the cell distribution in each final droplet (Right column)*

5.2 Results and discussion

5.2.1 Optimization of the chip design

The chips were optimized based on their ability to produce equal size droplets at the outlet through equal distribution of cell suspension through the channels. The designs (Fig 1 and Fig 2) that worked well in case of low throughput chips contained a central circular reservoir connected to inlet and the outlets radiated out of the central channel. We had four, five and six outlet designs with the outlet channels forming different angles with eact other and with the inlet channel. The design (Fig 1,f) that worked the best contained outlets placed at 60° with each other and the outlets adjacent to the inlet formed 30° with the inlet channel. This design helped the distribution of the suspension better due to the angular orientation. In all the designs, the inlet was 200 µm wide and the outlets were 50 µm wide. The central reservoir had a diameter of 3

mm and all the channels and the reservoir had a height of 200 μm. In case of high throughput designs, due to optimum and equal distribution channels, we observed the best result from chip which could accommodate 32 droplets in a single segment and it contained two segments leading to the formation of 64 droplets in a dual run. In future, the two segments can be integrated together to form 64 droplets in a single run.

5.2.2 Characterization of the chips

The low throughput chip was characterized by measuring the output droplet sizes for different densities of cells as well as the final count of the cells in these droplets. The result showed that, the output droplet sizes were almost near to the desired 20 μl in volume and it was almost uniform. The little variations were, we speculate related to manual punching of outlet holes which created uneven hole size at different outlets. On the other hand, we got higher numbers of cells than expected in each of the droplets. This was attributed to the excess volume of cell suspension in the channels and the reservoir which also contained few cells and those cells came to form the aggregate raising the number of cells in each droplet.

5.2.3 Increasing the throughput

The throughput increment was done by integrating the low throughput chips in a format that ensures the equal distribution of cell suspension through all the channels and that the liquid reaches all the outlets at the same time to make sure that uniformly sized droplet form in the outlets. But simple combining of the low throughput designs did not work well as after integration some of the outlets became very closer in proximity to each other. It led to the problem of droplet coalescence. The problem was solved by adopting a binary flow division on microfluidic platform.

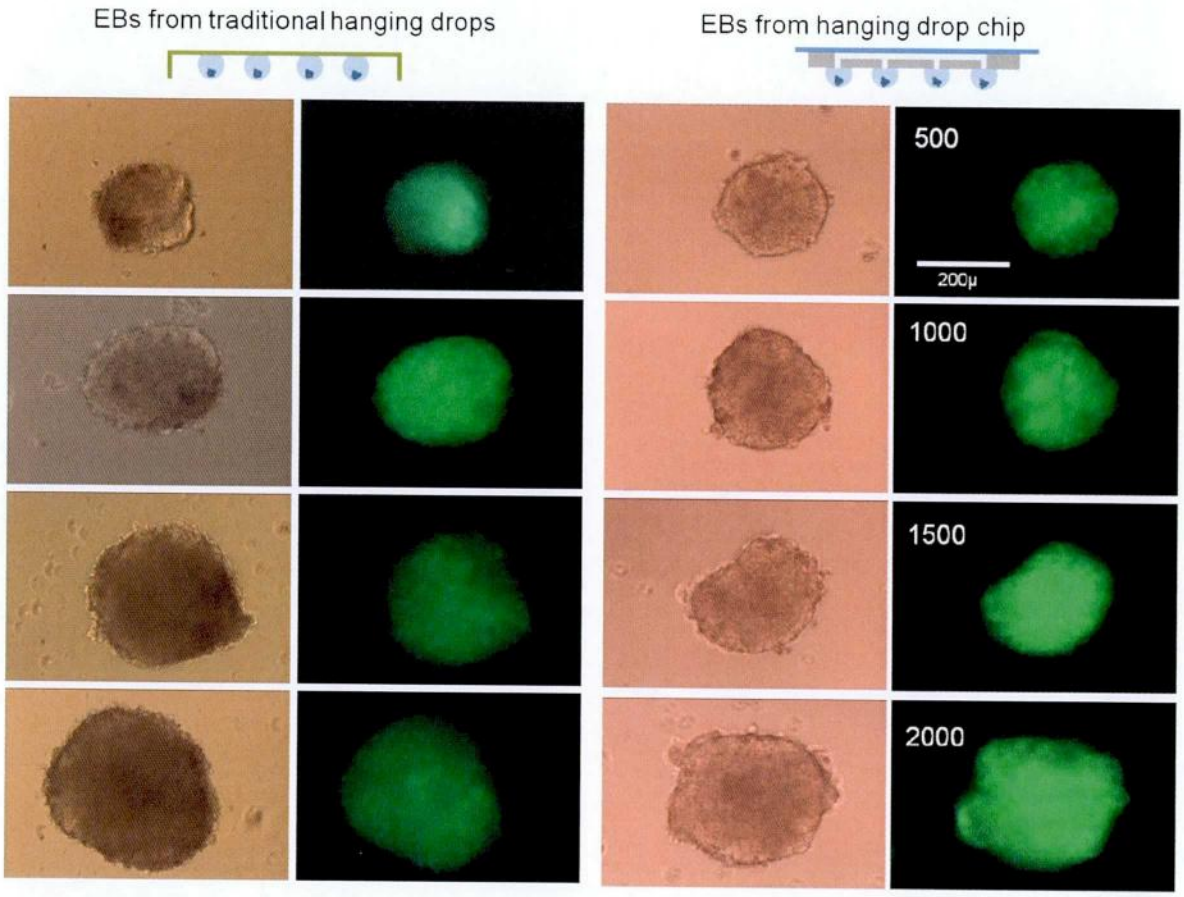

Figure 5 *Mouse ES cell EBs from control platform compared to EBs from hanging drop chips. The size differences for different cell concentrations were comparable to EBs from traditional platform. Left side column indicates light images and right side column fluorescence images.*

We designed straight channels of multiple levels starting with the wider and culminating with the smaller channels with binary flow division at each level (Fig 4d). After four levels of binary divisions with each branch giving us sixteen droplets of equal volumes with desired number of cells in each lane and we could make 64 droplets in total.

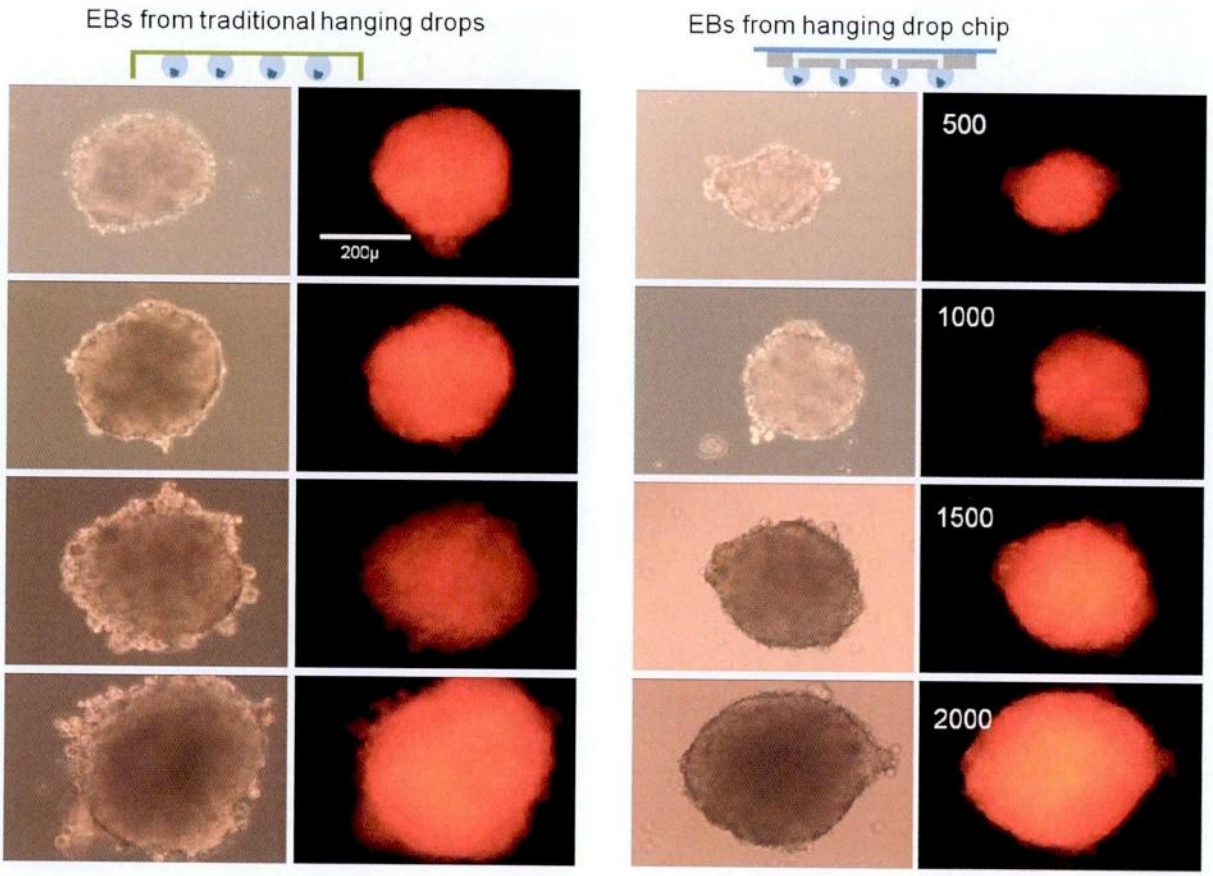

Figure 6 *Mouse iPS cell EBs from control platform compared to EBs from hanging drop chips. The size differences for different cell concentrations were comparable to EBs from traditional platform. Left side column indicates light images and right side column fluorescence images.*

5.2.4 Formation of hanging drop EBs on the chip

EBs of varying sizes (Fig 7 for mES EBs and Fig 8 for iPS EBs) were formed from varying cell density containing droplets form the hanging drop chips. We have used both mouse ES and iPS cells in this chip based EB formation study. In both the cases we could obtain EBs of comparable size and shape to those from control platform. The Sphericity of EBs from chips were also satisfactory. On the other hand, we have observed the changes in size with the cell numbers for mES and iPS EBs from the chip at par with the control EBs.

5.2.6 Differentiation into beating cardiomyocytes

The EBs from the chips and the control platform were plated onto 0.1% gelatin coated dishes and upon continuous culture, we observed the contractile beating colonies form these chip derived EBs. Compared to the EBs obtained from control platform, *i.e.* traditional hanging drop cultures onto the inverted tissue culture dishes, the EBs showed normal morphology and also normal proliferation upon plating. The differentiation into synchronously beating cardiomyocytes was also not affected by the production of cell aggregate using this chip platform.

5.3 Conclusion

Simple but effective microfluidic chip platforms to produce mouse ES and mouse iPS cell aggregates *i.e.* EBs of desired sizes and shapes is reported in this research. The microfluidic platforms reported here were for hanging drop gravity based embryoid body formation. Initially we wanted centrifugal force based aggregation system but due to the bubble formation issue on those devices in centrifugal devices, we opted to use gravity based hanging drop chips for cell aggregation. The chips were fabricated using PDMS based photolithography method. The chips of various designs and different throughputs were investigated and the optimum designs were selected based on optimization studies. Our chips successfully created ES and iPS EBs after three to four days of hanging drop culture. The chip derived EBs showed comparable in size and shape to traditional hanging drop EBs and were successfully grown and differentiated into contractile cardiomyocytes upon addition of cardiomyogenic enhancer GSK3β inhibitor to the cell culture medium. The chip has the potential for medium supplementing for long term EB culture and for being appended into an integrated EB and differentiation platform in the future.

5.4 References

[1] Weitzer, W. *Stem Cells* **2006**, 21–51.

[2] ten Berge, D.; Koole, W.; Fuerer, C.; Fish, M.; Eroglu, E.; Nusse, R. *Cell Stem Cell* **2008**, *3*, 508-518.

[3] Mauritz, C.; Schwanke, K.; Reppel, M.; Neef, S.; Katsirntaki, K.; Maier, L. S.; Nguemo, F.; Menke, S.; Haustein, M.; Hescheler, J.; others *Circulation* **2008**, *118*, 507.

[4] Wernig, M.; Zhao, J. P.; Pruszak, J.; Hedlund, E.; Fu, D.; Soldner, F.; Broccoli, V.; Constantine-Paton, M.; Isacson, O.; Jaenisch, R. *Proceedings of the National Academy of Sciences* **2008**, *105*, 5856.

[5] Dimos, J. T.; Rodolfa, K. T.; Niakan, K. K.; Weisenthal, L. M.; Mitsumoto, H.; Chung, W.; Croft, G. F.; Saphier, G.; Leibel, R.; Goland, R.; others *Science* **2008**, *321*, 1218.

[6] Kurosawa, H. *Journal of Bioscience and Bioengineering* **2007**, *103*, 389–398.

[7] Torisawa, Y.; Chueh, B.; Huh, D.; Ramamurthy, P.; Roth, T. M.; Barald, K. F.; Takayama, S. *Lab on a Chip* **2007**, *7*, 770–776.

[8] Fung, W. T.; Beyzavi, A.; Abgrall, P.; Nguyen, N. T.; Li, H. Y. *Lab on a Chip* **2009**, *9*, 2591–2595.

[9] Liu, L.; Luo, C.; Ni, X.; Wang, L.; Yamauchi, K.; Nomura, S. M.; Nakatsuji, N.; Chen, Y. *Biomedical Microdevices* **2010**, *12*, 505–511.

[10] Choi, Y. Y.; Chung, B. G.; Lee, D. H.; Khademhosseini, A.; Kim, J. H.; Lee, S. H. *Biomaterials* **2010**, 4296-4303.

[11] Hossain, M. M.; Shimizu, E.; Saito, M.; Rao, S. R.; Yamaguchi, Y.; Tamiya, E. *Analyst* **2010**, *135*, 1624-1630.

Chapter: 6

Discussion and Final remarks

A non-invasive, faster and inexpensive alternative for characterizing ES cell derived cardiomyocytes have been developed. The novel method was based on the analysis of the changes in the total pixel intensities in derivative images obtained from captured videos taken from in-vitro beating tissues. The intensity variation was then presented into the time and frequency domain intensity patterns which was the beating profile. In this approach, unlike the currently available approaches, the entire beating segment on the differentiated tissue was considered for analysis and characterization. This have ensured the simplicity of the method and enabled this method to reveal more information from the large patch of beating cells.

On the other hand, in terms of characterization parameters, the intensity variation based method was successfully applied in monitoring the initiation, propagation and maturation of beating of mESC derived cardiac muscle cells. Moreover, using our method - the beating frequency, the strength of beating, number of distinctly beating patches at a certain location on the culture dish could be obtained. Moreover, we used our proposed method in evaluating the response of differentiated cells to positive and negative inotropic agents. All of these are important in evaluating stem cell derived cardiomyocytes for subsequent applications after differentiation.

The main advantages of this approach are, we can do characterization of a large number of samples in short time i.e. the method is high throughput, after characterization, due to non-invasive nature of the method, the tissue will be available for further study or use and it can be expanded into an automated system of differentiated cardiomyocyte characterization.

In our study, we prepared a composite substrate containing functionalized MWCNT containing and gelatin. The novel substrate was characterized it by using FTIR, AFM, SEM,

Raman spectra analysis and 4-point conductivity measurement. The substrate was proven to be biocompatible for mES cell line we used and it supported the growth and differentiation of murine embryonic stem cells and directed the ES cells towards concurrent differentiation towards cardiomyocytes and neuronal cells. Cardiac differentiation preceded the neuronal differentiation and it was more prominent. The immunostaining using cardiac specific markers α-actinin, ANP and Troponin, the presence of differentiated cardiomyocytes with quite stronger organization and in higher numbers and patches compared to control culture on bare gelatin. The cardiomyocytes on composite substrate demonstrated stronger beating compared to control in their eating profiles. Neuronal nuclear markers Neu-N confirmed the presence of differentiated neurons on CNT composite substrate while no such differentiation was seen in case of gelatin only control plates.

In order to study the direct nanomaterials interaction with mES cells, mES cells were exposed directly to carboxylate modified multiwalled CNT dispersion made in 0.1% gelatin solution as well as in milli-Q water. The toxicity of CNT on mES cells due to the direct exposure was studied by MTS assay. The role of f-MWCNTs on EB formation and EB morphology was then investigated. Subsequently, the formed EBs were plated onto 0.1% gelatin coated culture dishes for subsequent growth and differentiation. We studied the differentiation through optical imaging and immunostaining. The role of exposure of ES cells to different concentrations of CNT at the EB formation stage was investigated. We have seen the formation of EBs of comparable size and shape with better sphericity in case of CNT treatments. The attachment of EBs to gelatin substrate was remarkable and it showed cellular organizations through cystic sac like structure formation. Upon continuous culture beating cardiomyocyte were observed from f-

MWCNT exposed EBs which showed stronger beating compared to control in their beating profiles as produced by our image analysis method.

In this doctoral research, I have also tried to develop gravity and centrifugation based microfluidic chips for cell aggregation. The successful gravity based microfluidic hanging drop chips is reported here. The chip fabricated off biocompatible PDMS and was bonded to glass through oxygen plasma treatment to construct the flow channels. In this study, the chips were glued to the upper lid of tissue culture dish but it can be made into independent device. The chip was successfully used to for ES and iPS cell aggregation. The EBs formed from the chips showed growth comparable to control EBs from traditional hanging drop cultures and upon the addition of cardiac differentiation enhancer GSK3β inhibitor to the differentiation medium, we observed cardiac differentiation from EBs derived from chips. The microfluidic hanging drop chips were designed in such a way that it is amenable to the future addition of a second layer at the bottom in order to make ES/iPS cell aggregation, differentiation and further investigations on an integrated single chip. Such integrated chips may open up new windows of microfluidic based stem cell research.

The image analysis method combined with the Mesoscale cell-nanomaterial interaction and the microfluidic cell aggregation hanging drop chips formed a niche of application in stem cell research with wider applicability in future researches. These research works represented a lot of promises towards their infringement and substantial contributions into the era of regenerative medicine.

However, before closing the discussion on the researches included in this thesis, I should also mention the obvious point of caution. Like any other researches in different fields of human interest where our understandings are not very apparent and comprehensive, we need to be cautious about the outcomes. Science has always been a two-edged blade – and depending on the edge that we use for cutting by it, science can harvest positive impact or it may become a tool to do harm against the mankind.

The interactions of mES cells with nanomaterials is opening newer avenues of applications and promises for us, however, as we do not understand these nano-scale interactions well enough right now, we should always have to remain vigilant about the precarious possibilities of this of cutting edge - the widely accepted CNT toxicity is an issue worth mention in this regard. Aside the foreseeable positive impacts of nano-scale in mES cell research, it may also do undesirable modulation of mES or other cells which can pose potential risks, for example, through undesired genetic mutation and manipulations. While we will be looking forward for the augmented applications of nanomaterials for studying ES cells in order to open up newer horizons, we shall have to find out the undesirable means of using such interactions for enabling us to harness the full potential of these approaches in a positive manner to yield the desirable outcomes. In the end, it is the concerned and concerted efforts of human intellect that brings novel breakthroughs to change our lives towards a more meaningful end.

List of publications

Original Papers included in this thesis

[1] **M. M. Hossain**, E. Shimizu, M. Saito, S. R. Rao, Y. Yamaguchi and E. Tamiya. Non-invasive characterization of mouse embryonic stem cell derived cardiomyocytes based on the intensity variation in digital beating video. ***Analyst,*** 2010, **135**, 1624 - 1630

[2] **M. M. Hossain**, S. R. Rao, M. Saito, T. Hasegawa, Y. Yamaguchi and E. Tamiya. 2010. Effects of the exposure to functionalized multiwalled carbon nanotubes on embryoid body formation from mouse embryonic stem cells their subsequent growth and cardiomyogenic differentiation. *Submitted*

[3] **M. M. Hossain**, S. R. Rao, M. Saito, Y. Yamaguchi and E. Tamiya. 2010. Carboxylate functionalized Multiwalled Carbon nanotube modified gelatin substrate enhances cardiac differentiation and promote neuronal differentiation of mouse embryonic stem cells. *Submitted*

[4] **M. M. Hossain**, S. R. Rao, M. Saito, Y. Yamaguchi and E. Tamiya. Microfluidic chip for high throughput, uniform Embryoid Body formation from mouse ES and iPS cells and their long term culture. *In preparation*

Original papers not part of this thesis

[1] M. U. Ahmed, M. Saito, **M. M. Hossain**, Rao, S.R., Furui, S., Hino, A., Takamura, Y.; Takagi, M. and Tamiya, E. 2009. Electrochemical genosensor for rapid detection of GMO using loop-mediated isothermal amplification. *Analyst*, **134**, 966–972.

[2] M. U. Ahmed, Q. Hasan, **M. M. Hossain**, M. Saito, and E. Tamiya, 2009. Meat species identification based on the loop mediated isothermal amplification and electrochemical DNA sensor, *Food Control* (**2009**) (doi: 10.1016/j.foodcont.2009.09.001)

[3] M. U. Ahmed, **M. M. Hossain,** and E. Tamiya 2008. Electrochemical Biosensors for Medical and Food Applications. *Electroanalysis*, Vol **20 (6)**, 616 – 626

[4] S. R. Rao, **M. M. Hossain**, H. Yoshikawa and E. Tamiya. Embryonic Stem Cell Developmental Processes Probing Based on Surface-Enhanced Raman Scattering from Gold Nanoparticles. *Submitted*

[5] K. Yamanaka, M. Saito, K. Kondou, **M. M. Hossain**, R. Koketsu, T. Sasaki, N. Nagatani, K. Ikuta, and E. Tamiya. Microfluidic RT-PCR device and electrochemical DNA sensor for rapid detection of influenza AH1pdm virus. *Submitted*

Seminars and Conferences

Hossain, M. M.; Ahmed, M.U.; Saito, M. and Tamiya, E. *Conductive biocompatible polymer patterning inside microfluidic channel for cellular investigation* at 75 the Convention of Electrochemical Society of Japan (ECSJ) in Yamanishi, Japan, March 29-31, 2008

Hossain, M. M., Saito, M. and Tamiya, E.. *Electrochemical patterning of conductive polymer wall inside microfluidic channel for biosensor application*, at 10th World Congress on Biosensors Shanghai, China. May 16, 2008

Hossain, M. M.,Rao S.R. and Tamiya, E. *Electro-active cells on Microfluidic cell chips: Culture, Stimulation and Manipulation*, at 5th International Stem Cell School in Regenerative Medicine in Berlin, Germany, October 20-22, 2008.

Marie curie fellowship for Stem cell school on regenerative medicine

A. Fifth International School on Regenerative Medicine 2008, Berlin and Rostock, Germany.

Lecture week: Signaling processes and systems biology in neural stem cells, Berlin, Germany, October 20 – 22, 2008.

Practical Course: Culture and transplantation of neural stem cells, at Albrecht-Kossel Institute for Neuroregeneration, University of Rostock, Rostock, Germany, October 24-27, 2008

B. Seventh International School on Regenerative Medicine 2009, Prague, Czech Republic.

Lecture week: Stem cells, biomaterials and nanotechnologies in regenerative medicine, Prague, Czech Republic, November 2– 4, 2009.

Practical Course: Patch-clamp recording and calcium imaging of stem cells, at Institute of Experimental Medicine ASCR, Prague, Czech Republic, November 5– 7, 2009.

Acknowledgements

All praise is to Allah - the creator almighty.

In the beginning, I would like to offer my earnest appreciation to the Japanese Ministry of Education, Culture, Science and Technology (MEXT) for offering me the Monbukagakusho scholarship to do this doctoral research.

I was fortunate to get Professor Eiichi Tamiya as my supervisor in the doctoral study. It was a long story and a memorable one - how I was introduced to Tamiya sensei's laboratory at Japan Advanced Institute of Science and Technology (JAIST) after winning the highly competitive selection for Monbukagakusho Scholarship arranged by Japanese Embassy in Bangladesh. I express my sincere gratitude and the deepest appreciation to him for guiding this research with care and adept supervision towards a meaningful end. My gratitude to him is, firstly - for accepting me a doctoral student in his LAB, secondly - for bring me as a member of his new laboratory at Osaka University, thirdly – for exposing me to the exciting field of stem cell research and fourthly – for his unprecedented support and insights towards the all the research works reported in this thesis.

My heartfelt thanks goes to Associate Professor Yoshinori Yamaguchi, Assistant Professor Masato Saito and Assistant Professor Hiroyuki Yoshikawa for their supports, guidance, advices, suggestions, comments and helps of all-sort without which it would be difficult for me to bring this work into the shape it is now. I would like to offer my gratitude for the special helps and guidance from Dr Sathuluri Ramachandra Rao, the senior post-doctoral fellow at Tamiya lab for all his supports, comments, long-meaningful-discussions and above all special helps in communications, which will remain as an inevitable part of this research. Special thanks to Dr Keiichiro Yamanaka for his kind help in AFM imaging.

I would like to thank Professor Yoshiki Sawa of the Division of Cardiovascular Surgery, Department of Surgery, Graduate School of Medicine, Osaka University for his support with iPS cells. My gratitude to Assistant Professor Atsuhiro Saito and Assistant Professor Mitsuhiro Ebara of Medical Centre for Translational Research for their insightful discussions. I am grateful to Kenji Miki san, doctoral student of Prof. Sawa's Laboratory for his help regarding STO and iPS cells as well as for his supports in cell culture and imaging.

Special thanks go to Associate Professor Kenzo Maehashi and Assistant Professor Yasuhide Ohno of Prof. Matsumoto's laboratory at The Institute of Scientific and Industrial Research (ISIR) of Osaka University for their help in CNT-gelatin substrate characterization.

My special appreciation is to Mr Toshiaki Hasegawa, staff of the Research Center for Ultra-High Voltage Electron Microscopy (HVEM) at Osaka University for his heartily support in TEM imaging of my samples.

I would like to offer my sincere thankfulness to all the members at Tamiya laboratory whom I came across during my period of stay here. I am thankful of Dr Minhaz Uddin Ahmed, Dr Ha Minh Hiep and Dr Ryohei Yasukuni for their strong supports during their stay at Prof. Tamiya's laboratory. I would like to mention special helps from Yasuhito Sugano san, Hoa Qynh Li san and Eiichi Shimizu san and Trung Ba Nguyen in various ways.

I would like to take this opportunity to thank my friends, relatives and well wishers here in Osaka and in JAIST as well as in Bangladesh for their encouragements and moral support for me and for my work. In this opportunity,

Without the selfless support from my beloved family members – my loving parents and three caring brothers, I won't be able to bear the tough ask of this research. Deep appreciation is to Meher Nigar Munmun for her virtual presence with me all along my lonely life here in Japan and for being a persuasive source of inspiration for me.